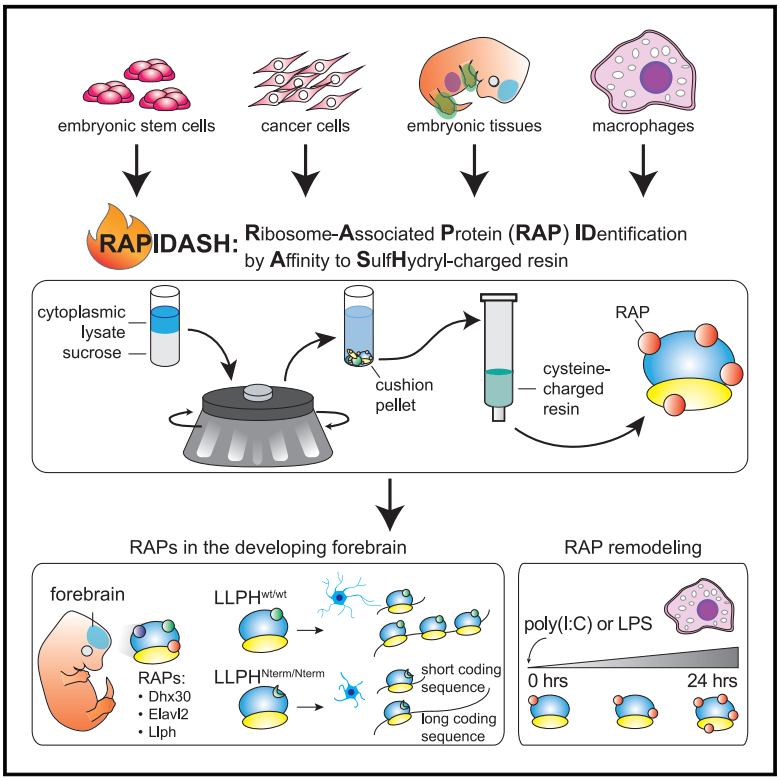
Molecular Cell

Resource

RAPIDASH: Tag-free enrichment of ribosome-associated proteins reveals composition dynamics in embryonic tissue, cancer cells, and macrophages

Graphical abstract



Authors

Teodorus Theo Susanto, Victoria Hung, Andrew G. Levine, ..., Alma L. Burlingame, Davide Ruggero, Maria Barna

Correspondence

davide.ruggero@ucsf.edu (D.R.), mbarna@stanford.edu (M.B.)

In brief

Susanto et al. developed a tag-free method to characterize ribosome-associated proteins from any sample. They identified hundreds of candidate ribosome-associated proteins, some of which were dynamic across embryonic tissues or during responses to cell stimuli. These included proteins that may be important for neural development or during immune activation.

Highlights

- Tag-free method to enrich ribosomes and associated proteins from any sample
- Dhx30 and Elavl2 are embryonic forebrain ribosome-associated proteins (RAPs)
- The RAP Llph may be important for neural development and translation of long mRNAs
- Macrophages exhibit ribosome composition changes upon different stimuli

Susanto et al., 2024, Molecular Cell *84*, 3545–3563
September 19, 2024 © 2024 Elsevier Inc. All rights reserved, including those for text and data mining, AI training, and similar technologies.
https://doi.org/10.1016/j.molcel.2024.08.023

CellPress

Molecular Cell

CellPress

Resource

RAPIDASH: Tag-free enrichment of ribosome-associated proteins reveals composition dynamics in embryonic tissue, cancer cells, and macrophages

Teodorus Theo Susanto,[1,9,12] Victoria Hung,[1,12] Andrew G. Levine,[2,3,4,12] Yuxiang Chen,[1] Craig H. Kerr,[1,10] Yongjin Yoo,[5] Juan A. Oses-Prieto,[6] Lisa Fromm,[3,4,7] Zijian Zhang,[1,8] Travis C. Lantz,[1,8] Kotaro Fujii,[1,11] Marius Wernig,[5,8] Alma L. Burlingame,[6] Davide Ruggero,[3,4,7,*] and Maria Barna[1,13,*]

[1]Department of Genetics, Stanford University School of Medicine, Stanford, CA 94305, USA
[2]Department of Laboratory Medicine, University of California, San Francisco, San Francisco, CA, USA
[3]Department of Urology, University of California, San Francisco, San Francisco, CA, USA
[4]Helen Diller Family Comprehensive Cancer Center, University of California, San Francisco, San Francisco, CA, USA
[5]Institute for Stem Cell Biology and Regenerative Medicine and Department of Pathology, Stanford University School of Medicine, Stanford, CA 94305, USA
[6]Department of Pharmaceutical Chemistry, University of California, San Francisco, San Francisco, CA 94158, USA
[7]Department of Cellular and Molecular Pharmacology, University of California, San Francisco, San Francisco, CA, USA
[8]Department of Chemical and Systems Biology, Stanford University School of Medicine, Stanford, CA 94305, USA
[9]Present address: Genomic Institute of Singapore, ASTAR, Singapore 138672, Singapore
[10]Present address: Inceptive, Palo Alto, CA 94040, USA
[11]Present address: Department of Molecular Genetics & Microbiology, University of Florida, Gainesville, FL 32610, USA
[12]These authors contributed equally
[13]Lead contact
*Correspondence: davide.ruggero@ucsf.edu (D.R.), mbarna@stanford.edu (M.B.)
https://doi.org/10.1016/j.molcel.2024.08.023

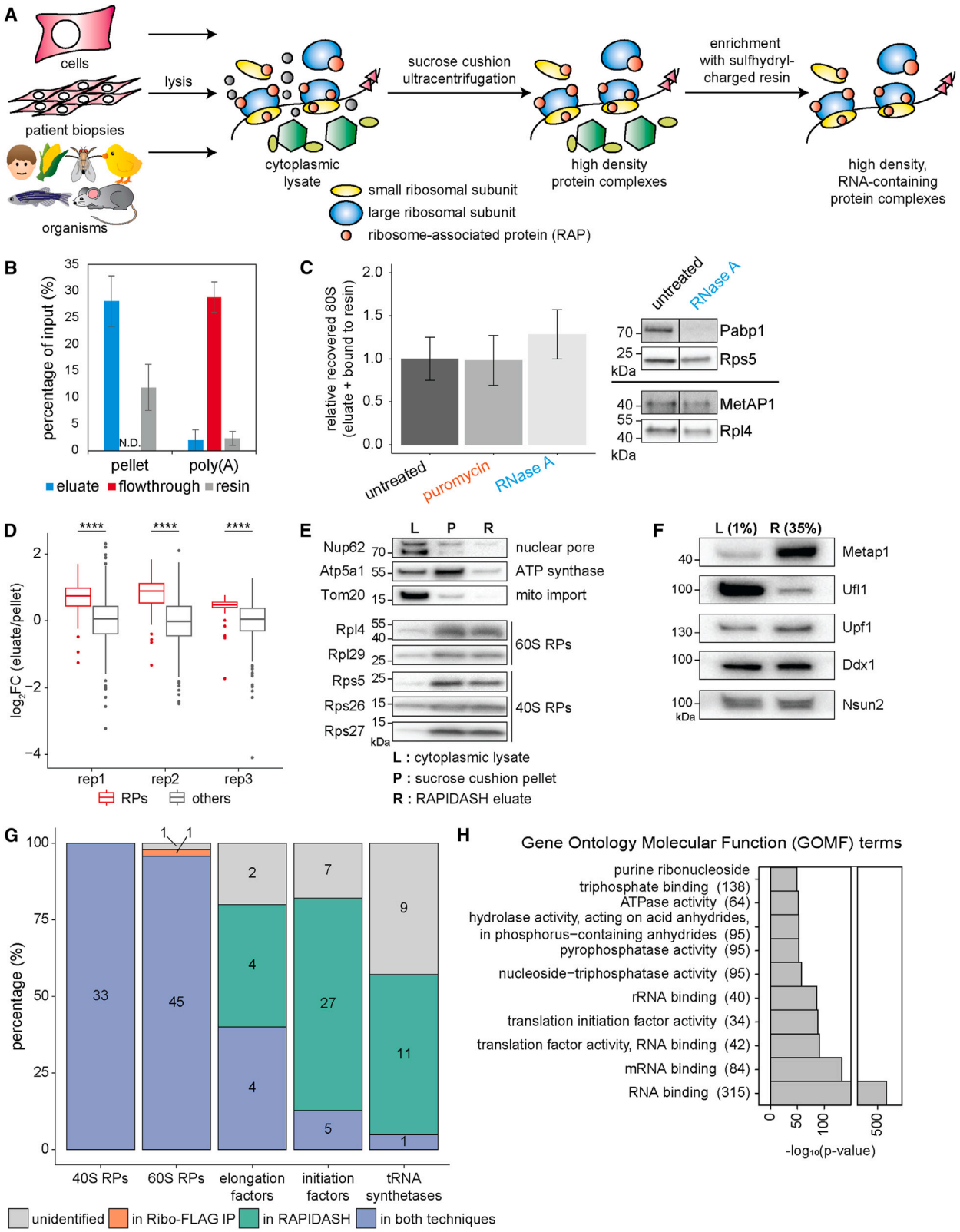
SUMMARY

Ribosomes are emerging as direct regulators of gene expression, with ribosome-associated proteins (RAPs) allowing ribosomes to modulate translation. Nevertheless, a lack of technologies to enrich RAPs across sample types has prevented systematic analysis of RAP identities, dynamics, and functions. We have developed a label-free methodology called RAPIDASH to enrich ribosomes and RAPs from any sample. We applied RAPIDASH to mouse embryonic tissues and identified hundreds of potential RAPs, including Dhx30 and Llph, two forebrain RAPs important for neurodevelopment. We identified a critical role of LLPH in neural development linked to the translation of genes with long coding sequences. In addition, we showed that RAPIDASH can identify ribosome changes in cancer cells. Finally, we characterized ribosome composition remodeling during immune cell activation and observed extensive changes post-stimulation. RAPIDASH has therefore enabled the discovery of RAPs in multiple cell types, tissues, and stimuli and is adaptable to characterize ribosome remodeling in several contexts.

INTRODUCTION

Recently, ribosomes have emerged as direct regulators of gene expression. Interestingly, ribosome-associated proteins (RAPs) such as RNA-binding proteins allow for specificity and regulation over mRNA translation. A handful of RAPs have been further functionally characterized, such as methionine aminopeptidase (MetAP),[1] fragile X messenger ribonucleoprotein (RNP) 1 protein (FMRP),[2–4] pyruvate kinase M (PKM),[5,6] RNA-binding protein with multiple splicing (RBPMS),[7] UFM1-specific ligase 1 (UFL1),[5,8] and cyclin-dependent kinase 1 (CDK1).[5,9,10] MetAP directly binds to ES27L,[1] a region of the ribosome that has expanded ribosomal RNA (rRNA) known as expansion segments (ESs), and cleaves the initiator methionine of polypeptides as they are synthesized. Surprisingly, MetAP is important for translation fidelity.[1] FMRP inhibits the translation of neuronal mRNAs.[2–4] PKM directly interacts with ribosomes and acts as a translational activator for a subset of mRNAs.[5,6] RBPMS is an RNA-binding protein that regulates the translation of mRNAs crucial for mesoderm differentiation.[7] In addition to these proteins, post-translational modification enzymes interact with and modify the ribosome. UFL1 is the sole known enzyme that deposits a post-translational modification known as UFMylation on proteins such as Rpl26, which is associated with an increase in the stalling of endoplasmic reticulum (ER) translocon-associated ribosomes.[8,11,12] Lastly, CDK1 phosphorylates Rpl12,

All rights are reserved, including those for text and data mining, AI training, and similar technologies.



(legend on next page)

which promotes translation of mitosis-related mRNAs.[9] Thus, RAPs connect the ribosome and mRNA translation to many important cellular functions.

Although RAPs diversify translational control, a lack of methods to rapidly and systematically identify RAPs in different tissue and cell types has stymied our ability to understand fundamental aspects of RAP biology. For example, how many RAPs exist, and do RAPs differ between cell types, tissues, and species? Most prior work has relied on fractionation of cell lysate according to density[13,14] or size[15] to identify RAPs. However, these techniques are highly nonspecific. For example, ER microsomes have heterogeneous densities that are present throughout most fractions, including those containing ribosomes (Figure S1A). Our lab used a genetic approach, which we refer to as Ribo-FLAG immunoprecipitation (IP), where core ribosomal proteins (RPs) were endogenously tagged with FLAG epitope tag to enable the IP of ribosomes and RAPs for subsequent analysis by mass spectrometry (MS). This enabled the discovery of hundreds of RAPs in mouse embryonic stem cells (mESCs), collectively known as the ribo-interactome.[5] Although Ribo-FLAG IP is exceptionally specific, the reliance on genetic editing hinders the implementation of this strategy in many different sample types, such as tissues or patient samples. A chemical approach, active ribosome capture-MS (ARC-MS), was recently reported as an orthogonal strategy to isolate ribosomes and RAPs.[7] Here, Click chemistry is employed to isolate ribosomes and RAPs for analysis by MS. However, this technique requires treating samples with azidohomoalanine and biases the findings toward ribosomes at the early steps of translation.[7]

We sought to develop a methodology that relies on the biophysical properties of the ribosome without genetic tagging or chemical modification, namely, the fact that it contains an rRNA core. In our approach, high-density protein complexes are pelleted by sucrose cushion ultracentrifugation and then undergo chromatography with cysteine-charged sulfolink resin to enrich those that contain RNA, which are mostly ribosomal complexes (Figure 1A). We called this methodology RAP identification by affinity to sulfhydryl-charged resin (RAPIDASH).

Herein, we have used RAPIDASH on mouse embryonic forebrain, limb, and liver tissues and show that ribosomes differ in RAP composition across tissue types. We focused on candidates in the forebrain and characterized Dhx30, Elavl2, and learning-associated protein of slug with 18 kDa (LAPS18)-like protein homolog (Llph) as bona fide RAPs. We further characterized the role of LLPH in human induced neurons, which revealed a critical role of LLPH in neural development and function. In addition, we discovered LLPH has a selective role in translational control, particularly for long transcripts that may require more ribosome-directed control of mRNA translation. We also applied RAPIDASH to characterize RAP dynamics in cancer cells and primary murine macrophages that are treated with different stimuli. This demonstrated the broad applicability of RAPIDASH to many sample types and its ability to characterize dynamic remodeling of ribosome composition.

RESULTS

Characterization of RAPIDASH in mESCs and cancer cells

We turned to a chromatographic technique that had been used to isolate active ribosomes from bacteria[17] and yeast[18] by binding of RNA moieties, likely rRNA, to a cysteine-charged resin. While the sulfhydryl-charged resin was used to isolate ribosomes, this protocol did not maintain interactions between ribosomes and RAPs. We made several changes to the protocol developed for yeast ribosomes[18] to optimize the binding and elution of RAP-bound mammalian ribosomes: the centrifugation was performed prior to resin chromatography, the

Figure 1. Characterization of the RAPIDASH method in mESCs

(A) Schematic of the RAPIDASH protocol. Cytoplasmic lysates from any sample undergo sucrose cushion ultracentrifugation and sulfhydryl-charged resin chromatography to enrich RNA-containing, high-density complexes.

(B) Characterization of the cysteine-charged sulfolink resin. Sucrose cushion pellet samples and poly(A) RNA isolated from mESCs underwent cysteine-charged sulfolink resin chromatography. The percentage of RNA relative to input amount is plotted for the flowthrough, eluate, and resin-bound samples. N.D., not detected. Error bars are ± standard error of the mean (SEM).

(C) Characterization of binding to the cysteine-charged sulfolink resin for 80S ribosomes isolated from untreated, puromycin-treated, or RNase A-treated mESC samples. Left: the percentage of input RNA that was eluted from or bound to the resin was normalized to that for the untreated sample for three technical replicates. Error bars are ± SEM. Right: untreated and RNase A-treated 80S samples were probed by western blotting for the presence of Pabp1, MetAP1, Rps5, and Rpl4. The horizontal black line separates sister blots loaded with the same samples. The vertical black line represents an omitted lane.

(D) Boxplot of normalized $\log_2$ fold change (FC) of RAPIDASH eluate over sucrose cushion pellet tandem mass tag (TMT) mass spectrometry ratios from three biological replicates of mESCs. Ribosomal proteins (RPs) (red) are significantly enriched over other proteins (gray) by RAPIDASH compared to sucrose cushion ultracentrifugation alone based on Welch's t test. p values: rep1 = 5.58×10^{-19}; rep2 = 4.96×10^{-22}; rep3 = 3.89×10^{-15}.

(E) Western blotting of mESC sucrose cushion pellet and RAPIDASH eluate samples to assess the specificity of RAPIDASH. Approximately equal amounts of RPs (see Figure S3D) for sucrose cushion pellet and RAPIDASH eluate samples were analyzed by western blotting for Nup62, Atp5a1, and Tom20. Rpl4, Rpl29, Rps5, Rps26, and Rps27 are RPs. Cytoplasmic lysate is an input control. Molecular weight markers are in kilodaltons (kDa).

(F) Western blot detection of known RAPs enriched by RAPIDASH. A representative blot with 1% of the mESC cytoplasmic lysate volume and 35% of the RAPIDASH eluate volume was probed for the known RAPs: Metap1, Ufl1, Upf1, Ddx1, and Nsun2.[1,5] Molecular weight markers are in kDa.

(G) Bar graph showing the translational machinery identified by Ribo-FLAG immunoprecipitation (IP)[5] or RAPIDASH. Ribo-FLAG IP proteins were identified by FLAG IP liquid chromatography-tandem mass spectrometry (LC-MS/MS) of endogenously FLAG-tagged Rpl36 or Rps17 in mESCs.[5] Three biological replicates of RAPIDASH were performed for each of the same cell lines and analyzed by LC-MS/MS. Proteins identified in at least three RAPIDASH samples were compared against the Ribo-FLAG IP proteins. The percentage of translational machinery components identified only in Ribo-FLAG IP (red), only in RAPIDASH (green), in both techniques (blue), or none (gray) are displayed.

(H) Gene Ontology (GO) term analysis of mESC proteins enriched by RAPIDASH. Proteins that were identified in RAPIDASH-enriched mESC samples were analyzed by Manteia.[16] The ten most significant GO molecular function (GOMF) terms at level 4 or lower are shown. p values displayed were corrected by the Benjamini-Hochberg method.

ultracentrifugation speed and time were altered, and the buffers were changed to maintain interactions with salt-sensitive RAPs. We isolated ribosomes using the protocol for yeast ribosomes or our optimized RAPIDASH protocol. The peptides derived from the enriched proteins from each sample were labeled with tandem mass tags (TMTs) so the relative levels of the proteins could be quantified by MS. Out of the 212 proteins identified, only 61 proteins gave quantifiable signal in the reporter ion channel for the original chromatography protocol (Table S1). Most of the quantified proteins were RPs. This number of proteins is far below what was identified by other methods used to characterize RAPs, which suggests the original chromatography protocol, while suitable to purify the core ribosome, cannot be used to comprehensively identify RAPs.

We found that sucrose cushion pellet material binds to and elutes from the cysteine-charged resin. Importantly, poly(A)-enriched RNA does not bind to the resin (Figure 1B). When mESC lysate underwent the cysteine-charged resin chromatography, the flowthrough, which contains the RNP complexes that do not bind to the resin, overwhelmingly was composed of small, non-ribosomal RNPs, while the eluate contained a greater proportion of ribosomes (Figure S1B). This suggests the cysteine-charged resin preferentially binds ribosomes instead of small RNPs. Performing the entire RAPIDASH protocol eliminates small RNPs but retains ribosomes (Figure S1B).

Next, we asked whether the binding of ribosomes to the resin depends on the nascent polypeptide chain, mRNA, or RAPs. We isolated 80S ribosomes from untreated samples or samples treated with puromycin to release nascent polypeptide chains[18]; RNase A to digest single-stranded RNAs[19–21]; or a high concentration of ammonium chloride to remove RAPs[22] (Figure S1C). The RNase A-treated sample was probed by western blotting to confirm the loss of Pabp1, a protein that depends on mRNA to associate with the ribosome, and to test for the presence of MetAP1, which binds the ribosome independently of mRNA[1,23,24] (Figure 1C). The ammonium chloride-treated sample was analyzed by western blotting to confirm the loss of the salt-sensitive RAPs Naa15 and MetAP1 (Figure S1D). We then performed chromatography with these samples and quantified the RNA (80S ribosomes) that either remained bound to the cysteine-charged resin or was eluted. In all samples, the amount of RNA in the flowthrough samples was not detectable, which indicates they successfully bound to the cysteine-charged resin. The untreated, puromycin-treated, and RNase A-treated samples showed similar amounts of RNA that either remained bound to or were eluted from the resin (Figure 1C). This suggests that the presence of polypeptide chains or mRNA does not affect the binding of ribosomes to the cysteine-charged resin. However, the combined amount of eluted RNA and RNA that remained bound to the resin for the ammonium chloride-treated 80S ribosomes was lower relative to that of untreated 80S ribosomes (Figure S1E). One possible explanation for this is that stripping off RAPs exposes more rRNA, which causes the ribosomes to bind more strongly to the cysteine-charged resin and consequently be more difficult to elute.

Next, we asked whether the cysteine-charged resin chromatography differentially enriches ribosomes translating a subset of mRNAs. RNA sequencing (RNA-seq) showed that less than 7% of genes change significantly (adjusted $p < 0.05$, absolute fold change [FC] ≥ 2) between samples that underwent the entire RAPIDASH protocol versus sucrose cushion ultracentrifugation alone (Figures S2A–S2C). This suggests the cysteine-charged resin chromatography is largely unbiased in terms of which mRNA-engaged ribosomes bind and elute.

We used TMT-MS to assess whether the cysteine-charged resin chromatography step allows for further enrichment of RPs compared with only performing sucrose cushion ultracentrifugation (Figure S3A). Figure 1D shows that compared with sucrose cushion ultracentrifugation alone, RAPIDASH significantly enriches RPs over other proteins. Although there might be a slight bias for 60S (large subunit) RPs over 40S (small subunit) RPs, this is not significant across all three replicates (Figure S3B).

We then asked whether non-ribosomal, large protein complexes are depleted after the entire RAPIDASH protocol compared with sucrose cushion ultracentrifugation alone. We ranked the proteins by their average enrichment ratios of RAPIDASH compared with sucrose cushion ultracentrifugation across three replicates and asked which Gene Ontology (GO) cellular component (GOCC) terms are enriched for proteins that are in the bottom 10%. The most significantly enriched terms for these proteins were related to mitochondria, nucleus, cytoskeleton, and vesicles (Figure S3C; Table S2). To confirm the depletion of non-ribosomal, large complexes and structures by RAPIDASH, we compared ultracentrifugation pellets versus RAPIDASH eluate samples for components of these complexes. As expected, when approximately equal amounts of RPs were loaded for each sample (Figure S3D), the nuclear pore complex (Nup62), adenosine triphosphate (ATP) synthase (Atp5a1), and the translocase of the outer membrane (TOM) complex (Tom20) were depleted in the RAPIDASH sample compared with the sucrose cushion ultracentrifugation pellet sample (Figure 1E). Subsequently, we assessed whether the RAPIDASH workflow can maintain interactions between ribosomes and their associated proteins. The known RAPs Ufl1,[5,8] Upf1,[25] Ddx1,[5] Nsun2,[5] and Metap1[1] were all present in mESC RAPIDASH samples (Figures 1F and S3E).

We next wanted to assess the sensitivity of RAPIDASH in capturing translation components. We detected 793 proteins present in at least 3 out of 6 replicates (Table S3, column O = 1). Figure 1G shows the comparison of proteins in translational machinery that are identified by Ribo-FLAG IP using Byonic (v2.12.0)[26] and analyzed by significance analysis of interactome (SAINT) (v2.5.0)[27] as described previously,[5] or in at least three out of six RAPIDASH samples identified using MaxQuant (v2.4.2.0).[28,29] RAPIDASH identified all RPs except for Uba52 (Rpl40) and Rpl41. Compared with Ribo-FLAG IP, RAPIDASH captured more translation elongation factors, initiation factors, and transfer RNA (tRNA) synthetases (Figure 1G). In addition, RAPIDASH detected 298 out of the 428 (70%) proteins identified by Ribo-FLAG IP[5] (Table S3, column P = 1), which suggests RAPIDASH yields a high-quality list of candidate RAPs. We also compared our mESC RAPIDASH data to the recent work of ARC-MS in human embryonic stem cells (hESCs).[7] Out of the 793 proteins identified in RAPIDASH MS samples, there are 380 proteins that were also identified by ARC-MS in hESCs (Table S3, column Q = 1). This good overlap suggests that

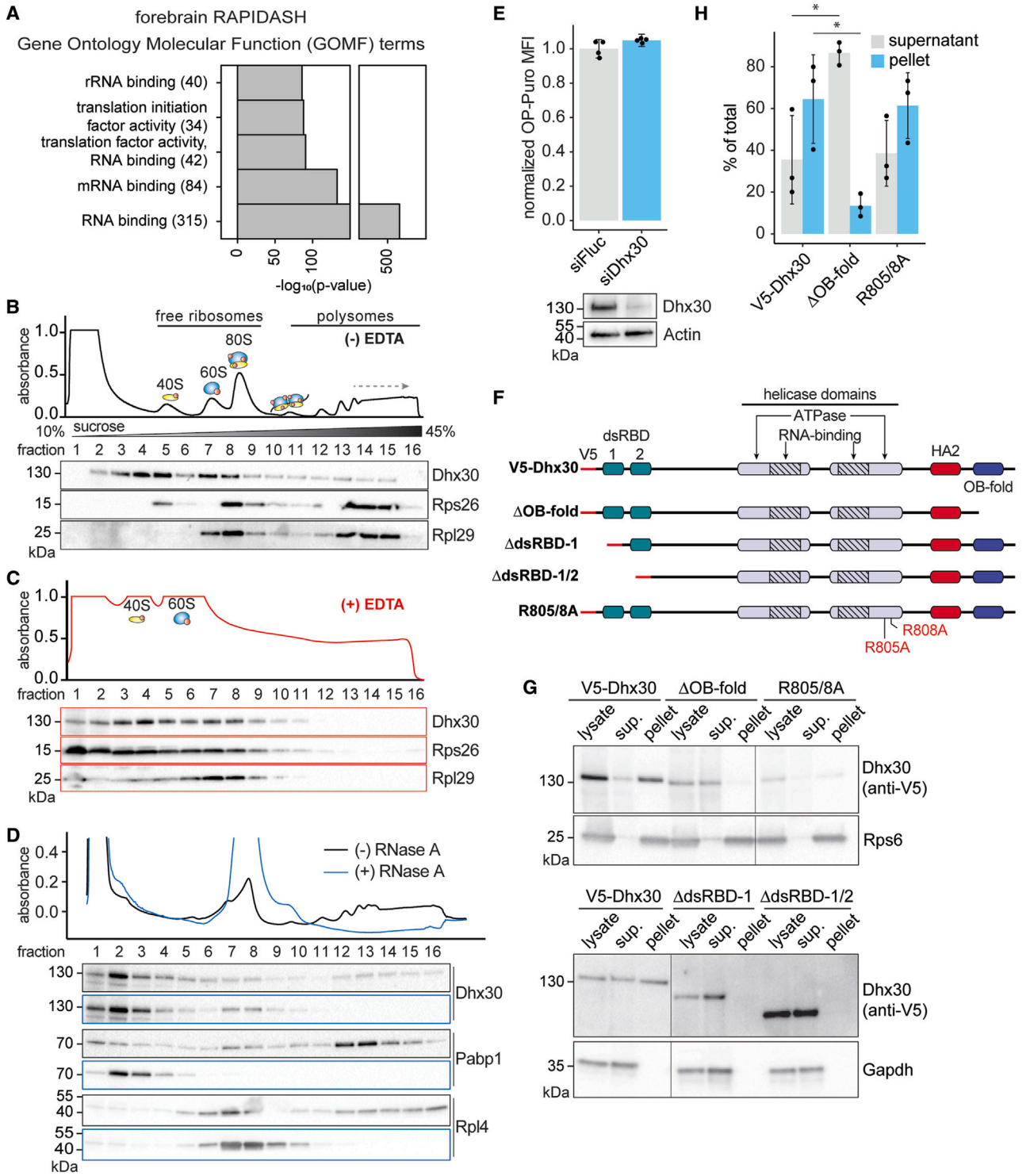


Figure 2. Characterization of Dhx30 as a bona fide mRNA-independent RAP

(A) Analysis of GO terms in forebrain MS data. RAPIDASH was performed on E12.5 mouse forebrain samples. These samples were analyzed by LC-MS/MS. The top 5 most significant GOMF terms at level 4 or lower as analyzed by Manteia[16] are shown. *p* values displayed were corrected by the Benjamini-Hochberg method.

(B and C) Sucrose gradient and western blotting analysis of Dhx30. Sucrose gradient fractionation was performed on mESC cytoplasmic lysate without (B) or with (C) EDTA treatment. The proteins from each fraction were precipitated and analyzed by western blotting; lanes were loaded with equal volumes of precipitated protein sample. RPs are markers for the 40S and 60S ribosomal subunits. Molecular weight markers are in kDa.

(legend continued on next page)

RAPIDASH is finding many RAPs identified by ARC-MS. Since ARC-MS is disposed toward finding proteins that are involved in the early steps of translation, the non-overlapping proteins may be RAPs that are more involved in other steps of translation, such as elongation or termination. Other non-overlapping proteins may be RAPs in mice but not humans or vice versa. GO analysis using Manteia[16] on mESC RAPIDASH liquid chromatography-tandem MS (LC-MS/MS) samples, half of the ten most significant GO molecular function (GOMF) terms are related to RNA binding or translation (Figure 1H).

Lastly, we tested the ability of RAPIDASH to detect RAP interactions with ribosomes in a distinct cancer cell type. For this experiment, we used PC3 cells, an aggressive metastatic human prostate cancer cell line in which constitutive mammalian target of rapamycin (mTOR) hyperactivation is essential for its tumorigenic potential.[30] We used RAPIDASH to isolate ribosomes complexes from PC3 cells that had been grown for 24 h in the presence or absence of the mTOR inhibitor Rapalink-1 and performed TMT-MS (Table S4). Although mTORC1 controls RP abundance, we did not observe major differences in RPs in our cells at these early conditions upon Rapalink-1 treatment. However, TMT-MS detected select proteins with altered associations with ribosomes upon mTOR inhibition: eIF4G1 and G3BP2 (Table S4). The translation initiation factor eIF4G1 decreased association with ribosomes upon mTOR inhibition, consistent with work showing that eIF4G1 is sequestered away from the ribosome when mTOR is inactive,[31] and G3BP2 was recently shown to regulate mTOR signaling.[32] In addition, two other proteins, PA2G4 (Ebp1) and PDCD4, also changed their association with the ribosome upon mTOR inhibition but were just below the stringent FC cutoffs that we set (Table S4). PA2G4, which regulates proteostasis through interactions with the 60S exit tunnel,[33] also decreased association with ribosomes upon mTOR inhibition. The translation inhibitor PDCD4[34] increased ribosome association upon mTOR inhibition. The significance of the differential interactions of these RAPs with ribosomes in cancer cells and downstream of mTOR signaling remains an interesting area of exploration.

Application of RAPIDASH to the developing mouse forebrain identifies Dhx30 as a RAP

We next sought to identify RAPs present in the developing mouse forebrain tissue. We performed RAPIDASH on E12.5 forebrains followed by LC-MS/MS. This analysis yielded 518 protein identifications present in 2 out of 3 replicates (Table S5, column L = 1). GO analysis[16] of the data showed significantly enriched GOMF terms such as RNA binding and mRNA binding (Figure 2A), suggesting that proteins identified are bona fide RAPs with potential forebrain-specific functions.

To identify hits for further functional characterization, we separated the identified proteins into two classes: (1) proteins that regulate translation but are not known ribosome binders and (I2) proteins that bind the ribosome but are not known to regulate translation. Following this schema, we identified Dhx30 as a paradigm class I protein. Dhx30 belongs to the DExH (Asp-Glu-X-His) class of RNA helicases. DExD/H-box RNA helicases are highly conserved enzymes that use the energy of ATP to remodel RNA secondary structure and are vital for regulating various aspects of the RNA life cycle that when perturbed can lead to disease.[35]

Biallelic loss of *Dhx30* leads to embryonic lethality in mice exhibiting distinct early neural defects.[36] Strikingly, mutations mapped to the helicase and RNA-binding domains of human DHX30 have been directly identified in pediatric neurodevelopmental disease resulting in gait abnormalities or inability to walk, speech impairment, and severe intellectual disability.[37,38] Dhx30 has been implicated in cytoplasmic translational regulation and has been suggested to bind to mRNAs that carry a 3′ UTR CG-rich motif mediating p53-dependent death (CGPD-motif) and decrease their translation.[39]

We observed that Dhx30 co-fractionates with ribosomal subunits, mature 80S ribosomes, and polysomes (Figure 2B). Furthermore, ethylenediaminetetraacetic acid (EDTA)-mediated dissociation of mature 80S ribosomes and polysomes disrupts the Dhx30 co-fractionation profile along the gradient (Figure 2C). Our findings further indicate Dhx30 interaction with the ribosome is mRNA-independent, as Dhx30 still co-fractionates with 80S ribosomes after RNase A treatment (Figure 2D). Knockdown of Dhx30 with small interfering RNA (siRNA) did not significantly change the global protein synthesis rate (Figure 2E). These data support prior literature describing Dhx30 mediation of translation of specific subsets of mRNAs.[39,40]

Dhx30 has two oligonucleotide/oligosaccharide binding (OB)-fold domains, two double-stranded RNA-binding domains (dsRBDs), a core of two helicase domains, and a helicase-associated domain (HA2)[37] (Figure 2F). To test which domain is involved in ribosome interactions, we generated a variety of V5-tagged Dhx30 mutants that harbor either human disease-relevant

(D) Sucrose gradient fractionation and western blotting analysis of Dhx30 after RNase A treatment. The mESC cytoplasmic lysate was treated with (blue) or without (black) RNase A, fractionated, and probed by western blotting as in (B). Rpl4 is a marker for large ribosomal subunit, and Pabp1 is a marker for mRNA-dependent ribosome association. Molecular weight markers are in kDa.

(E) Effect of Dhx30 knockdown on global protein synthesis. Protein synthesis in mESCs was measured by O-propargyl-puromycin (OP-Puro) incorporation. Top: OP-Puro median fluorescence intensity (MFI) between siFluc (a control siRNA) and siDhx30 (siRNA against Dhx30) across four biological replicates. Error bars are ± SEM. Bottom: western blotting of Dhx30 in mESCs treated with siFluc or siDhx30. Actin is a loading control. Molecular weight markers are in kDa.

(F) Illustration of Dhx30 constructs. Oligonucleotide/oligosaccharide binding (OB) fold domain; and double-stranded RNA-binding domains (dsRBDs).

(G) Ribosome association of Dhx30 mutants. mESCs were transfected with V5-tagged Dhx30 mutants, lysed, and subjected to sucrose cushion ultracentrifugation. The lysate, pellet, and supernatant (sup.) were probed by western blotting for the presence of the V5, Rps6, and Gapdh. Top: V5-Dhx30, ΔOB-fold, and R805/8A constructs. Bottom: V5-Dhx30, ΔdsRBD-1, and ΔdsRBD-1/2 constructs. Molecular weight markers are in kDa.

(H) Quantification of the proportion of Dhx30 mutants in the sucrose cushion pellet or supernatant. Three biological replicates of mESCs were transfected with V5-Dhx30, ΔOB-fold, and R805/8A constructs as in (G) and analyzed by western blotting for the presence of Dhx30. Data are plotted as a percentage of the total amount of Dhx30 found in the combined pellet and supernatant fraction. Error bars are ± standard deviation. Significance was calculated using a two-tailed Welch's t test.

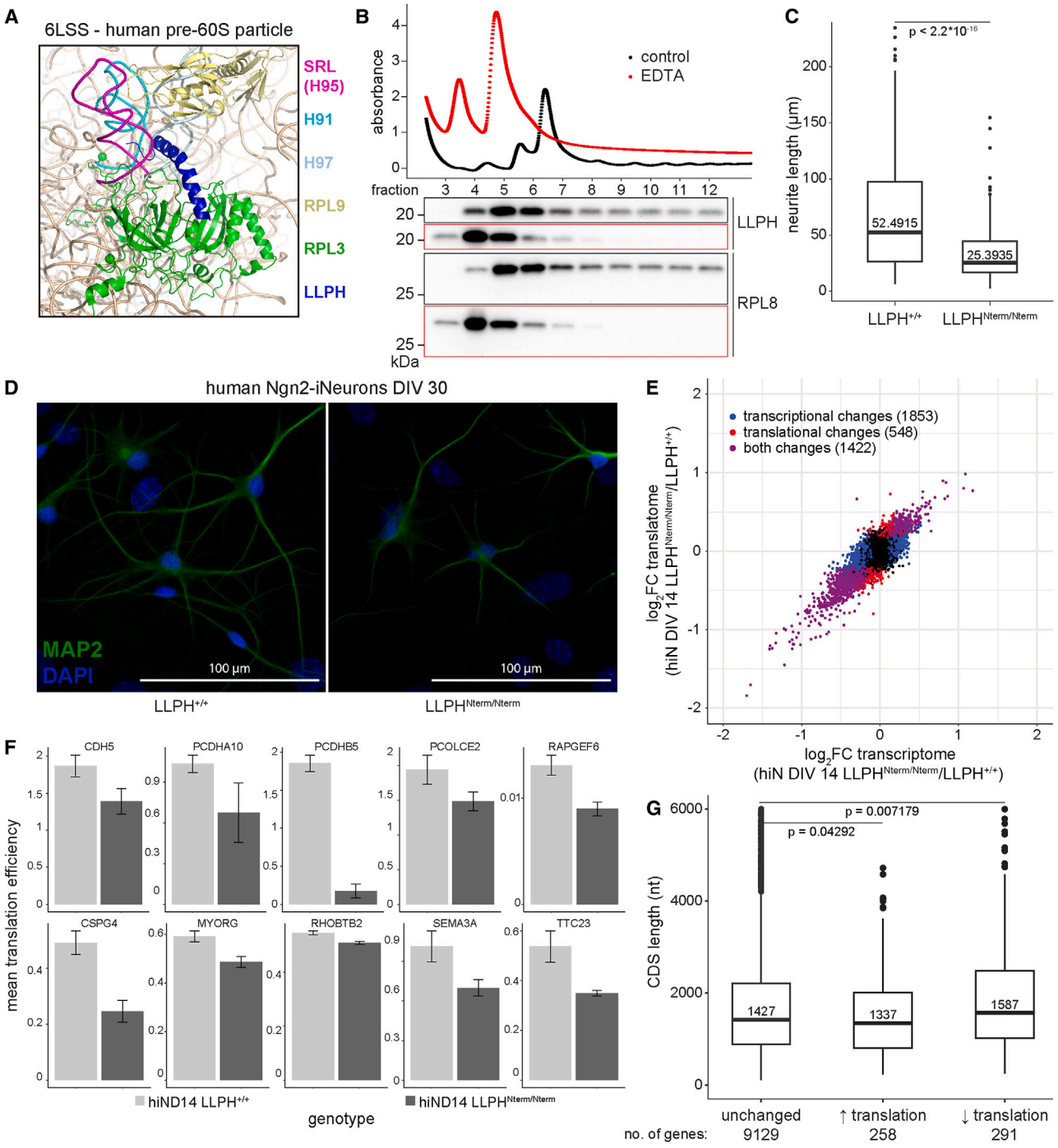


Figure 3. LLPH is a RAP with a role in neurodevelopment

(A) LLPH binding location on the ribosome. Previously published cryo-EM data show LLPH binds near the sarcin-ricin loop (SRL) of the human pre-60S particle (Protein Data Bank ID: 6LSS).[46] Helices 91, 95 (SRL), and 97 as well as RPL9, RPL3, and LLPH are colored.

(B) Sucrose gradient and western blotting analysis of LLPH co-fractionation with ribosomes. P493-6 cell lysate treated with (red) or without (black) EDTA was fractionated, and the proteins from each fraction were precipitated and analyzed by western blotting as in Figure 2B. RPL8 is a marker for large ribosomal subunit-containing fractions. Molecular weight markers are in kDa.

(C) Measurement of traced primary neurite lengths of individual LLPH$^{+/+}$ and LLPH$^{Nterm/Nterm}$ human Ngn2-induced neurons (hiNs) at days *in vitro* (DIV) 30. The median neurite length is displayed. The *p* value was calculated using the Wilcoxon signed-rank test.

(D) Representative fluorescence images of fixed DIV 30 wild-type and LLPH$^{Nterm/Nterm}$ hiNs. Wild-type and LLPH$^{Nterm/Nterm}$ hiNs were fixed and stained with a primary antibody against MAP2 and 4′,6-diamidino-2-phenylindole (DAPI).

(legend continued on next page)

mutations that inactivate helicase activity (R805/8A)[37] or domain truncations (Figure 2F) and transfected them into mESCs. Although the R805/8A mutant expressed at a lower level compared with wild-type Dhx30 and thus may be less stable, we observed that whatever R805/8A protein was expressed was enriched in the pellet compared with the supernatant, which suggests helicase activity is not required for ribosome binding (Figures 2G and 2H). Although the ΔOB-fold mutant also expressed at a lower level and thus may also be less stable, the protein that was present did not associate with the pellet (Figures 2G and 2H), which suggests the ΔOB-fold may play an important role in Dhx30 stability, ribosome association, or both. Additionally, we observed almost complete loss of ribosome association in samples that expressed the ΔdsRBD construct (Figure 2G). Taken together, these data suggest Dhx30 may bind the ribosome through its OB-fold and dsRBDs. These findings thereby identify a bona fide RAP from our RAPIDASH results and begin to delineate the domains of Dhx30 that bind to the ribosome.

LLPH as a RAP is important for neurodevelopment

Our forebrain data also yielded a paradigm class II protein called Llph. The homolog, LAPS18, was first functionally characterized in *Limax marginatus*, where it was suggested to be a secreted protein important for long-term memory formation.[41] By contrast, work studying the *Aplysia kurodai* homolog *Aplysia* LAPS18-like protein (ApLLP) described ApLLP as a nuclear protein enriched in the nucleolus that is important for the switch to long-term facilitation.[42,43] In mice, Llph is highly expressed in the developing mouse brain, but its expression wanes once the pup is born. Further work studying mouse Llph characterized it as a cell-permeable protein that is important for neural development.[44] Our RAPIDASH data suggest Llph may link the ribosome to a critical role in neural development and function.

Recently, cryoelectron microscopy (cryo-EM) structures of the pre-60S particle in yeast[45] and humans[46] have captured the N terminus of LLPH binding to the ribosome at the base of sarcin-ricin loop (Figure 3A), a highly conserved sequence critical for GTP hydrolysis of EF1A and EEF2, which enables proper translocation during protein synthesis.[47,48] Therefore, LLPH may be important for regulating translation elongation.

First, we confirmed LLPH is a RAP. Because LLPH is easier to detect in human samples than mouse samples, we used P493-6 lymphoblastoid cells, which express LLPH at a high level. P493-6 cell lysate was fractionated, and the fractions were probed by western blotting for the presence of LLPH (Figures 3B and S4A). This showed LLPH associates mainly with the 60S subunit but is also present in mature ribosomes and polysomes. Treatment of the lysate with EDTA or RNase A shows that LLPH co-migrates with the 60S subunit (Figures 3B and S4A).

We next established an A549 cell line that expresses LLPH-FLAG when treated with doxycycline. IP of LLPH-FLAG from these cells following doxycycline treatment and analysis by MS revealed LLPH binds to the ribosome. Additional binding partners, which include the elongation factor EEF2; the RAPs PA2G4, SERBP1, and CCDC124; the RTRAF-RTCB-DDX1-FAM98B complex; and the BTF3-NACA complex, hint at a possible role in translational control (Figure S4B; Table S6). For example, EEF2 is involved with ribosome translocation.[49] PA2G4, as stated above, is an RNA-binding protein that binds near the exit tunnel on the 60S subunit that regulates proteostasis[33] and is also involved in growth regulation.[50–52] SERBP1 and CCDC124 bind to hibernating ribosomes and help the recovery of translation.[53] The RTRAF-RTCB-DDX1-FAM98B complex binds to the cap of the mRNA and increases the rate of translation.[54] The BTF3-NACA binds to the nascent polypeptide and prevents non-ER proteins from being trafficked to the ER.[55,56] These data suggest that LLPH may participate in different steps of translational control.

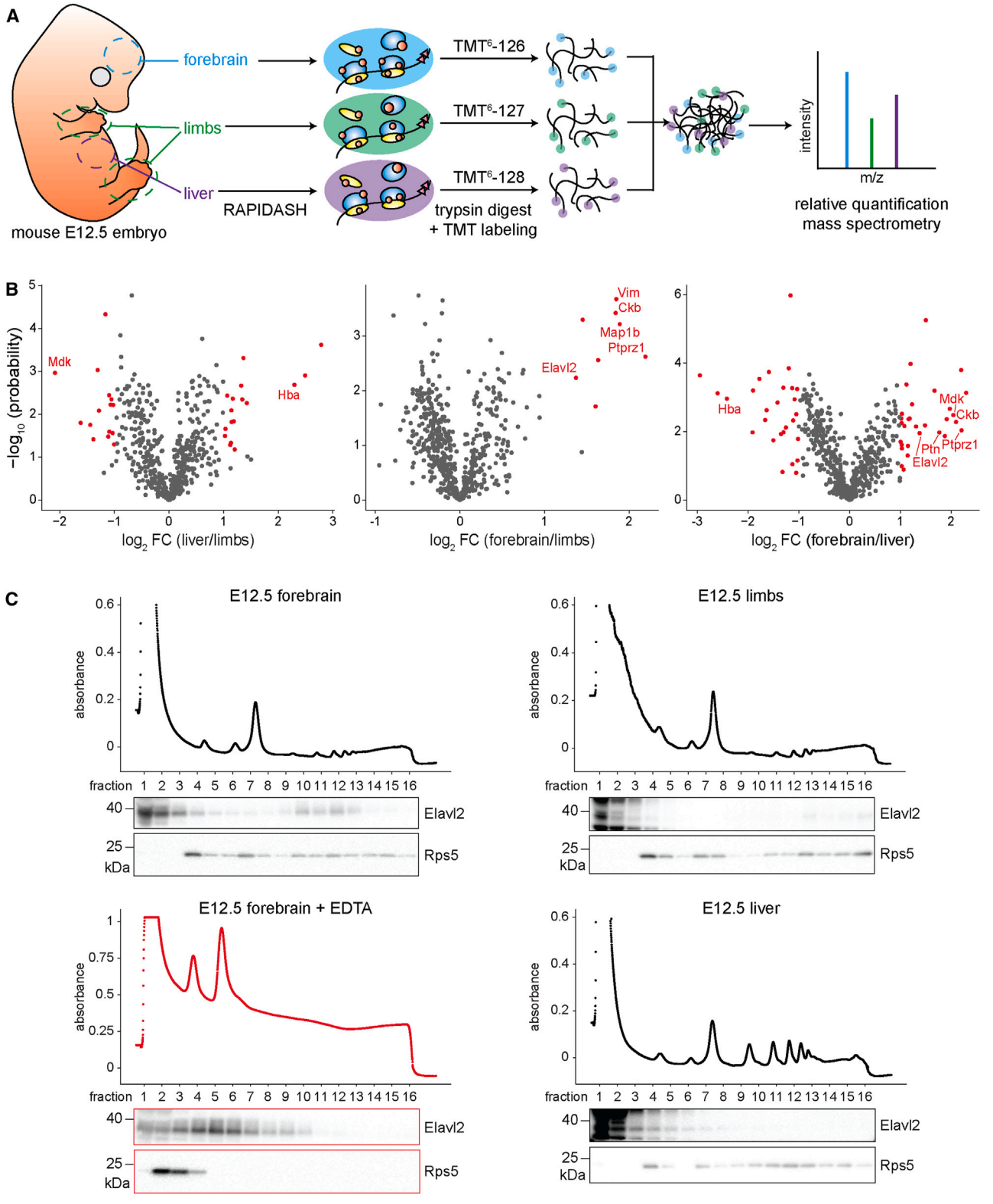
Next, we wanted to directly characterize LLPH's role as a RAP in neurons. CRISPR-Cas9 was used to edit LLPH in H1-hESCs so that only the N-terminal 24 amino acids of LLPH, plus five extra amino acids that were the result of the genomic editing, were expressed ($LLPH^{Nterm/Nterm}$) (Figure S4C). Importantly, $LLPH^{Nterm/Nterm}$ hESCs are indistinguishable from wild-type hESCs in terms of growth (Figure S4D). We differentiated these hESCs into induced neurons (hiNs).[57] Our data reveal LLPH binds to the ribosome in an RNase-independent manner (Figure S4E). We assessed the morphology of the hiNs and observed that $LLPH^{Nterm/Nterm}$ neurons form shorter neurites with fewer secondary and tertiary neurites compared with the wild-type control neurons (Figures 3C and 3D).

We next carried out ribosome profiling at an early stage during differentiation (days *in vitro* [DIV] 14) to determine whether a difference in translation preceded the morphological differences (Figure 3E; Table S7). Genes that were translationally downregulated in $LLPH^{Nterm/Nterm}$ mutant hiNs included those involved with the extracellular matrix (ECM), such as a cadherin and two protocadherins and CDH5, PCDHA10, and PCDH5B; procollagen C-endopeptidase enhancer 2 (PCOLCE2),[58] and the guanine exchange factor RAPGEF6, which has been linked to neuritogenesis[59] (Figure 3F). This is striking because the ECM is important for many aspects of neurodevelopment.[60,61] In addition, several non-ECM genes important for neurodevelopment are also translationally downregulated in the $LLPH^{Nterm/Nterm}$ mutant hINs compared with wild-type hINs, such as CSPG4,[62] MYORG,[63]

(E) Comparison of ribosome sequencing (Ribo-seq) and RNA-seq data for DIV 14 $LLPH^{+/+}$ and $LLPH^{Nterm/Nterm}$ hiNs (n = 3 biological replicates). Blue genes significantly change (Benjamini-Hochberg procedure false discovery rate [FDR] < 0.1 and absolute fold change [FC] ≥ 2) in mRNA abundance only; red genes change in ribosome occupancy only; purple genes change in mRNA abundance and ribosome occupancy.

(F) Representative genes with lower mean translation efficiency differences in $LLPH^{Nterm/Nterm}$ versus $LLPH^{+/+}$ hiNs. Top: representative genes with downregulated translation efficiency in $LLPH^{Nterm/Nterm}$ compared with $LLPH^{+/+}$ that are involved in building the extracellular matrix. Bottom: representative genes known to be linked to neurodevelopmental defects.

(G) Boxplots of coding sequence (CDS) length for genes that are translationally upregulated, downregulated, or unchanged when comparing $LLPH^{Nterm/Nterm}$ and $LLPH^{+/+}$ hiNs. Significance was calculated using the Mann-Whitney U test. The median CDS lengths are displayed. Only genes with CDS lengths shorter than 6,000 nucleotides are displayed; the full plot is shown in Figure S4F.



(legend on next page)

RHOBTB2,[64,65] SEMA3A,[66] and TTC23[67,68] (Figure 3F). These may help explain why LLPH$^{Nterm/Nterm}$ hiNs fail to produce neurites of the same length as wild-type hiNs.

Finally, because the binding site of LLPH on the ribosome suggests a role in regulating elongation, we asked whether genes that are translationally downregulated in LLPH$^{Nterm/Nterm}$ hiNs have any correlation with length since elongation rate is known to be negatively correlated with coding sequence length.[69] We strikingly found translationally downregulated genes are enriched for those with longer coding sequences compared with those that show no change in translation when comparing LLPH$^{Nterm/Nterm}$ and wild-type LLPH hiNs, which suggests LLPH may have a role in promoting elongation (Figures 3G and S4F). This is intriguing in the context of neurons because neuronal genes can have long coding sequences. Since coding sequence length also negatively correlates with translation fidelity,[70] regulation of elongation may be crucial to faithfully translate neuronal genes.

Identification and characterization of tissue-specific RAPs in developing mouse embryo

We next asked whether RAPs change across embryonic tissues, specifically E12.5 limbs, forebrain, and liver, by using TMT-MS (Figure 4A).

We detected 566 proteins across all four replicates of three tissues (Table S8). Proteins that had FC $\geq$ 2 or a false discovery rate (FDR) < 0.1 when comparing one tissue to another were considered enriched in a particular tissue. Comparing forebrain and limb samples to liver samples yielded more proteins that passed the significance cutoffs than for forebrain versus limb samples (Figure 4B). This might be due to the more homogeneous cell composition in liver tissue compared with the other tissues, which highlights the inter-tissue differences. Hemoglobin subunit alpha (Hba) was shown to be enriched in the liver as a RAP compared with the other two tissues, which hints at a previously described role for the ribosome's role in heme bioavailability regulation.[71] Hkdc1, a kinase that phosphorylates hexose to hexose-6-phosphate in glycolysis, is enriched as a RAP in the liver relative to the other two tissues. This finding is reminiscent of how Pkm, another metabolic kinase, was shown to directly interact with ER ribosomes and regulate translation of specific mRNAs.[5]

The forebrain and limbs had very few RAPs that were differentially enriched; all RAPs that were differentially enriched between these two tissues were enriched in the forebrain relative to the limbs. Creatine kinase b (Ckb), a kinase important for energy transduction in energy-intensive tissues (e.g., muscle, heart, and brain),[72] is enriched as a RAP in the forebrain over both the liver and limbs. Vimentin is an intermediate filament protein that is crucial for spatially organizing organelles within cells, and it has been implicated in cell adhesion,[73,74] cell migration,[74] and neural development. It has also been observed to bind to ribosomes *in vitro*, which suggests vimentin may help anchor ribosomes in the complex spatial architecture of neurons.[75]

Strikingly, we also identified the secreted growth factors midkine (Mdk) and pleiotrophin (Ptn) as putative RAPs across all three tissues, although they were both enriched in the forebrain relative to the liver (Figure 4B). Their receptor is a brain-specific transmembrane protein tyrosine phosphatase Ptprz1,[76] which was also found to be a forebrain-enriched RAP. All three of these proteins are involved in neural development. It is tempting to speculate that the ribosome is a substrate for Ptprz1, and the binding of the ligands Mdk or Ptn may modulate phosphatase activity on the ribosome and initiate a translational program that is important for neural development.

Finally, Elavl2 is an RNA-binding protein that is a forebrain-enriched RAP compared with both liver and limbs. Elavl2 is a paradigm class I protein; although it is an RNA-binding protein that has been suggested to be a translation repressor in ovaries,[77] it is possible that in these embryonic tissues, Elavl2 is also a direct ribosome binder. Elavl2 was more enriched in the ribosome fractions in the forebrain compared with other tissues (Figure 4C), which suggests its role on the ribosome may be important for brain development. Taken together, RAPIDASH has revealed hundreds of potential RAPs in embryonic tissues that may play a role in tissue-specific functions.

RAPIDASH reveals dynamic ribosome composition remodeling during macrophage stimulation

Finally, we leveraged RAPIDASH to understand how an acute stimulus could temporally remodel ribosome complexes within a given cell type. Mechanistically, macrophages sense the presence of bacterial and viral pathogens via germline-encoded pattern recognition receptors.[78] For example, Toll-like receptor 4 (TLR4) senses invasion by gram-negative bacteria via binding to their outer cell membrane component lipopolysaccharide (LPS). At the same time, TLR3 alerts the macrophage to potential viral infection via binding to double-stranded RNA.

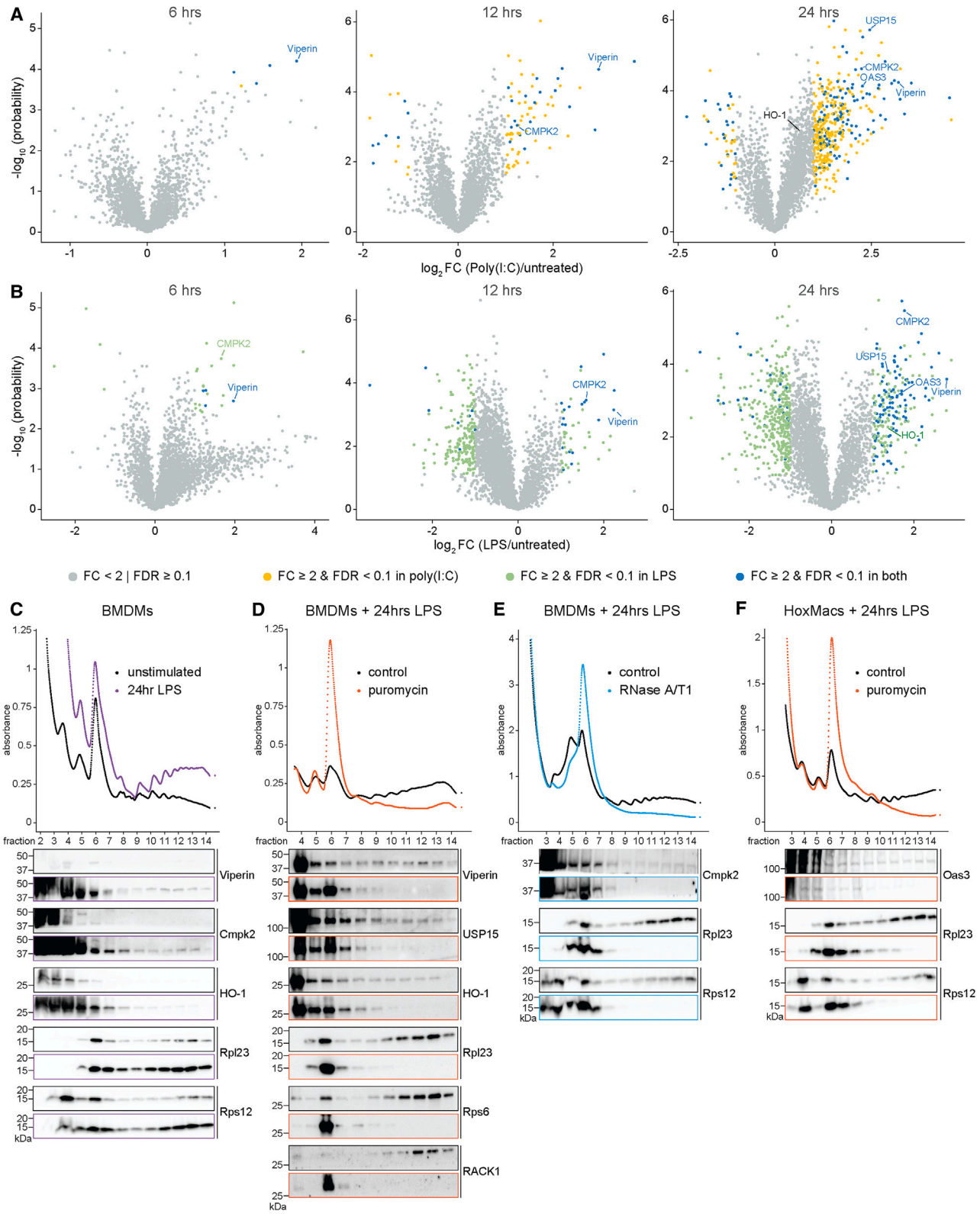
RAPIDASH in unstimulated primary murine bone marrow-derived macrophages (BMDMs) identified a total of 1,240 proteins with at least one peptide in each of three replicates (Table S9, column O = 1). As expected, GO term analysis showed strong enrichment for ribosome- and translation-related processes (Figure S5A). RPs were highly enriched: 32 of 33 small (97%) and 41 of 47 large (87%) ribosomal subunit proteins detected were present in the top 15% most abundant proteins. The top 15% proteins also included subunits of the translation

Figure 4. Characterization of tissue-specific RAPs in E12.5 mouse embryos

(A) Schematic of the strategy to quantify tissue-specific RAPs by TMT mass spectrometry. Four biological replicates of forebrain, limb, and liver tissues from mouse embryos underwent RAPIDASH. Peptides derived from the enriched proteins were labeled with TMT reagents and analyzed by LC-MS/MS.

(B) Volcano plots comparing RAPs identified in different tissues. Putative RAPs identified in: liver to limbs (left), forebrain to limbs (center), forebrain to liver (right) are shown using volcano plots graphing $-\log_{10}(p \text{ value})$ against $\log_2$(FC). Proteins present in at least three out of four biological replicates with absolute $\log_2$FC $\geq$ 1 and FDR < 0.10 are defined as significantly differentially enriched (red). Significance was calculated using a paired Welch's t test.

(C) Characterization of Elavl2 as a forebrain-enriched RAP. E12.5 mouse embryonic forebrain, limb, and liver tissues were lysed, treated with (red line) or without (black lines) EDTA, and separated by sucrose gradient fractionation. The proteins from each fraction were precipitated and analyzed by western blotting for the presence of Elavl2 or Rps5, a marker for the ribosome. Lanes were normalized by equal volume of samples. Molecular weight markers are in kDa.



(legend on next page)

initiation factors eIF2, eIF3, and eIF5; the elongation factor EEF2; and the known RAP PA2G4.

We next performed TMT-MS on RAPIDASH samples from BMDMs 0, 2, 6, 12, and 24 h post-activation by the TLR3 agonist polyinosinic-polycytidylic acid (poly(I:C)). We found that ribosome complexes were gradually remodeled over time (Figure 5A; Table S10). By 24 h post-stimulation, 410 proteins were enriched 2-fold, and 50 proteins were de-enriched 2-fold compared with ribosome complexes in resting BMDMs. These included the interferon (IFN)-induced protein with tetratricopeptide (IFIT) repeats proteins IFIT1, IFIT2, and IFIT3, which inhibit translation of viral transcripts[79]; the ubiquitin-like protein ISG15, which is co-translationally ligated onto viral proteins thus interfering with their function[80]; and the E3 ubiquitin ligase for ISG15, Herc6.[81,82] We also identified the deubiquitylase USP15, which associates with polysomes and may stabilize newly synthesized (viral) proteins,[83,84] and the prolyl hydroxylase P4HA1, which has been demonstrated to co-translationally modify proline residues of flavivirus proteins.[85] Among the 59 proteins "ejected" from ribosome complexes upon TLR3 stimulation, we identified PDCD4, which, as we noted above, is a known ribosome-interacting translational inhibitor.[86] We also identified HMGB1, HMGB2, and HMGB3 proteins; HMGB2 in particular has recently been implicated in ribosome biogenesis[87] and has been identified as a putative RAP.[88] The function of this family of proteins on resting ribosome complexes remains to be explored.

Intriguingly, among RAPs that were highly enriched in TLR3-stimulated macrophages, we identified multiple cytoplasmic RNA sensors, such as members of the 2′,5′-oligoadenylate synthetase (OAS) family that are known to regulate translation in the context of viral infection but have not been previously identified as RAPs. It is tempting to speculate that these findings indicate a mode of on-ribosome sensing of immunostimulatory viral RNAs (which may, for example, provide a mechanism of selectively degrading "infected" ribosomes via local RNase L activation). Indeed, published work has confirmed the ability of one sensor, retinoic-acid inducible gene I (RIG-I), to localize to ribosomes via binding to an rRNA ES.[89]

In addition to RNA sensors, we identified several other IFN-stimulated RAPs in TLR3-activated macrophages. Among them, Viperin (encoded by the gene *Rsad2*) and CMPK2 have both recently been implicated in translational regulation.[90,91] Mechanistically, these proteins have been proposed to inhibit viral translation via induction of ribosome collisions. Strikingly, stimulation of BMDMs with LPS for 0, 2, 6, 12, and 24 h showed an overall remarkably similar effect on ribosome complexes as did activation with poly(I:C) (Figures 5B and S5B; Table S11). Of the 206 proteins enriched 2-fold 24 h after LPS stimulation, 111 were also 2-fold enriched, and an additional 20 were 1.5-fold enriched following 24 h of poly(I:C) stimulation. This similarity in ribosome remodeling may be because TLR3 and TLR4 signal through a shared downstream adapter protein, TIR (Toll/interleukin-1 [IL-1] receptor)-domain-containing adapter-inducing interferon-β (TRIF). The greater number of highly enriched RAPs identified following poly(I:C) stimulation (395) compared with LPS stimulation (198) may reflect the more robust TRIF-dependent signaling and IFN induction that occurs downstream of TLR3 ligation.

We confirmed several hits common to TLR3- and TLR4-stimulated macrophages as bona fide RAPs (Figures 5C–5F). Lastly, we did identify several intriguing RAPs that were selectively enriched following LPS treatment. These included the proteins caspase recruitment domain-containing protein 9 (CARD9 and SON DNA-binding protein (SON), which have known roles in immune defense[92,93] and been putatively identified as RAPs.[88]

Therefore, RAPIDASH has enabled the characterization of dynamic changes to ribosomes upon macrophage stimulation.

DISCUSSION

RAPIDASH can characterize RAPs in different sample types

We have developed a method called RAPIDASH that can enrich ribosomes and RAPs. The specificity of RAPIDASH is largely due to the cysteine-charged sulfolink resin chromatography step. Although the cysteine-charged sulfolink resin preferentially binds to rRNA compared with poly(A) RNA, the mechanism by which this specificity is achieved is unclear and could potentially be due to an affinity for structured RNA or RNA modifications that are present in rRNA.

Compared with Ribo-FLAG IP, RAPIDASH can be used on any sample, requires less input material, and has better coverage. We believe RAPIDASH can be used for many other cell types, tissues, organisms, and dynamic conditions, including clinical settings and non-model organisms. RAPIDASH is capable of processing low-input samples. Based on our proteomic data, a single E12.5 limb bud should yield on average about 350 ng of RAPs. In addition, while RAPIDASH can generate a decent-quality list of candidate RAPs, it is important to validate that these proteins are true hits, for example, by sucrose gradient fractionation of samples treated with EDTA.

Implications of RAPs with tissue-specific functions and RAPs during immune activation

Our findings in tissues suggest that RAPs may enable the ribosome to coordinate tissue-specific functions. For example, the helicase function of Dhx30 may regulate the translational specificity of the ribosome in neurons by denaturing secondary structures of select mRNAs. It would be interesting to identify the

Figure 5. RAPIDASH identifies RAPs in macrophages following Toll-like receptor (TLR) stimulation

(A and B) Volcano plots of murine bone marrow-derived macrophages (BMDMs) stimulated with lipopolysaccharide (LPS) (A) or polyinosinic-polycytidylic acid (poly(I:C)) (B) for 6, 12, or 24 h prior to isolation of ribosome complexes for TMT-MS analysis. The x axes show the $\log_2$FC of ribosome complex composition in activated versus unstimulated macrophages at 6 (left), 12 (middle), and 24 h (right). Significance was calculated using Student's t test.

(C–F) Characterization of candidate RAPs in unstimulated or stimulated BMDMs. Lysates from unstimulated or LPS-stimulated BMDMs (C–E) or macrophages differentiated from HoxB8-immortalized progenitor cells (F) were subjected to sucrose gradient. Total protein was extracted from individual fractions and subjected to western blot analysis for the indicated proteins. Lanes were loaded with equal volumes of precipitated protein. Puromycin and RNase treatments were performed as described in the STAR Methods section. Molecular weight markers are in kDa.

Table 1. Information for samples prepared for relative quantification by TMT MS. Each TMT replicate constitutes a single injection of the mixed protein samples.

TMT replicate	protein sample	amount of protein (μg)	TMT tag
RAPIDASH eluate vs. sucrose cushion pellet in mESCs, rep 1	sucrose cushion pellet	25	130
	RAPIDASH eluate	25	131
RAPIDASH eluate vs. sucrose cushion pellet in mESCs, rep 2	sucrose cushion pellet	25	130
	RAPIDASH eluate	25	131
RAPIDASH eluate vs. sucrose cushion pellet in mESCs, rep 3	sucrose cushion pellet	25	130
	RAPIDASH eluate	25	131
E12.5 mouse embryonic tissues, rep 1	limbs	15	126
	forebrain	15	127
	liver	15	128
E12.5 mouse embryonic tissues, rep 2	limbs	25	126
	forebrain	25	127
	liver	25	128
E12.5 mouse embryonic tissues, rep 3	limbs	13	126
	forebrain	13	127
	liver	13	128
E12.5 mouse embryonic tissues, rep 4	limbs	25	126
	forebrain	25	127
	liver	25	128

targets of Dhx30 and how their translational efficiency changes if Dhx30 carries the same mutations as in patients. Our data suggest LLPH may enable the proficient translation of neural developmental genes with long coding sequences, including those that are required for neurite outgrowth, which reveals a potential RAP-mediated mechanism for neural translation.

We have also identified various RAPs that could play a tissue-specific role in normal mouse development. Elavl2 is capable of binding both ribosome and mRNA; it remains to be seen precisely how this impacts translation of Elavl2 binding targets. Interestingly, we see cytoskeleton-related components such as Vimentin and Map1b being enriched in the forebrain. Other cytoskeletal components have previously been found to be associated with ribosomes, which hints at possible roles in localized translation.[94–97] Map1b has been shown to play a role in microtubule remodeling critical for axonal outgrowth.[98] Possibly, ribosomes are recruited alongside Map1b to distal growth cones, or facilitate central sprouting and peripheral regeneration of neurons.[98–100] Additionally, the identification of Ckb and Ptprz1, a kinase and phosphatase, respectively, as potential RAPs suggests they enable rapid translational responses to cell signals. Finally, we have applied RAPIDASH to stimulated macrophages over time and observed extensive changes in ribosome composition. These data suggest that pathogen detection leads to a translational rewiring to help macrophages overcome infection. Notably, activation of TLR3 and TLR4 leads to overlapping changes in ribosome composition, which suggests the usage of common mechanisms of translational control despite distinctions in inflammatory contexts.

Outlook

Thus, RAPIDASH has revealed a dynamic and diverse layer of ribosome composition that is important for tissue-specific functions and responses to acute stimuli, such as in macrophages and cancer cells. In the future, RAPIDASH can be used to characterize ribosome composition in a variety of samples to characterize how the ribosome acts as a cell signal integrator to regulate gene expression in health and disease.

Limitations of the study

While RAPIDASH is a versatile technique that can analyze ribosome composition across different cells, tissues, and organisms, there are some limitations. First, every protein identified by RAPIDASH is a candidate RAP. The cutoffs applied to the proteomic data in this manuscript were arbitrarily chosen and are fairly stringent; thus, there may be biologically relevant RAPs that fall below these cutoffs. Moreover, as stated above, every candidate RAP must be validated by orthogonal techniques, such as sucrose gradient fractionation experiments. Second, the lower limit of input required for MS-based proteomic analysis of RAPIDASH eluate has not been fully characterized and may present a barrier for certain sample types where the amount of input is extremely limiting. Finally, RAPs identified by RAPIDASH may not be exclusively localized to the ribosome, so it is important to carefully dissect a protein's function on the ribosome versus other extra-ribosomal functions.

RESOURCE AVAILABILITY

Lead contact

Requests for further information, resources, and reagents should be directed to the lead contact, Maria Barna (mbarna@stanford.edu).

Materials availability

Unique materials generated in this study will be available upon request.

Data and code availability

- Proteomic data have been deposited to the ProteomeXchange Consortium via the PRIDE[101] partner repository with these dataset identifiers: PRIDE: PXD054427 (TMT MS RAPIDASH and ribosome chromatographic purification [Meskauskas et al.[18]]) of E14 mESCs), PRIDE: PXD054298 (TMT MS RAPIDASH and sucrose cushion of E14 mESCs), PRIDE: PXD054300 (label-free MS RAPIDASH of Rpl36-FLAG and Rps17-FLAG E14 mESCs), PRIDE: PXD055144 (TMT MS RAPIDASH of PC3 cells), PRIDE: PXD054303 (label-free MS RAPIDASH of E12.5 mouse forebrain), PRIDE: PXD055152 (label-free MS of LLPH-FLAG IP of 293T cells), PRIDE: PXD054304 (TMT MS RAPIDASH of E12.5 mouse limbs, forebrain, and liver), PRIDE: PXD055154 (label-free MS RAPIDASH of mouse macrophages), and PRIDE: PXD055155 (TMT MS RAPIDASH of mouse macrophages). Sequencing data have been deposited to the Gene Expression Omnibus (GEO) with these identifiers: GEO: GSE274178 (RNA-seq of poly(A)-enriched RNA comparing sucrose cushion ultracentrifugation and RAPIDASH samples) and GEO: GSE274188 (ribosome profiling of hiNs).
- Original code has been deposited on GitHub/Zenodo at the following DOI: https://zenodo.org/doi/10.5281/zenodo.13286233.
- Any additional information required to reanalyze the data reported in this paper is available from the lead contact upon request.

ACKNOWLEDGMENTS

This work was funded by National Institute of Health (NIH) grants 5R21MH130323 and 5R01HD086634 (to M.B.), R38 HL143581 and K38 HL165490 (to A.G.L.), and R35CA242986 (to D.R.). D.R. was also supported by the American Cancer Society (Research Professor Award). MS for the LLPH-FLAG IP-MS experiment and for macrophages was provided by the Mass Spectrometry Resource at UCSF (A.L.B., Director) supported by the Dr. Miriam and Sheldon G. Adelson Medical Research Foundation (AMRF) and the UCSF Program for Breakthrough Biomedical Research (PBBR). T.T.S. was supported by a National Science Scholarship (PhD) from the Agency for Science, Technology, and Research. V.H. was the Fraternal Order of Eagles Fellow of the Damon Runyon Cancer Research Foundation (DRG 2314-17) and was also supported by the Katharine McCormick Advanced Postdoctoral Fellowship. C.H.K. was supported by a Stanford Dean's Fellowship and a Canadian Institutes of Health Research Postdoctoral Fellowship. Y.Y. was supported by the New York Stem Cell Foundation Druckenmiller Fellowship (NYSCF-D-F74). Y.C. was supported by a Stanford Dean's Fellowship. L.F. was supported by an EMBO Long-Term Fellowship. K.F. was supported by the Uehara Memorial Foundation and Human Frontier Science Program Fellowship. We thank H.D. Rosenblatt and Y. Bai for assistance with some experiments.

AUTHOR CONTRIBUTIONS

T.T.S., V.H., K.F., and M.B. developed the RAPIDASH technique. T.T.S., V.H., and Y.C. characterized the chromatography step. T.T.S. and V.H. performed the proteomic characterization and analysis of mESCs and embryonic tissues. C.H.K., V.H., and Y.C. performed the characterization of Dhx30. L.F. characterized RAP changes upon Rapalink-1 treatment in PC3 cells and LLPH in P493-6 and A549 cells. Y.Y. and M.W. aided in the design of the experiments in hiNs. T.T.S. performed the characterization of LLPH in hESCs and hiNs. T.C.L. and Z.Z. helped with additional experiments. A.G.L. and D.R. designed the macrophage experiments. A.G.L. performed the macrophage experiments. J.A.O.-P. and A.L.B. performed the MS and analysis of the PC3 data, the LLPH IP-MS data, and the macrophage data. T.T.S., V.H., A.G.L., J.A.O.-P., D.R., and M.B. wrote the paper with input from the other authors.

DECLARATION OF INTERESTS

The authors declare no competing interests.

STAR★METHODS

Detailed methods are provided in the online version of this paper and include the following:

- KEY RESOURCES TABLE
- EXPERIMENTAL MODEL AND STUDY PARTICIPANT DETAILS
  - Mice
  - Cells
- METHOD DETAILS
  - Western blotting for mESCs, human cells, and mouse embryonic tissues
  - Characterization of cysteine-charged sulfolink resin
  - Characterization of cysteine-charged sulfolink resin binding using 80S ribosomes from samples treated with puromycin, RNase A, or high salt
  - RAPIDASH for E14 mouse embryonic stem cells
  - Sucrose gradient fractionation for RAPIDASH characterization
  - RNA-seq analysis of cysteine-charged resin input and eluate samples
  - RNA-seq analysis
  - SYPRO Ruby for mESCs
  - Mass spectrometry of unlabeled tryptic digests
  - RAPIDASH and proteomic analysis of ribosomal complexes for PC3 cells
  - RAPIDASH for E12.5 tissues
  - TMT mass spectrometry
  - Mass spectrometry data analysis
  - Sucrose gradient fractionation of mESC lysates and subsequent western blotting
  - siRNA-mediated knockdown and OP-puromycin labeling
  - Transfection of Dhx30 mutant constructs, sucrose cushion ultracentrifugation, and western blotting
  - Sucrose gradient fractionation of P493-6 cells
  - H1-hESC cell culture and CRISPR
  - Lentivirus production
  - Generation of human induced neurons from H1-hESC with Ngn2 overexpression
  - Sucrose gradient fractionation of human induced neurons treated with or without RNase A and subsequent western blotting
  - Human induced neurons morphology analysis
  - LLPH-Flag immunoprecipitation
  - Cell viability assay
  - Ribosome profiling on human induced neurons
  - Ribosome profiling analysis
  - Sucrose Gradient Fractionation for mouse E12.5 tissues
  - RAPIDASH on macrophages
  - Proteomic analysis of ribosomal complexes in macrophages
  - Sucrose gradient fractionation experiments for macrophages
  - Western blotting for macrophage gradient fractions
- QUANTIFICATION AND STATISTICAL ANALYSIS

SUPPLEMENTAL INFORMATION

Supplemental information can be found online at https://doi.org/10.1016/j.molcel.2024.08.023.

Received: December 8, 2023
Revised: June 25, 2024
Accepted: August 20, 2024
Published: September 10, 2024

REFERENCES

1. Fujii, K., Susanto, T.T., Saurabh, S., and Barna, M. (2018). Decoding the function of expansion segments in ribosomes. Mol. Cell *72*, 1013–1020.e6. https://doi.org/10.1016/j.molcel.2018.11.023.

2. Darnell, J.C., Van Driesche, S.J., Zhang, C., Hung, K.Y.S., Mele, A., Fraser, C.E., Stone, E.F., Chen, C., Fak, J.J., Chi, S.W., et al. (2011). FMRP stalls ribosomal translocation on mRNAs linked to synaptic function and autism. Cell *146*, 247–261. https://doi.org/10.1016/j.cell.2011.06.013.

3. Ishizuka, A., Siomi, M.C., and Siomi, H. (2002). A Drosophila fragile X protein interacts with components of RNAi and ribosomal proteins. Genes Dev. *16*, 2497–2508. https://doi.org/10.1101/gad.1022002.

4. Chen, E., Sharma, M.R., Shi, X., Agrawal, R.K., and Joseph, S. (2014). Fragile X mental retardation protein regulates translation by binding directly to the ribosome. Mol. Cell *54*, 407–417. https://doi.org/10.1016/j.molcel.2014.03.023.

5. Simsek, D., Tiu, G.C., Flynn, R.A., Byeon, G.W., Leppek, K., Xu, A.F., Chang, H.Y., and Barna, M. (2017). The mammalian ribo-interactome reveals ribosome functional diversity and heterogeneity. Cell *169*, 1051–1065.e18. https://doi.org/10.1016/j.cell.2017.05.022.

6. Kejiou, N.S., Ilan, L., Aigner, S., Luo, E., Tonn, T., Ozadam, H., Lee, M., Cole, G.B., Rabano, I., Rajakulendran, N., et al. (2023). Pyruvate kinase M (PKM) binds ribosomes in a poly-ADP ribosylation dependent manner to induce translational stalling. Nucleic Acids Res. *51*, 6461–6478. https://doi.org/10.1093/nar/gkad440.

7. Bartsch, D., Kalamkar, K., Ahuja, G., Lackmann, J.-W., Hescheler, J., Weber, T., Bazzi, H., Clamer, M., Mendjan, S., Papantonis, A., et al. (2023). mRNA translational specialization by RBPMS presets the competence for cardiac commitment in hESCs. Sci. Adv. *9*, eade1792. https://doi.org/10.1126/sciadv.ade1792.

8. Wang, L., Xu, Y., Rogers, H., Saidi, L., Noguchi, C.T., Li, H., Yewdell, J.W., Guydosh, N.R., and Ye, Y. (2020). UFMylation of RPL26 links translocation-associated quality control to endoplasmic reticulum protein homeostasis. Cell Res. *30*, 5–20. https://doi.org/10.1038/s41422-019-0236-6.

9. Imami, K., Milek, M., Bogdanow, B., Yasuda, T., Kastelic, N., Zauber, H., Ishihama, Y., Landthaler, M., and Selbach, M. (2018). Phosphorylation of the ribosomal protein RPL12/uL11 affects translation during mitosis. Mol. Cell *72*, 84–98.e9. https://doi.org/10.1016/j.molcel.2018.08.019.

10. Haneke, K., Schott, J., Lindner, D., Hollensen, A.K., Damgaard, C.K., Mongis, C., Knop, M., Palm, W., Ruggieri, A., and Stoecklin, G. (2020). CDK1 couples proliferation with protein synthesis. J. Cell Biol. *219*, e201906147. https://doi.org/10.1083/jcb.201906147.

11. Makhlouf, L., Peter, J.J., Magnussen, H.M., Thakur, R., Millrine, D., Minshull, T.C., Harrison, G., Varghese, J., Lamoliatte, F., Foglizzo, M., et al. (2024). The UFM1 E3 ligase recognizes and releases 60S ribosomes from ER translocons. Nature *627*, 437–444. https://doi.org/10.1038/s41586-024-07093-w.

12. DaRosa, P.A., Penchev, I., Gumbin, S.C., Scavone, F., Wąchalska, M., Paulo, J.A., Ordureau, A., Peter, J.J., Kulathu, Y., Harper, J.W., et al. (2024). UFM1 E3 ligase promotes recycling of 60S ribosomal subunits from the ER. Nature *627*, 445–452. https://doi.org/10.1038/s41586-024-07073-0.

13. Mehta, P., Woo, P., Venkataraman, K., and Karzai, A.W. (2012). Ribosome purification approaches for studying interactions of regulatory proteins and RNAs with the ribosome. Methods Mol. Biol. *905*, 273–289. https://doi.org/10.1007/978-1-61779-949-5_18.

14. Britten, R.J., and Roberts, R.B. (1960). High-resolution density gradient sedimentation analysis. Science *131*, 32–33. https://doi.org/10.1126/science.131.3392.32.

15. Yoshikawa, H., Larance, M., Harney, D.J., Sundaramoorthy, R., Ly, T., Owen-Hughes, T., and Lamond, A.I. (2018). Efficient analysis of mammalian polysomes in cells and tissues using Ribo Mega-SEC. eLife *7*, e36530. https://doi.org/10.7554/eLife.36530.

16. Tassy, O., and Pourquié, O. (2014). Manteia, a predictive data mining system for vertebrate genes and its applications to human genetic diseases. Nucleic Acids Res. *42*, D882–D891. https://doi.org/10.1093/nar/gkt807.

17. Maguire, B.A., Wondrack, L.M., Contillo, L.G., and Xu, Z. (2008). A novel chromatography system to isolate active ribosomes from pathogenic bacteria. RNA *14*, 188–195. https://doi.org/10.1261/rna.692408.

18. Meskauskas, A., Leshin, J.A., and Dinman, J.D. (2011). Chromatographic purification of highly active yeast ribosomes. J. Vis. Exp. *3214*. https://doi.org/10.3791/3214.

19. Loring, H.S., Carpenter, F.H., and Roll, P.M. (1947). The hydrolysis of yeast ribonucleic acid by ribonucleinase; the extend of hydrolysis and the preparation on ribonucleinase-resistant fractions after ribonucleinase treatment. J. Biol. Chem. *169*, 601–608. https://doi.org/10.1016/S0021-9258(17)30877-3.

20. Schmidt, G., Cubiles, R., Swartz, B.H., and Thannhauser, S.J. (1947). The action of ribonucleinase on yeast nucleic acid. J. Biol. Chem. *170*, 759–760. https://doi.org/10.1016/S0021-9258(17)30859-1.

21. Brown, D.M., and Todd, A.R. (1952). 13. Nucleotides. Part X. Some observations on the structure and chemical behaviour of the nucleic acids. J. Chem. Soc. 52–58. https://doi.org/10.1039/JR9520000052.

22. Stöcklein, W., and Piepersberg, W. (1980). Binding of cycloheximide to ribosomes from wild-type and mutant strains of Saccharomyces cerevisiae. Antimicrob. Agents Chemother. *18*, 863–867. https://doi.org/10.1128/AAC.18.6.863.

23. Vetro, J.A., and Chang, Y.-H. (2002). Yeast methionine aminopeptidase type 1 is ribosome-associated and requires its N-terminal zinc finger domain for normal function in vivo. J. Cell. Biochem. *85*, 678–688. https://doi.org/10.1002/jcb.10161.

24. Gamerdinger, M., Jia, M., Schloemer, R., Rabl, L., Jaskolowski, M., Khakzar, K.M., Ulusoy, Z., Wallisch, A., Jomaa, A., Hunaeus, G., et al. (2023). NAC controls cotranslational N-terminal methionine excision in eukaryotes. Science *380*, 1238–1243. https://doi.org/10.1126/science.adg3297.

25. Ganesan, R., Mangkalaphiban, K., Baker, R.E., He, F., and Jacobson, A. (2022). Ribosome-bound Upf1 forms distinct 80S complexes and conducts mRNA surveillance. RNA *28*, 1621–1642. https://doi.org/10.1261/rna.079416.122.

26. Bern, M., Kil, Y.J., and Becker, C. (2012). Byonic: advanced peptide and protein identification software. Curr. Protoc. Bioinformatics *20*, 13.20.1–13.20.14. https://doi.org/10.1002/0471250953.bi1320s40.

27. Choi, H., Liu, G., Mellacheruvu, D., Tyers, M., Gingras, A.-C., and Nesvizhskii, A.I. (2012). Analyzing Protein-Protein Interactions from Affinity Purification-Mass Spectrometry Data with SAINT. CP in Bioinformatics *39*, 8.15.1–8.15.23. https://doi.org/10.1002/0471250953.bi0815s39.

28. Cox, J., and Mann, M. (2008). MaxQuant enables high peptide identification rates, individualized p.p.b.-range mass accuracies and proteome-wide protein quantification. Nat. Biotechnol. *26*, 1367–1372. https://doi.org/10.1038/nbt.1511.

29. Tyanova, S., Temu, T., Sinitcyn, P., Carlson, A., Hein, M.Y., Geiger, T., Mann, M., and Cox, J. (2016). The Perseus computational platform for comprehensive analysis of (prote)omics data. Nat. Methods *13*, 731–740. https://doi.org/10.1038/nmeth.3901.

30. Hsieh, A.C., Liu, Y., Edlind, M.P., Ingolia, N.T., Janes, M.R., Sher, A., Shi, E.Y., Stumpf, C.R., Christensen, C., Bonham, M.J., et al. (2012). The translational landscape of mTOR signalling steers cancer initiation and metastasis. Nature *485*, 55–61. https://doi.org/10.1038/nature10912.

31. Thoreen, C.C., Chantranupong, L., Keys, H.R., Wang, T., Gray, N.S., and Sabatini, D.M. (2012). A unifying model for mTORC1-mediated regulation of mRNA translation. Nature *485*, 109–113. https://doi.org/10.1038/nature11083.

32. Prentzell, M.T., Rehbein, U., Sandoval, M.C., Meulemeester, A.-S.D., Baumeister, R., Brohée, L., Berdel, B., Bockwoldt, M., Carroll, B., Chowdhury, S.R., et al. (2021). G3BPs tether the TSC complex to lysosomes and suppress mTORC1 signaling. Cell *184*, 655–674.e27. https://doi.org/10.1016/j.cell.2020.12.024.

33. Kraushar, M.L., Krupp, F., Harnett, D., Turko, P., Ambrozkiewicz, M.C., Sprink, T., Imami, K., Günnigmann, M., Zinnall, U., Vieira-Vieira, C.H., et al. (2021). Protein synthesis in the developing neocortex at near-atomic resolution reveals Ebp1-mediated neuronal proteostasis at the 60S tunnel exit. Mol. Cell *81*, 304–322.e16. https://doi.org/10.1016/j.molcel.2020.11.037.

34. Yang, H.-S., Jansen, A.P., Komar, A.A., Zheng, X., Merrick, W.C., Costes, S., Lockett, S.J., Sonenberg, N., and Colburn, N.H. (2003). The transformation suppressor Pdcd4 is a novel eukaryotic translation initiation Factor 4A binding protein that inhibits translation. Mol. Cell. Biol. *23*, 26–37. https://doi.org/10.1128/MCB.23.1.26-37.2003.

35. Parsyan, A., Svitkin, Y., Shahbazian, D., Gkogkas, C., Lasko, P., Merrick, W.C., and Sonenberg, N. (2011). mRNA helicases: the tacticians of translational control. Nat. Rev. Mol. Cell Biol. *12*, 235–245. https://doi.org/10.1038/nrm3083.

36. Zheng, H.-J., Tsukahara, M., Liu, E., Ye, L., Xiong, H., Noguchi, S., Suzuki, K., and Ji, Z.-S. (2015). The novel helicase helG (DHX30) is expressed during gastrulation in mice and has a structure similar to a human DExH box helicase. Stem Cells Dev. *24*, 372–383. https://doi.org/10.1089/scd.2014.0077.

37. Lessel, D., Schob, C., Küry, S., Reijnders, M.R.F., Harel, T., Eldomery, M.K., Coban-Akdemir, Z., Denecke, J., Edvardson, S., Colin, E., et al. (2017). De novo missense mutations in DHX30 impair global translation and cause a neurodevelopmental disorder. Am. J. Hum. Genet. *101*, 716–724. https://doi.org/10.1016/j.ajhg.2017.09.014.

38. Cross, L.A., McWalter, K., Keller-Ramey, J., Henderson, L.B., and Amudhavalli, S.M. (2020). A report of gonadal mosaicism in DHX30-related neurodevelopmental disorder. Clin. Dysmorphol. *29*, 161–164. https://doi.org/10.1097/MCD.0000000000000316.

39. Rizzotto, D., Zaccara, S., Rossi, A., Galbraith, M.D., Andrysik, Z., Pandey, A., Sullivan, K.D., Quattrone, A., Espinosa, J.M., Dassi, E., et al. (2020). Nutlin-induced apoptosis is specified by a translation program regulated by PCBP2 and DHX30. Cell Rep. *30*, 4355–4369.e6. https://doi.org/10.1016/j.celrep.2020.03.011.

40. Bosco, B., Rossi, A., Rizzotto, D., Hamadou, M.H., Bisio, A., Giorgetta, S., Perzolli, A., Bonollo, F., Gaucherot, A., Catez, F., et al. (2021). DHX30 coordinates cytoplasmic translation and mitochondrial function contributing to cancer cell survival. Cancers *13*, 4412. https://doi.org/10.3390/cancers13174412.

41. Nakaya, T., Kawahara, S., Watanabe, S., Lee, D.-S., Suzuki, T., and Kirino, Y. (2001). Identification and expression of a novel gene in odour-taste associative learning in the terrestrial slug. Genes Cells *6*, 43–56. https://doi.org/10.1046/j.1365-2443.2001.00397.x.

42. Kim, H., Lee, S.-H., Han, J.-H., Lee, J.-A., Cheang, Y.-H., Chang, D.-J., Lee, Y.-S., and Kaang, B.-K. (2006). A nucleolar protein ApLLP induces ApC/EBP expression required for long-term synaptic facilitation in Aplysia neurons. Neuron *49*, 707–718. https://doi.org/10.1016/j.neuron.2006.01.035.

43. Kim, H., Chang, D.-J., Lee, J.-A., Lee, Y.-S., and Kaang, B.-K. (2003). Identification of nuclear/nucleolar localization signal in Aplysia learning associated protein of slug with a molecular mass of 18 kDa homologous protein. Neurosci. Lett. *343*, 134–138. https://doi.org/10.1016/S0304-3940(03)00269-6.

44. Yu, N.-K., Kim, H.F., Shim, J., Kim, S., Kim, D.W., Kwak, C., Sim, S.-E., Choi, J.-H., Ahn, S., Yoo, J., et al. (2016). A transducible nuclear/nucleolar protein, mLLP, regulates neuronal morphogenesis and synaptic transmission. Sci. Rep. *6*, 22892. https://doi.org/10.1038/srep22892.

45. Wu, S., Tutuncuoglu, B., Yan, K., Brown, H., Zhang, Y., Tan, D., Gamalinda, M., Yuan, Y., Li, Z., Jakovljevic, J., et al. (2016). Diverse roles of assembly factors revealed by structures of late nuclear pre-60S ribosomes. Nature *534*, 133–137. https://doi.org/10.1038/nature17942.

46. Liang, X., Zuo, M.-Q., Zhang, Y., Li, N., Ma, C., Dong, M.-Q., and Gao, N. (2020). Structural snapshots of human pre-60S ribosomal particles before and after nuclear export. Nat. Commun. *11*, 3542. https://doi.org/10.1038/s41467-020-17237-x.

47. Shao, S., Murray, J., Brown, A., Taunton, J., Ramakrishnan, V., and Hegde, R.S. (2016). Decoding mammalian ribosome-mRNA states by translational GTPase complexes. Cell *167*, 1229–1240.e15. https://doi.org/10.1016/j.cell.2016.10.046.

48. Voorhees, R.M., and Ramakrishnan, V. (2013). Structural basis of the translational elongation cycle. Annu. Rev. Biochem. *82*, 203–236. https://doi.org/10.1146/annurev-biochem-113009-092313.

49. Spahn, C.M.T., Gomez-Lorenzo, M.G., Grassucci, R.A., Jørgensen, R., Andersen, G.R., Beckmann, R., Penczek, P.A., Ballesta, J.P.G., and Frank, J. (2004). Domain movements of elongation factor eEF2 and the eukaryotic 80S ribosome facilitate tRNA translocation. EMBO J. *23*, 1008–1019. https://doi.org/10.1038/sj.emboj.7600102.

50. Hou, X., and Tang, W. (2021). Pseudogene PA2G4P4 promotes oncogene PA2G4 expression and nuclear translocation to affect glioblastoma cell viability and apoptosis. Life Sci. *265*, 118793. https://doi.org/10.1016/j.lfs.2020.118793.

51. Xu, Y., Cai, H., Tu, W., Ding, L., and Luo, R. (2021). Increased PA2G4 expression is an unfavorable factor in nasopharyngeal carcinoma. Appl. Immunohistochem. Mol. Morphol. *29*, 513–518. https://doi.org/10.1097/PAI.0000000000000918.

52. Wild, K., Aleksić, M., Lapouge, K., Juaire, K.D., Flemming, D., Pfeffer, S., and Sinning, I. (2020). MetAP-like Ebp1 occupies the human ribosomal tunnel exit and recruits flexible rRNA expansion segments. Nat. Commun. *11*, 776. https://doi.org/10.1038/s41467-020-14603-7.

53. Wells, J.N., Buschauer, R., Mackens-Kiani, T., Best, K., Kratzat, H., Berninghausen, O., Becker, T., Gilbert, W., Cheng, J., and Beckmann, R. (2020). Structure and function of yeast Lso2 and human CCDC124 bound to hibernating ribosomes. PLOS Biol. *18*, e3000780. https://doi.org/10.1371/journal.pbio.3000780.

54. Pazo, A., Pérez-González, A., Oliveros, J.C., Huarte, M., Chavez, J.P., and Nieto, A. (2019). hCLE/RTRAF-HSPC117-DDX1-FAM98B: A new cap-binding complex that activates mRNA translation. Front. Physiol. *10*, 92. https://doi.org/10.3389/fphys.2019.00092.

55. Möller, I., Beatrix, B., Kreibich, G., Sakai, H., Lauring, B., and Wiedmann, M. (1998). Unregulated exposure of the ribosomal M-site caused by NAC depletion results in delivery of non-secretory polypeptides to the Sec61 complex. FEBS Lett. *441*, 1–5. https://doi.org/10.1016/S0014-5793(98)01440-9.

56. Beatrix, B., Sakai, H., and Wiedmann, M. (2000). The α and β subunit of the nascent polypeptide-associated complex have distinct functions *. J. Biol. Chem. *275*, 37838–37845. https://doi.org/10.1074/jbc.M006368200.

57. Zhang, Y., Pak, C., Han, Y., Ahlenius, H., Zhang, Z., Chanda, S., Marro, S., Patzke, C., Acuna, C., Covy, J., et al. (2013). Rapid single-step induction of functional neurons from human pluripotent stem cells. Neuron *78*, 785–798. https://doi.org/10.1016/j.neuron.2013.05.029.

58. Steiglitz, B.M., Keene, D.R., and Greenspan, D.S. (2002). PCOLCE2 encodes a functional procollagen C-proteinase enhancer (PCPE2) that is a collagen-binding protein differing in distribution of expression and post-translational modification from the previously described PCPE1. J. Biol. Chem. *277*, 49820–49830. https://doi.org/10.1074/jbc.M209891200.

59. Maeta, K., Edamatsu, H., Nishihara, K., Ikutomo, J., Bilasy, S.E., and Kataoka, T. (2016). Crucial role of Rapgef2 and Rapgef6, a family of guanine nucleotide exchange factors for Rap1 small GTPase, in formation of apical surface adherens junctions and neural progenitor development in the mouse cerebral cortex. eNeuro *3*, ENEURO.0142-16.2016. https://doi.org/10.1523/ENEURO.0142-16.2016.

60. Long, K.R., and Huttner, W.B. (2019). How the extracellular matrix shapes neural development. Open Biol. *9*, 180216. https://doi.org/10.1098/rsob.180216.

61. Melrose, J., Hayes, A.J., and Bix, G. (2021). The CNS/PNS extracellular matrix provides instructive guidance cues to neural cells and neuroregulatory proteins in neural development and repair. Int. J. Mol. Sci. *22*, 5583. https://doi.org/10.3390/ijms22115583.

62. de Vrij, F.M., Bouwkamp, C.G., Gunhanlar, N., Shpak, G., Lendemeijer, B., Baghdadi, M., Gopalakrishna, S., Ghazvini, M., Li, T.M., Quadri, M., et al. (2019). Candidate CSPG4 mutations and induced pluripotent stem cell modeling implicate oligodendrocyte progenitor cell dysfunction in familial schizophrenia. Mol. Psychiatry *24*, 757–771. https://doi.org/10.1038/s41380-017-0004-2.

63. Arkadir, D., Lossos, A., Rahat, D., Abu Snineh, M., Schueler-Furman, O., Nitschke, S., Minassian, B.A., Sadaka, Y., Lerer, I., Tabach, Y., et al. (2019). MYORG is associated with recessive primary familial brain calcification. Ann. Clin. Transl. Neurol. *6*, 106–113. https://doi.org/10.1002/acn3.684.

64. Niu, X., Sun, Y., Yang, Y., Cheng, M., Tan, Q., Zhang, J., and Zhang, Y. (2021). RHOBTB2 gene associated epilepsy and paroxysmal movement disorder: two cases report and literature review. Acta Epileptol. *3*, 20. https://doi.org/10.1186/s42494-021-00056-y.

65. Straub, J., Konrad, E.D.H., Grüner, J., Toutain, A., Bok, L.A., Cho, M.T., Crawford, H.P., Dubbs, H., Douglas, G., Jobling, R., et al. (2018). Missense variants in RHOBTB2 cause a developmental and epileptic encephalopathy in humans, and altered levels cause neurological defects in Drosophila. Am. J. Hum. Genet. *102*, 44–57. https://doi.org/10.1016/j.ajhg.2017.11.008.

66. Young, J., Metay, C., Bouligand, J., Tou, B., Francou, B., Maione, L., Tosca, L., Sarfati, J., Brioude, F., Esteva, B., et al. (2012). SEMA3A deletion in a family with Kallmann syndrome validates the role of semaphorin 3A in human puberty and olfactory system development. Hum. Reprod. *27*, 1460–1465. https://doi.org/10.1093/humrep/des022.

67. Maccani, J.Z.J., Koestler, D.C., Lester, B., Houseman, E.A., Armstrong, D.A., Kelsey, K.T., and Marsit, C.J. (2015). Placental DNA methylation related to both infant toenail mercury and adverse neurobehavioral outcomes. Environ. Health Perspect. *123*, 723–729. https://doi.org/10.1289/ehp.1408561.

68. Salles, J., Eddiry, S., Lacassagne, E., Laurier, V., Molinas, C., Bieth, É., Franchitto, N., Salles, J.-P., and Tauber, M. (2021). Patients with PWS and related syndromes display differentially methylated regions involved in neurodevelopmental and nutritional trajectory. Clin. Epigenet. *13*, 159. https://doi.org/10.1186/s13148-021-01143-0.

69. Lyu, X., Yang, Q., Zhao, F., and Liu, Y. (2021). Codon usage and protein length-dependent feedback from translation elongation regulates translation initiation and elongation speed. Nucleic Acids Res. *49*, 9404–9423. https://doi.org/10.1093/nar/gkab729.

70. Kapur, M., and Ackerman, S.L. (2018). mRNA translation gone awry: translation fidelity and neurological disease. Trends Genet. *34*, 218–231. https://doi.org/10.1016/j.tig.2017.12.007.

71. Mestre-Fos, S., Ito, C., Moore, C.M., Reddi, A.R., and Williams, L.D. (2020). Human ribosomal G-quadruplexes regulate heme bioavailability. J. Biol. Chem. *295*, 14855–14865. https://doi.org/10.1074/jbc.RA120.014332.

72. Wallimann, T., Wyss, M., Brdiczka, D., Nicolay, K., and Eppenberger, H.M. (1992). Intracellular compartmentation, structure and function of creatine kinase isoenzymes in tissues with high and fluctuating energy demands: the 'phosphocreatine circuit' for cellular energy homeostasis. Biochem. J. *281*, 21–40. https://doi.org/10.1042/bj2810021.

73. Tsuruta, D., and Jones, J.C.R. (2003). The vimentin cytoskeleton regulates focal contact size and adhesion of endothelial cells subjected to shear stress. J. Cell Sci. *116*, 4977–4984. https://doi.org/10.1242/jcs.00823.

74. Eckes, B., Dogic, D., Colucci-Guyon, E., Wang, N., Maniotis, A., Ingber, D., Merckling, A., Langa, F., Aumailley, M., Delouvée, A., et al. (1998). Impaired mechanical stability, migration and contractile capacity in vimentin deficient fibroblasts. J. Cell Sci. *111*, 1897–1907. https://doi.org/10.1242/jcs.111.13.1897.

75. Traub, P., and Nelson, W.J. (1982). Interaction of the intermediate filament protein vimentin with ribosomal subunits and ribosomal RNA in vitro. Mol. Biol. Rep. *8*, 239–247. https://doi.org/10.1007/BF00776586.

76. Xia, Z., Ouyang, D., Li, Q., Li, M., Zou, Q., Li, L., Yi, W., and Zhou, E. (2019). The expression, functions, interactions and prognostic values of PTPRZ1: a review and bioinformatic analysis. J. Cancer *10*, 1663–1674. https://doi.org/10.7150/jca.28231.

77. Chalupnikova, K., Solc, P., Sulimenko, V., Sedlacek, R., and Svoboda, P. (2014). An oocyte-specific ELAVL2 isoform is a translational repressor ablated from meiotically competent antral oocytes. Cell Cycle *13*, 1187–1200. https://doi.org/10.4161/cc.28107.

78. Kagan, J.C., and Barton, G.M. (2014). Emerging principles governing signal transduction by pattern-recognition receptors. Cold Spring Harb. Perspect. Biol. *7*, a016253. https://doi.org/10.1101/cshperspect.a016253.

79. Diamond, M.S., and Farzan, M. (2013). The broad-spectrum antiviral functions of IFIT and IFITM proteins. Nat. Rev. Immunol. *13*, 46–57. https://doi.org/10.1038/nri3344.

80. Durfee, L.A., Lyon, N., Seo, K., and Huibregtse, J.M. (2010). The ISG15 conjugation system broadly targets newly synthesized proteins: implications for the antiviral function of ISG15. Mol. Cell *38*, 722–732. https://doi.org/10.1016/j.molcel.2010.05.002.

81. Oudshoorn, D., van Boheemen, S., Sánchez-Aparicio, M.T., Rajsbaum, R., García-Sastre, A., and Versteeg, G.A. (2012). HERC6 is the main E3 ligase for global ISG15 conjugation in mouse cells. PLoS One *7*, e29870. https://doi.org/10.1371/journal.pone.0029870.

82. Ketscher, L., Basters, A., Prinz, M., and Knobeloch, K.-P. (2012). mHERC6 is the essential ISG15 E3 ligase in the murine system. Biochem. Biophys. Res. Commun. *417*, 135–140. https://doi.org/10.1016/j.bbrc.2011.11.071.

83. Faronato, M., Patel, V., Darling, S., Dearden, L., Clague, M.J., Urbé, S., and Coulson, J.M. (2013). The deubiquitylase USP15 stabilizes newly synthesized REST and rescues its expression at mitotic exit. Cell Cycle *12*, 1964–1977. https://doi.org/10.4161/cc.25035.

84. Kusakabe, S., Suzuki, T., Sugiyama, Y., Haga, S., Horike, K., Tokunaga, M., Hirano, J., Zhang, H., Chen, D.V., Ishiga, H., et al. (2019). USP15 participates in hepatitis C virus propagation through regulation of viral RNA translation and lipid droplet formation. J. Virol. *93*, e01708–e01718. https://doi.org/10.1128/JVI.01708-18.

85. Aviner, R., Li, K.H., Frydman, J., and Andino, R. (2021). Cotranslational prolyl hydroxylation is essential for Flavivirus biogenesis. Nature *596*, 558–564. https://doi.org/10.1038/s41586-021-03851-2.

86. Di Paolo, A., Eastman, G., Mesquita-Ribeiro, R., Farias, J., Macklin, A., Kislinger, T., Colburn, N., Munroe, D., Sotelo Sosa, J.R., Dajas-Bailador, F., et al. (2020). PDCD4 regulates axonal growth by translational repression of neurite growth-related genes and is modulated during nerve injury responses. RNA *26*, 1637–1653. https://doi.org/10.1261/rna.075424.120.

87. Bianco, C., and Mohr, I. (2019). Ribosome biogenesis restricts innate immune responses to virus infection and DNA. eLife *8*, e49551. https://doi.org/10.7554/eLife.49551.

88. Cho, N.H., Cheveralls, K.C., Brunner, A.-D., Kim, K., Michaelis, A.C., Raghavan, P., Kobayashi, H., Savy, L., Li, J.Y., Canaj, H., et al. (2022). OpenCell: endogenous tagging for the cartography of human cellular organization. Science *375*, eabi6983. https://doi.org/10.1126/science.abi6983.

89. Lässig, C., Matheisl, S., Sparrer, K.M.J., de Oliveira Mann, C.C., Moldt, M., Patel, J.R., Goldeck, M., Hartmann, G., García-Sastre, A., Hornung, V., et al. (2015). ATP hydrolysis by the viral RNA sensor RIG-I prevents

unintentional recognition of self-RNA. eLife *4*, e10859. https://doi.org/10.7554/eLife.10859.

90. Hsu, J.C.-C., Laurent-Rolle, M., Pawlak, J.B., Xia, H., Kunte, A., Hee, J.S., Lim, J., Harris, L.D., Wood, J.M., Evans, G.B., et al. (2022). Viperin triggers ribosome collision-dependent translation inhibition to restrict viral replication. Mol. Cell *82*, 1631–1642.e6. https://doi.org/10.1016/j.molcel.2022.02.031.
91. Pawlak, J.B., Hsu, J.C.-C., Xia, H., Han, P., Suh, H.-W., Grove, T.L., Morrison, J., Shi, P.-Y., Cresswell, P., and Laurent-Rolle, M. (2023). CMPK2 restricts Zika virus replication by inhibiting viral translation. PLoS Pathog. *19*, e1011286. https://doi.org/10.1371/journal.ppat.1011286.
92. Hu, A., Hu, Z., Zou, H., Zhang, J., Zhang, D., Wang, H., Zhong, J., and Chen, B. (2022). CARD9 in host immunity to fungal, bacterial, viral, and parasitic infections: an update. Front. Microbiol. *13*, 1021837. https://doi.org/10.3389/fmicb.2022.1021837.
93. Gregory, D.J., DeLoid, G.M., Salmon, S.L., Metzger, D.W., Kramnik, I., and Kobzik, L. (2020). SON DNA-binding protein mediates macrophage autophagy and responses to intracellular infection. FEBS Lett. *594*, 2782–2799. https://doi.org/10.1002/1873-3468.13851.
94. Lenk, R., Ransom, L., Kaufmann, Y., and Penman, S. (1977). A cytoskeletal structure with associated polyribosomes obtained from HeLa cells. Cell *10*, 67–78. https://doi.org/10.1016/0092-8674(77)90141-6.
95. Toh, B.H., Lolait, S.J., Mathy, J.P., and Baum, R. (1980). Association of mitochondria with intermediate filaments and of polyribosomes with cytoplasmic actin. Cell Tissue Res. *211*, 163–169. https://doi.org/10.1007/BF00233731.
96. Traub, P., Bauer, C., Hartig, R., Grüb, S., and Stahl, J. (1998). Colocalization of single ribosomes with intermediate filaments in puromycin-treated and serum-starved mouse embryo fibroblasts. Biol. Cell *90*, 319–337. https://doi.org/10.1111/j.1768-322X.1998.tb01042.x.
97. Hamill, D., Davis, J., Drawbridge, J., and Suprenant, K.A. (1994). Polyribosome targeting to microtubules: enrichment of specific mRNAs in a reconstituted microtubule preparation from sea urchin embryos. J. Cell Biol. *127*, 973–984. https://doi.org/10.1083/jcb.127.4.973.
98. Fischer, I., and Romano-Clarke, G. (1991). Association of microtubule-associated protein (MAP1B) with growing axons in cultured hippocampal neurons. Mol. Cell. Neurosci. *2*, 39–51. https://doi.org/10.1016/1044-7431(91)90038-P.
99. Gordon-Weeks, P.R., and Fischer, I. (2000). MAP1B expression and microtubule stability in growing and regenerating axons. Microsc. Res. Tech. *48*, 63–74. https://doi.org/10.1002/(SICI)1097-0029(20000115)48:2<63::AID-JEMT2>3.0.CO;2-1.
100. Bouquet, C., Soares, S., von Boxberg, Y., Ravaille-Veron, M., Propst, F., and Nothias, F. (2004). Microtubule-associated protein 1B controls directionality of growth cone migration and axonal branching in regeneration of adult dorsal root ganglia neurons. J. Neurosci. *24*, 7204–7213. https://doi.org/10.1523/JNEUROSCI.2254-04.2004.
101. Perez-Riverol, Y., Bai, J., Bandla, C., García-Seisdedos, D., Hewapathirana, S., Kamatchinathan, S., Kundu, D.J., Prakash, A., Frericks-Zipper, A., Eisenacher, M., et al. (2022). The PRIDE database resources in 2022: a hub for mass spectrometry-based proteomics evidences. Nucleic Acids Res. *50*, D543–D552. https://doi.org/10.1093/nar/gkab1038.
102. Rodrik-Outmezguine, V.S., Okaniwa, M., Yao, Z., Novotny, C.J., McWhirter, C., Banaji, A., Won, H., Wong, W., Berger, M., de Stanchina, E., et al. (2016). Overcoming mTOR resistance mutations with a new-generation mTOR inhibitor. Nature *534*, 272–276. https://doi.org/10.1038/nature17963.
103. Frankish, A., Carbonell-Sala, S., Diekhans, M., Jungreis, I., Loveland, J.E., Mudge, J.M., Sisu, C., Wright, J.C., Arnan, C., Barnes, I., et al. (2023). GENCODE: reference annotation for the human and mouse genomes in 2023. Nucleic Acids Res. *51*, D942–D949. https://doi.org/10.1093/nar/gkac1071.
104. Hooper, M., Hardy, K., Handyside, A., Hunter, S., and Monk, M. (1987). HPRT-deficient (Lesch–Nyhan) mouse embryos derived from germline colonization by cultured cells. Nature *326*, 292–295. https://doi.org/10.1038/326292a0.
105. Pajic, A., Spitkovsky, D., Christoph, B., Kempkes, B., Schuhmacher, M., Staege, M.S., Brielmeier, M., Ellwart, J., Kohlhuber, F., Bornkamm, G.W., et al. (2000). Cell cycle activation by c-myc in a Burkitt lymphoma model cell line. Int. J. Cancer *87*, 787–793. https://doi.org/10.1002/1097-0215(20000915)87:6<787::AID-IJC4>3.0.CO;2-6.
106. Thomson, J.A., Itskovitz-Eldor, J., Shapiro, S.S., Waknitz, M.A., Swiergiel, J.J., Marshall, V.S., and Jones, J.M. (1998). Embryonic stem cell lines derived from human blastocysts. Science *282*, 1145–1147. https://doi.org/10.1126/science.282.5391.1145.
107. Clauser, K.R., Baker, P., and Burlingame, A.L. (1999). Role of Accurate Mass Measurement (±10 ppm) in Protein Identification Strategies Employing MS or MS/MS and Database Searching. Anal. Chem. *71*, 2871–2882. https://doi.org/10.1021/ac9810516.
108. Schindelin, J., Arganda-Carreras, I., Frise, E., Kaynig, V., Longair, M., Pietzsch, T., Preibisch, S., Rueden, C., Saalfeld, S., Schmid, B., et al. (2012). Fiji: an open-source platform for biological-image analysis. Nat. Methods *9*, 676–682. https://doi.org/10.1038/nmeth.2019.
109. Arshadi, C., Günther, U., Eddison, M., Harrington, K.I.S., and Ferreira, T.A. (2021). SNT: a unifying toolbox for quantification of neuronal anatomy. Nat. Methods *18*, 374–377. https://doi.org/10.1038/s41592-021-01105-7.
110. Martin, M. (2011). Cutadapt removes adapter sequences from high-throughput sequencing reads. EMBnet.journal *17*, 10–12. https://doi.org/10.14806/ej.17.1.200.
111. Dobin, A., Davis, C.A., Schlesinger, F., Drenkow, J., Zaleski, C., Jha, S., Batut, P., Chaisson, M., and Gingeras, T.R. (2013). STAR: ultrafast universal RNA-seq aligner. Bioinformatics *29*, 15–21. https://doi.org/10.1093/bioinformatics/bts635.
112. Pertea, G., and Pertea, M. (2020). GFF Utilities: GffRead and GffCompare. F1000Res *9*. ISCB Comm J-304. https://doi.org/10.12688/f1000research.23297.2.
113. Patro, R., Duggal, G., Love, M.I., Irizarry, R.A., and Kingsford, C. (2017). Salmon provides fast and bias-aware quantification of transcript expression. Nat. Methods *14*, 417–419. https://doi.org/10.1038/nmeth.4197.
114. Love, M.I., Huber, W., and Anders, S. (2014). Moderated estimation of fold change and dispersion for RNA-seq data with DESeq2. Genome Biol. *15*, 550. https://doi.org/10.1186/s13059-014-0550-8.
115. Smith, T., Heger, A., and Sudbery, I. (2017). UMI-tools: modeling sequencing errors in Unique Molecular Identifiers to improve quantification accuracy. Genome Res. *27*, 491–499. https://doi.org/10.1101/gr.209601.116.
116. Langmead, B., and Salzberg, S.L. (2012). Fast gapped-read alignment with Bowtie 2. Nat. Methods *9*, 357–359. https://doi.org/10.1038/nmeth.1923.
117. Robinson, M.D., McCarthy, D.J., and Smyth, G.K. (2010). edgeR: a Bioconductor package for differential expression analysis of digital gene expression data. Bioinformatics *26*, 139–140. https://doi.org/10.1093/bioinformatics/btp616.
118. Ritchie, M.E., Phipson, B., Wu, D., Hu, Y., Law, C.W., Shi, W., and Smyth, G.K. (2015). limma powers differential expression analyses for RNA-sequencing and microarray studies. Nucleic Acids Res. *43*, e47. https://doi.org/10.1093/nar/gkv007.
119. Law, C.W., Chen, Y., Shi, W., and Smyth, G.K. (2014). voom: precision weights unlock linear model analysis tools for RNA-seq read counts. Genome Biol. *15*, R29. https://doi.org/10.1186/gb-2014-15-2-r29.

120. Guan, S., Price, J.C., Prusiner, S.B., Ghaemmaghami, S., and Burlingame, A.L. (2011). A data processing pipeline for mammalian proteome dynamics studies using stable isotope metabolic labeling. Mol. Cell. Proteomics *10*, M111.010728. https://doi.org/10.1074/mcp.M111.010728.

121. Rosenfeld, J., Capdevielle, J., Guillemot, J.C., and Ferrara, P. (1992). In-gel digestion of proteins for internal sequence analysis after one- or two-dimensional gel electrophoresis. Anal. Biochem. *203*, 173–179. https://doi.org/10.1016/0003-2697(92)90061-B.

122. McGlincy, N.J., and Ingolia, N.T. (2017). Transcriptome-wide measurement of translation by ribosome profiling. Methods *126*, 112–129. https://doi.org/10.1016/j.ymeth.2017.05.028.

STAR★METHODS

KEY RESOURCES TABLE

REAGENT or RESOURCE	SOURCE	IDENTIFIER
Antibodies		
Rabbit polyclonal anti-NUP62	Proteintech	Cat# 13916-1-AP; RRID: AB_2267660
Rabbit polyclonal anti-ATP5A1	Proteintech	Cat# 14676-1-AP; RRID: AB_2061761
Rabbit polyclonal anti-TOM20	Proteintech	Cat# 11802-1-AP; RRID: AB_2207530
Rabbit polyclonal anti-RPL4	Proteintech	Cat# 11302-1-AP; RRID: AB_2181909
Rabbit monoclonal anti-RPL10A [EPR12344]	Abcam	Cat# ab174318; RRID: AB_3532168
Mouse monoclonal anti-RPS5	Abcam	Cat# ab58345; RRID: AB_2180899
Rabbit polyclonal anti-RPS26	Proteintech	Cat# 14909-1-AP; RRID: AB_2180361
Goat polyclonal anti-RPS27	Fisher Scientific	Cat# PIPA518092; RRID: AB_10980328
Mouse monoclonal anti-METAP1	R&D Systems	Cat# MAB3537-SP; RRID: AB_2144061
Rabbit polyclonal anti-UFL1	Bethyl Laboratories	Cat# A303-456A; RRID: A303-456A
Rabbit polyclonal anti-UPF1	Proteintech	Cat# 23379-1-AP; RRID: AB_11232421
Rabbit polyclonal anti-DDX1	Bethyl Laboratories	Cat# A300-520A; RRID: AB_451045
Rabbit polyclonal anti-NSUN2	Proteintech	Cat# 20854-1-AP; RRID: AB_10693629
Rabbit polyclonal anti-DHX30	Abcam	Cat# ab85687; RRID: AB_1860273
Mouse polyclonal anti-RPL29	Abcam	Cat# ab88514; RRID: AB_2042834
Rabbit polyclonal anti-PABP1	Cell Signaling Technology	Cat# 4992; RRID: AB_10693595
Rabbit polyclonal anti-NAA15	Sigma Aldrich	Cat# HPA023589-100UL; RRID: AB_1854311
Rabbit monoclonal anti-RPS19 [EPR10423]	Abcam	Cat# ab181365; RRID: AB_3532170
Mouse monoclonal anti-β-Actin (8H10D10)	Cell Signaling Technology	Cat# 3700S; RRID: AB_2242334
Rabbit monoclonal anti-RPS6 (5G10)	Cell Signaling Technology	Cat# 2217; RRID: AB_331355
Mouse monoclonal anti-V5 tag (SV5-Pk1)	Invitrogen	Cat# R960-25; RRID: AB_2792973
Mouse monoclonal anti-GAPDH (D4C6R)	Cell Signaling Technology	Cat# 97166; RRID: AB_2756824
Rabbit polyclonal anti-LLPH	Invitrogen	Cat# PA5-66207; RRID: AB_2664587
Rabbit polyclonal anti-RPS20	Proteintech	Cat# 15692-1-AP; RRID: AB_10596626
Rabbit polyclonal anti-RPL8	Proteintech	Cat# 16981-1-AP; RRID: AB_2182071
Rabbit polyclonal anti-ELAVL2	Proteintech	Cat# 14008-1-AP; RRID: AB_2096356
Chicken polyclonal anti-MAP2A/B	EnCor Biotechnology	Cat# CPCA-MAP2; RRID: AB_2138173
Rabbit polyclonal anti-RPL23	Bethyl Laboratories	Cat# A305-008A; RRID: AB_2621202
Mouse monoclonal anti-RPS6 (54D2)	Cell Signaling Technology	Cat# 2317S; RRID: AB_2238583
Rabbit polyclonal anti-RPS12	Proteintech	Cat# 16490-1-AP; RRID: AB_2146233
Rabbit polyclonal anti-USP15	Proteintech	Cat# 14354-1-AP; RRID: AB_2257148
Mouse monoclonal anti-Viperin [MaP.VIP]	Abcam	Cat# ab107359; RRID: AB_10888107
Mouse polyclonal anti-CMPK2	Abnova	Cat# H00129607-A01; RRID: AB_535248
Rabbit polyclonal anti-HO-1	Enzo	Cat# ADI-SPA-895-F; RRID: AB_10618757
Rabbit polyclonal anti-RACK1	Cell Signaling Technology	Cat# 4716S; RRID: AB_490864
Rabbit polyclonal anti-OAS3	Proteintech	Cat# 21915-1-AP; RRID: AB_2876880
Chemicals, Peptides, and Recombinant Proteins		
EmbryoMax® 0.1% Gelatin Solution	Millipore	Cat# ES-006-B
Gelatin from bovine skin	Sigma Aldrich	Cat# G9391
KnockOut™ DMEM	Gibco	Cat# 10829-018
EmbryoMax® ES Cell Qualified FBS	Millipore	Cat# ES-009-B

(*Continued on next page*)

Continued

REAGENT or RESOURCE	SOURCE	IDENTIFIER
EmbryoMax® L-Glutamine Solution (100X), 200mM	Millipore	Cat# TMS-002-C
EmbryoMax® Penicillin-Streptomycin Solution, 100X	Millipore	Cat# TMS-AB2-C
EmbryoMax® MEM, Non Essential Amino Acids (100X)	Millipore	Cat# TMS-001-C
2-Mercaptoethanol	Gibco	Cat# 21985023
mouse leukemia inhibitory factor (LIF) protein	Gemini Bio	Cat# 400-495
Ham's F-12K (Kaighn's) Medium	Gibco	Cat# 21127022
DMEM	Gibco	Cat# 11965-092
Fetal Bovine Serum, certified, heat inactivated	Gibco	Cat# 10082147
Penicillin-Streptomycin (10,000 U/mL)	Gibco	Cat# 15140122
HEPES (1 M)	Gibco	Cat# 15630080
Sodium pyruvate (100 mM)	Gibco	Cat# 11360070
GlutaMAX™ supplement	Gibco	Cat# 35050061
mCSF medium derived from 3T3-mCSF cells	Hiten Madhani's lab at UCSF	N/A
LPS-EK Ultrapure	Invivogen	Cat# tlrl-peklps
Poly(I:C) (HMW)	Invivogen	Cat# tlrl-pic
RPMI 1640 Medium	Gibco	Cat# 11875093
β-Estradiol	Sigma Aldrich	Cat# E2758-1G
Flt3L medium derived from B16-FLT3 cells.	Averil Ma's lab at UCSF	N/A
Laemmli SDS-Sample Buffer 6X, Reducing	Bioworld	Cat# 10570021-1
4–20% Criterion™ TGX™ Gels	Bio-rad	Cat# 5671095
4–20% Mini-PROTEAN® TGX™ Precast Protein Gels	Bio-rad	Cat# 4561096
Tris/Glycine/SDS	Bio-rad	Cat# 1610772
Trans-Blot Turbo RTA Midi 0.2 μm PVDF Transfer Kit	Bio-rad	Cat# 1704273
Trans-Blot Turbo RTA Mini 0.2 μm PVDF Transfer Kit	Bio-rad	Cat# 1704272
TWEEN® 20	Sigma Aldrich	Cat# P9416-100ML
PBS Tablets	Fisher Scientific	Cat# BP2944100
Bovine Serum Albumin	Sigma Aldrich	Cat# A9647-100G
Sodium azide	Sigma Aldrich	Cat# S2002-25G
HRP-conjugated anti-mouse	Cytiva	Cat# NA931-1ML
HRP-conjugated anti-rabbit	Cytiva	Cat# NA934-1ML
HRP-conjugated anti-goat antibody	R&D Systems	Cat# HAF019
Clarity Western ECL Substrate	Bio-rad	Cat# 1705061
SuperSignal™ West Femto Maximum Sensitivity Substrate	Thermo Scientific	Cat# 34095
Cycloheximide	Sigma Aldrich	Cat# C7698-1G
DPBS, no calcium, no magnesium	Gibco	Cat# 14190250
HEPES	Sigma Aldrich	Cat# H3375-100G
Potassium hydroxide	Sigma Aldrich	Cat# 221473-500G
Magnesium acetate tetrahydrate	Sigma Aldrich	Cat# M5661-250G
Ammonium chloride	Sigma Aldrich	Cat# A9434-500G
Pierce™ DTT (Dithiothreitol), No-Weigh™ Format	Thermo Scientific	Cat# A39255

(*Continued on next page*)

Continued

REAGENT or RESOURCE	SOURCE	IDENTIFIER
Triton™ X-100	Sigma Aldrich	Cat# T8787
Sodium deoxycholate	Sigma Aldrich	Cat# D6750
Glycerol	Sigma Aldrich	Cat# G9012-100ML
TURBO™ DNase (2 U/μL)	Invitrogen	Cat# AM2238
SUPERase·In™ RNase Inhibitor (20 U/μL)	Invitrogen	Cat# AM2696
Halt™ Protease and Phosphatase Inhibitor Single-Use Cocktail, EDTA-Free (100X)	Thermo Scientific	Cat# 78443
UltraPure™ DNase/RNase-Free Distilled Water	Invitrogen	Cat# 10977015
Sucrose	Sigma Aldrich	Cat# 8510-500GM
Chloroform	Sigma Aldrich	Cat# 3150
Ethanol	Gold Shield Distributors	Cat# 412804
SulfoLink™ Coupling Resin	Thermo Scientific	Cat# 20402
Tris Hydrochloride	Fisher Scientific	Cat# BP153-500
EDTA (0.5 M), pH 8.0, RNase-free	Invitrogen	Cat# AM9262
L-Cysteine	Sigma Aldrich	Cat# 168149-25G
Buffer Kit, RNase-free	Invitrogen	Cat# AM9010
TRIzol™ reagent	Invitrogen	Cat# 15596026
Trypsin-EDTA (0.5%), no phenol red	Gibco	Cat# 15400054
Puromycin	Invivogen	Cat# ant-pr-1
GTP Solution, Tris buffered	Thermo Scientific	Cat# R1461
Restore™ PLUS Western Blot Stripping Buffer	Thermo Scientific	Cat# 46430
TRIzol™ LS Reagent	Invitrogen	Cat# 10296010
Methanol (HPLC)	Fisher Scientific	Cat# A452SK-1
Acetic Acid, Glacial	Fisher Scientific	Cat# A38-212
Water (HPLC)	Fisher Scientific	Cat# W5-4
SYPRO Ruby	Invitrogen	Cat# S12000
Ammonium bicarbonate	Sigma Aldrich	Cat# 09830-500G
Guanidinium hydrochloride	Sigma Aldrich	Cat# G3272
Urea	Sigma Aldrich	Cat# U1250-1KG
Ammonium formate	Sigma Aldrich	Cat# 09735
Pierce™ Iodoacetamide, No-Weigh™ Format	Thermo Scientific	Cat# A39271
Trypsin/Lys-C Mix, Mass Spec Grade	Promega	Cat# V5073
Heptafluorobutyric acid	Sigma Aldrich	Cat# 52411-5ML-F
Formic Acid	Fisher Scientific	Cat# A117-50
HALO Peptide ES-C18 Bulk Packing 2.7 μm beads	MAC-MOD Analytical	Cat# 942120202
Rapalink-1	Lab of Kevan Shokat[102]	N/A
Tris(2-carboxyethyl)phosphine hydrochloride	Sigma Aldrich	Cat# C4706
Lysyl Endopeptidase®, Mass Spectrometry Grade (Lys-C)	Fujifilm	Cat# 125-05061
Trypsin Protease, MS Grade	Thermo Scientific	Cat# 90057
Acetonitrile	Fisher Scientific	Cat# A955-500
Hydroxylamine solution	Sigma Aldrich	Cat# 467804-10ML
Fetal Bovine Serum	Sigma Aldrich	Cat# TMS-013-B
DMEM/F-12, HEPES, no phenol red	Gibco	Cat# 11039021
HEPES, 1.0M buffer soln., pH 8.0	Fisher Scientific	Cat# AAJ63578AK

(*Continued on next page*)

Continued

REAGENT or RESOURCE	SOURCE	IDENTIFIER
Trifluoroacetic acid	Fluka	Cat# 40967
Opti-MEM™ I Reduced Serum Medium, no phenol red	Gibco	Cat# 11058021
DharmaFECT 1 Transfection Reagent	Horizon	Cat# T-2001
O-propargyl-puromycin (OPP)	Vector Laboratories	Cat# CCT-1407
HBSS, no calcium, no magnesium, no phenol red	Gibco	Cat# 14175095
Paraformaldehyde, 16% w/v aq. soln., methanol free	Thermo Scientific	Cat# 43368-9M
Saponin	Sigma Aldrich	Cat# 47036
Lipofectamine™ 2000 Transfection Reagent	Invitrogen	Cat# 11668019
mTeSR™1 Complete Kit	STEMCELL Technologies	Cat# 85850
Geltrex™ LDEV-Free, hESC-Qualified, Reduced Growth Factor Basement Membrane Matrix	Gibco	Cat# A1413302
StemPro™ Accutase™ Cell Dissociation Reagent	Gibco	Cat# A1110501
Thiazovivin	Tocris	Cat# 3845
Cas9-NLS protein	QB3-Berkeley Macrolab	N/A
Polyethylenimine hydrochloride	Sigma Aldrich	Cat# 764965-1G
Matrigel® Basement Membrane Matrix, LDEV-free, 5 mL	Corning	Cat# 356234
Polybrene	Tocris	Cat# 7711
PolyFect Transfection Reagent	Qiagen	301105
DMEM/F-12	Gibco	Cat# 11320033
N-2 Supplement (100X)	Gibco	Cat# 17502048
Insulin from bovine pancreas	Sigma Aldrich	Cat# I6634-100MG
Sodium hydroxide	Fisher Scientific	Cat# SS255-1
Doxycycline hydrochloride	Fisher Scientific	Cat# BP26535
Puromycin dihydrochloride from *Streptomyces alboniger*	Sigma Aldrich	Cat# P8833-25MG
Cytosine β-D-arabinofuranoside (AraC)	Sigma Aldrich	Cat# C1768-1G
Neurobasal™ Medium	Gibco	Cat# 21103049
Gem21 NeuroPlex™ Serum-Free Supplement	Gemini	Cat# 400-160
HyClone™ HyClone Characterized FBS, Canadian Origin	Cytiva	Cat# SH30396.03
Goat serum, heat inactivated	MP Biomedicals	Cat# 092939249
Goat anti-Chicken IgY (H+L) Secondary Antibody, Alexa Fluor™ 647	Invitrogen	Cat# A-21449
DAPI solution	Thermo Scientific	Cat# 62248
Fluoromount-G	SouthernBiotech	Cat# 0100-01
ANTI-FLAG® M2 Affinity Gel	Sigma Aldrich	Cat# A2220
NP-40	Thermo Scientific	Cat# 85124
Octaethylene glycol monododecyl ether (Nikkol)	Sigma Aldrich	Cat# P8925-1G
Micrococcal Nuclease (MNase)	Thermo Scientific	Cat# EN0181
FLAG® Peptide	Millipore	Cat# F3290-4MG
ProtoBlue Safe Colloidal Coomassie Blue G-250	National Diagnostics	Cat# EC-722
RNase A, affinity purified, 1 mg/mL	Invitrogen	Cat# AM2271

(*Continued on next page*)

Continued

REAGENT or RESOURCE	SOURCE	IDENTIFIER
RNase T1 (1000 U/μL)	Invitrogen	Cat# EN0541
Bromophenol Blue	Fisher Scientific	Cat# MBX14107
Formamide	Promega	Cat# H5052
10x Tris-Borate-EDTA buffer	Sigma Aldrich	Cat# T4415-1L
TEMED	Invitrogen	Cat# 15524010
Ammonium persulfate	Sigma Aldrich	Cat# A3678-25G
GlycoBlue™ Coprecipitant (15 mg/mL)	Invitrogen	Cat# AM9516
Isopropyl Alcohol	Sigma Aldrich	Cat# PX1835
O'RangeRuler 20 bp DNA Ladder	Thermo Scientific	Cat# SM1323
Glycogen	Invitrogen	Cat# 10814-010
Critical Commercial Kits and Assays		
Qubit™ RNA High Sensitivity (HS) kit	Invitrogen	Cat# Q32852
PureLink™ RNA Mini kit	Invitrogen	Cat# 12183025
NEBNext® Poly(A) mRNA Magnetic Isolation Module	New England Biolabs	Cat# E7490L
RNA Clean & Concentrator-5	Zymo Research	Cat# R1016
Amicon® Ultra Centrifugal Filter, 3 kDa MWCO	Millipore	Cat# UFC8003
ProteoExtract® Protein Precipitation Kit	Millipore	Cat# 539180
Bio-Rad Protein Assay Dye Reagent Concentrate	Bio-rad	Cat# 5000006
TMTsixplex™ Isobaric Label Reagent Set, 5 x 0.8 mg	Thermo Scientific	Cat# 90066
Zombie Violet™ Fixable Viability Kit	BioLegend	Cat# 423113
Click-iT™ Plus Alexa Fluor™ 555 Picolyl Azide Toolkit	Invitrogen	Cat# C10642
Precision gRNA Synthesis Kit	Invitrogen	Cat# A29377
P3 Primary Cell 4D-Nucleofector™ X Kit S	Lonza	Cat# V4XP-3032
Lenti-X™ Concentrator	Takara	Cat# 631232
CellTiter-Glo® 2.0 Cell Viability Assay	Promega	Cat# G9242
NEBNext® Ultra™ II Directional RNA Library Prep Kit for Illumina	New England Biolabs	Cat# E7760L
Direct-zol RNA Microprep Kits	Zymo Research	Cat# R2060
5′ DNA Adenylation Kit	New England Biolabs	Cat# E2610S
Oligo Clean & Concentrator	Zymo Research	Cat# D4060
CircLigase ssDNA Ligase	Biosearch Technologies	Cat# CL4111K
DNA Clean & Concentrator-5	Zymo Research	Cat# D4003
Bioanalyzer High Sensitivity DNA kit	Agilent	Cat# 5067-4626
Qubit™ dsDNA High Sensitivity (HS) kit	Invitrogen	Cat# Q33231
TMTpro™ 18-plex Label Reagent Set, 5 mg	Thermo Scientific	Cat# A52045
Monarch Gel Extraction Kit	NEB	Cat# T1020S
Monarch PCR Purification Kit	NEB	Cat# T1030S
QIAGEN Plasmid Plus Midi Kit (100)	Qiagen	Cat# 12945
QIAGEN Plasmid Mini Kit (100)	Qiagen	Cat# 12125
Deposited Data		
GENCODE release M34 (GRCm39)	Frankish et al.[103]	https://www.gencodegenes.org/mouse/release_M34.html
TMT MS RAPIDASH and ribosome chromatographic purification[18] of E14 mESCs.	This manuscript	PXD054427

(*Continued on next page*)

Continued

REAGENT or RESOURCE	SOURCE	IDENTIFIER
TMT MS RAPIDASH and sucrose cushion of E14 mESCs.	This manuscript	PXD054298
label-free MS RAPIDASH of L36-FLAG and S17-FLAG E14 mESCs	This manuscript	PXD054300
label-free MS RAPIDASH of E12.5 mouse forebrain	This manuscript	PXD054303
TMT MS RAPIDASH of E12.5 mouse limbs, forebrain, and liver	This manuscript	PXD054304
RNA-seq comparing sucrose cushion ultracentrifugation and RAPIDASH samples	This manuscript	GSE274178
Ribosome profiling of hiNs	This manuscript	GSE274188
Original code to analyze RNA-seq and ribosome profiling data	This manuscript	https://zenodo.org/doi/10.5281/zenodo.13286233
Experimental Models: Cell Lines		
Mouse: E14 embryonic stem cells (E14-mESC)	Hooper et al.[104]	N/A
Rpl36-FLAG E14-mESC	Simsek et al.[5]	N/A
Rps17-FLAG E14-mESC	Simsek et al.[5]	N/A
PC-3	ATCC	Cat# CRL-1435
A549	ATCC	Cat# CCL-185
293T	ATCC	Cat# CRL-3216
P493-6	Helmholtz Center Munich, Munich, Germany[105]	N/A
COS1	ATCC	Cat# CRL-1650
H1-human embryonic stem cells (H1-hESCs)	Thomson et al.[106], WiCell	Cat# WA01
Murine bone marrow-derived macrophages (BMDMs)	This manuscript	N/A
HoxB8-immortalized murine progenitor cells	Lab of Averil Ma at UCSF	N/A
Experimental Models: Organisms		
FVB/NJ mouse	The Jackson Laboratory	Cat# 001800
C57BL/6J mouse	The Jackson Laboratory	Cat# 000664
Oligonucleotides		
siGENOME Non-Targeting Control siRNAs #2	Horizon	Cat# D-001210-02-05
siGENOME Mouse Dhx30 siRNA SMARTPool	Horizon	Cat# M-053738-00-0005
Recombinant DNA		
pCE-mp53DD	Addgene	Cat# 41856
pCAG-V5-Dhx30	This manuscript	N/A
pCAG-ΔOB-fold	This manuscript	N/A
pCAG-R805/8A	This manuscript	N/A
pCAG-ΔdsRBD-1	This manuscript	N/A
pCAG-ΔdsRBD-1/2	This manuscript	N/A
pMD2.G	Addgene	Cat# 12259
psPAX2	Addgene	Cat# 12260
FUW-TetO-Ngn2-T2A-Bsd	Zhang et al.[57]	N/A
FUW-rtTA	Zhang et al.[57]	N/A
pHR-TRE3G-LLPH-FLAG-P2A-BFP	This manuscript	N/A
pHR-TRE3G-GFP-FLAG-P2A-BFP	This manuscript	N/A

(*Continued on next page*)

Continued

REAGENT or RESOURCE	SOURCE	IDENTIFIER
Software and Algorithms		
Xcalibur™ Software	Thermo Scientific	v3.0
Protein Prospector	Clauser et al.[107]	N/A
MaxQuant	Cox and Mann[28]	v2.4.2.0
Perseus	Tyanova et al.[29]	v2.0.11
CellQuest Pro	BD Biosciences	N/A
FlowJo	BD Biosciences	v10
Fiji	Schindelin et al.[108]	v2.35
SNT	Arshadi et al.[109]	v4.1.2
PeakChart	Brandel	v1.02
Cutadapt	Martin[110]	v4.7; v2.4
STAR	Dobin et al.[111]	v2.7.11b
gffread	Pertea and Pertea[112]	v0.12.7
Salmon	Patro et al.[113]	v1.10.3 and v1.4.0
DESeq2	Love et al.[114]	v1.44.0
FASTX-Toolkit	http://hannonlab.cshl.edu/	v0.0.14
UMI-tools	Smith et al.[115]	v1.01
Bowtie 2	Langmead and Salzberg[116]	v2.3.4.3
edgeR	Robinson et al.[117]	v.3.42.4
limma	Ritchie et al.[118] and Law et al.[119]	v3.56.2
Other		
DNA LowBind Tubes	Eppendorf	Cat# 10051232
Pierce™ Micro-Spin Columns	Thermo Scientific	Cat# 89879
1 mL, Open-Top Thickwall Polycarbonate Tube	Beckman Coulter	Cat# 343778
Falcon® Round-Bottom Polypropylene Test Tubes With Cap	Corning	Cat# 352059
Pierce™ Centrifuge Columns, 5 mL	Thermo Scientific	Cat# 89897
13.2 mL, Thinwall Polypropylene Tubes, 14 x 89mm - 50Pk	Beckman Coulter	Cat# 331372
C18 ZipTip	Millipore	Cat# ZTC18S960
OMIX C18 pipette tips	Agilent	Cat# A57003100
C18 SepPak	Waters	Cat# WAT051910
Mobicol column	Boca Scientific	Cat# M1050
Mobicol filter (Small/Lower), 10 μm pore size	Boca Scientific	Cat# M2110
96 Well Black Polystyrene Microplate	Corning	Cat# CLS3603
20G x 1.5" hypodermic needles	Santa Cruz Biotechnology	Cat# sc-359535
Costar® Spin-X® centrifuge tube filters, 0.22 μm pore cellulose acetate membrane	Corning	Cat# 8160
Trans-Blot® Turbo™ Transfer System	Bio-Rad	Cat# 1704150
ChemiDoc™ XRS+ System	Bio-Rad	Cat# 1708265
TLA120.2 rotor	Beckman Coulter	Cat# 357656
Gradient Master	Biocomp Instruments	Cat# 108
Qubit™ 4 Fluorometer	Invitrogen	Cat# Q33238
SW 41 Ti Swinging-Bucket Rotor	Beckman Coulter	Cat# 331362
L8-80M ultracentrifuge	Beckman Coulter	N/A
Density Gradient Fraction System	Brandel	Cat# BR-188
NanoDrop™ 2000c Spectrophotometer	Invitrogen	Cat# ND-2000C

(*Continued on next page*)

Continued

REAGENT or RESOURCE	SOURCE	IDENTIFIER
Acquity UPLC (ultra performance liquid chromatography) M-class system	Waters	N/A
Orbitrap Elite Mass Spectrometer	Thermo Scientific	N/A
PicoFrit SELF/P PicoTip emitter	New Objective	Cat# PF360-75-15-N-5
2 μm, 50 μm x 150 mm, EASY-Spray™ C18 Reversed Phase HPLC Column	Thermo Scientific	Cat# ES801
2 μm 75 μm x 50 cm PepMap RSLC C18 EASY-Spray™ column	Thermo Scientific	Cat# ES903
Orbitrap Eclipse Tribrid Mass Spectrometer	Thermo Scientific	N/A
LSR II Flow Cytometer	BD Biosciences	N/A
FACSAria III	BD Biosciences	N/A
4D-Nucleofector® X Unit	Lonza	Cat# AAF-1003X
LSM 780 Confocal Microscope	Zeiss	N/A
Agilent 2100 Bioanalyzer	Agilent	N/A
SW 60 Ti Swinging-Bucket Rotor	Beckman Coulter	Cat# 335649
Orbitrap Exploris™ 480	Thermo Scientific	N/A
L8-70M ultracentrifuge	Beckman Coulter	N/A
Fractionator base unit	Biocomp Instruments	Cat# 152

EXPERIMENTAL MODEL AND STUDY PARTICIPANT DETAILS

Mice

Embryonic tissue-related experiments

Mouse protocols were reviewed and approved by the Stanford Administrative Panel on Laboratory Animal Care (APLAC, protocol #27463). Mice were housed at Stanford University with standard conditions: 12 hour light-dark cycle, ambient temperatures between 68 and 79°F, humidity between 30 and 70%, free access to chow, acidified water, and filtered air flow. Wild-type FVB/NJ mice were purchased from Jackson Laboratories. For timed pregnancies, one male and one female were housed together, and the female was checked daily for plugs. The day the vaginal plug was observed was considered embryo stage E0.5. At E12.5, the pregnant female was euthanized by CO_2 inhalation followed by cervical dislocation to collect the embryos.

Macrophage-related experiments

Wild-type C57BL/6J mice were purchased from Jackson Laboratories. Animals were housed in a specific-pathogen free environment in the Laboratory Animal Research Center at UCSF. All experiments conformed to ethics and guidelines approved by the UCSF Institutional and Animal Care and Use Committee.

Cells

Wild-type E14 mouse embryonic stem cells (XY) (mESCs) were a gift from Barbara Panning's lab (UCSF). The Rpl36-FLAG mESC and Rps17-FLAG mESC lines were as described previously.[5] All mESC lines were maintained on cell culture dishes coated with 0.1% (w/v) gelatin (EmbryoMax® 0.1% Gelatin Solution, Millipore, ES-006-B) in sterile milliQ water in cell culture incubators at 5% CO_2, 37°C in mESC media containing KnockOut™ DMEM (Dulbecco's Modified Eagle Media; Thermo Fisher Scientific, 10829-018) with 15% ES quality fetal bovine serum (FBS) (Millipore, ES-009-B), 2 mM EmbryoMax® L-glutamine (Millipore, TMS-002-C), 1x EmbryoMax® Penicillin/Streptomycin (Millipore, TMS-AB2-C), 1x EmbryoMax® MEM, non essential amino acids (Millipore, TMS-001-C), 0.055 mM 2-mercaptoethanol (Gibco, 21985023), and 10^3 U/mL mouse leukemia inhibitory factor (LIF) protein (Gemini, 400-495). Specific experiments noted below grew mESCs on cell culture dishes coated with a 0.1% (w/v) gelatin (Sigma Aldrich, G9391) solution in sterile milliQ water prepared in lab. Cells were typically passaged every other day at a 1:6 ratio for maintenance. On days where the cells were not split, the media was changed to fresh mESC media.

PC3 cells were maintained in Ham's F12K media (Gibco, 21127022) with 10% heat-inactivated FBS (Gibco, 10082147), 100 U/mL Penicillin, 100 μg/mL Streptomycin (Gibco, 15140122) in cell culture incubators at 5% CO_2, 37°C.

P493-6 cells were cultured in RPM1-1640, 100 U/mL Penicillin, 100 μg/mL Streptomycin, 10% tetracycline-free fetal calf serum (FCS), and 50 μM beta-mercaptoethanol (all from Gibco). Cells were cultured at 37°C, 5% CO_2.

A549 cells were cultured at 37°C, 5% CO_2 in F12K media with 10% FBS, 100 U/mL Penicillin, and 100 μg/mL Streptomycin.

293T and COS1 cells were grown in DMEM (Gibco, 11965-092), 10% FBS, 100 U/mL Penicillin, 100 μg/mL Streptomycin at 37°C, 5% CO_2.

H1-human embryonic stem cells (XY) (hESCs) were cultured in mTeSR1 media (STEMCELL Technologies, 85850) on plastic dishes coated with Geltrex (Gibco, A1413302). H7-hESCs were passaged 1:10 using Accutase (Gibco, A1110501) and cultured overnight in mTeSR1 supplemented with 2 μM thiazovivin (Tocris, 3845) to promote cell survival.

For differentiation of primary bone marrow derived-macrophages (BMDMs), whole bone marrow from femurs and tibias was plated on polystyrene dishes (five 10-cm dishes per mouse, either male or female) for six days in complete DMEM (10% heat-inactivated FBS, 10 mM HEPES (Gibco, 15630080), 100 U/mL Penicillin, 100 μg/mL Streptomycin (Gibco), 1 mM Sodium Pyruvate (Gibco, 11360070), 1x Glutamax (Gibco, 35050061), and 55 μM 2-mercaptoethanol (Gibco)) supplemented with 10% mCSF medium derived from 3T3-mCSF cells (a kind gift from Hiten Modani's lab at UCSF). BMDMs were replated overnight on tissue-culture-treated dishes prior to activation with LPS (100 ng/mL, Invivogen) or poly(I:C) (2 μg/mL, Invivogen). All plates were kept in cell culture incubators at 5% CO_2, 37°C.

For some experiments, macrophages were generated from HoxB8-immortalized murine progenitor cells (a kind gift from Averil Ma's lab at UCSF). HoxB8 cells were maintained in an undifferentiated state in complete RPMI (10% heat-inactivated FBS, Glutamax, HEPES, Penicillin/Streptomycin) supplemented with β-estradiol (1 μM) and 5% Flt3L medium derived from B16-FLT3 cells. For macrophage differentiation, HoxB8 progenitor cells were washed twice in complete RPMI without β-estradiol and plated on polystyrene dishes in complete DMEM supplemented with 10% mCSF medium for six days. On day six, macrophages were replated onto tissue-culture treated dishes overnight prior to activation. Cells were maintained in cell culture incubators at 5% CO_2, 37°C.

Cell lines did not undergo further authentication.

METHOD DETAILS

Western blotting for mESCs, human cells, and mouse embryonic tissues

Related to Figures 1, 2, 3, 4, S1, S3, and S4. Protein samples were resuspended in 1X sodium dodecyl sulfate (SDS) Laemmli buffer (Fisher Scientific, 50-196-784). Protein samples were then denatured in a thermocycler for 10 minutes at 95°C. Sucrose gradient fractionation samples were separated on 4–20% Criterion™ TGX™ Gels (Bio-Rad, 5671095), and others were separated on 4–20% Mini-PROTEAN® TGX™ Precast Protein Gels (Bio-Rad, 456-1096). The gels were run with 1x Tris/Glycine/SDS buffer (Bio-Rad, 161-0772) until the bromophenol blue dye front reached the bottom of the gel. Unless otherwise stated, semi-dry transfer was performed using a Trans-Blot® Turbo™ RTA Midi (Bio-Rad, 170-4273) or Mini (Bio-Rad, 170-4272) PVDF Transfer Kit on a Trans-Blot® Turbo™ Transfer System (Bio-Rad, 1704150). Each transferred membrane was rinsed once with PBS (Fisher Scientific, BP2944100) + 0.1% (v/v) TWEEN® 20 (Sigma Aldrich, P9416-100ML) (PBST) and then blocked in 5% (w/v) bovine serum albumin (BSA; Sigma, A9647-100G) in PBST for 30 minutes in room temperature or overnight at 4°C. The membranes were rocked in primary antibody solutions in 5% (w/v) BSA, 0.02% (w/v) sodium azide (Sigma Aldrich, S2002-25G) in PBST overnight at 4°C. After the primary antibody incubation, the membrane was then washed four times with PBST for 5 minutes each time. HRP-conjugated anti-mouse (Cytiva, NA931-1ML) and anti-rabbit (Cytiva, NA934-1ML) secondary antibodies were diluted at 1:5000 in 5% milk in PBST. HRP-conjugated anti-goat antibody (R&D Systems, HAF019) was used at a 1:1000 dilution in 5% milk in PBST. The membranes were rocked in secondary antibody solutions for 1 hour at room temperature. The membrane was then washed again four times with PBST for 5 minutes each time. The membrane was then developed with Clarity Western ECL Substrate (Bio-Rad, 170-5061) or SuperSignal™ West Femto Maximum Sensitivity Substrate (Thermo Fisher Scientific, 34095) for at least 5 minutes before imaging it with a ChemiDoc XRS+ System (Bio-Rad, 1708265). The primary antibodies used in this paper are: Nup62 (Proteintech, 13916-1-AP); Atp5a1 (Proteintech, 14676-1-AP); Tom20 (Proteintech, 11802-1-AP); Rpl4 (Proteintech, 11302-1-AP); Rps5 (Abcam, ab58345); Rps26 (Proteintech, 14909-1-AP); Rps27 (Fisher Scientific, PIPA518092); Metap1 (R&D Systems, MAB3537-SP); Ufl1 (Bethyl Laboratories, A303-456A); Upf1 (Proteintech, 23379-1-AP); Ddx1 (Bethyl Laboratories, A300-520A); Nsun2 (Proteintech, 20854-1-AP); Dhx30 (Abcam, ab85687); Rpl29 (Abcam, ab88514); Pabp1 (Cell Signaling Technology, 4992); Naa15 (Sigma Aldrich, HPA023589-100UL), Rps19 (Abcam, ab181365); β-Actin (8H10D10) (Cell Signaling Technology, 3700S); Rps6 (Cell Signaling Technology, 2217); V5 Tag (Thermo Fisher, R960-25); GAPDH (D4C6R) (Cell Signaling Technology, 97166); Llph (Invitrogen, PA5-66207); Rps20 (Proteintech, 15692-1-AP); RPL8 (Proteintech, 16981-1-AP); and Elavl2 (Proteintech, 14008-1-AP).

Characterization of cysteine-charged sulfolink resin

mESC ribosome cushion pellet preparation

Related to Figure 1B. E14 mESCs were harvested when they were ~70% confluent. The old media was changed with the fresh mESC media 1 hour prior to harvest and then supplemented with 100 μg/mL cycloheximide (CHX; Sigma Aldrich, C7698-1G) for 3 minutes. The cells were then washed with pre-warmed Dulbecco's Phosphate-Buffered Saline (DPBS; Gibco, 14190-250) twice, trypsinized, and neutralized with cold mESC media; all solutions were supplemented with 100 μg/mL CHX. After neutralization, cells were then washed once with 100 μg/mL CHX in cold DPBS. All centrifugation steps were done at 200 x g at 4°C for 3 minutes. These mESC pellets were then flash frozen in liquid nitrogen for temporary storage at -80°C, or immediately lysed in 350 μL cold lysis buffer A (20 mM HEPES (Sigma Aldrich, H3375-100G), adjusted to pH 7.6 by KOH (Sigma Aldrich, 221473-500G) (HEPES-KOH), 15 mM magnesium acetate ($Mg(OAc)_2$) (Sigma Aldrich, M5661-250G), 60 mM NH_4Cl (Sigma Aldrich, A9434-500G), 1 mM dithiothreitol (DTT; Pierce, A39255), 100 μg/mL CHX, 1% Triton X-100 (Sigma Aldrich, T8787), 0.5% sodium deoxycholate (Sigma Aldrich, D6750), 8% glycerol (Sigma Aldrich, G9012-100ML), 20 U/mL TURBO DNase (Ambion, AM2238), 200 U/mL SUPERase·In™ RNase

Inhibitor (Ambion, AM2696), 1× Halt™ Protease and Phosphatase Inhibitor (Thermo Scientific, 78443), in nuclease-free water (Invitrogen, 10977015)) at 4°C for 30 minutes with occasional vortexing every 10 minutes. Lysates were cleared by sequential centrifugation at 800 ×g for 5 minutes, 800 ×g for 5 minutes, 8000 ×g for 5 minutes and 21,300 ×g for 5 minutes. Cleared supernatant were loaded onto 700 μL 1 M sucrose cushion buffer (20 mM HEPES-KOH, pH 7.6, 15mM $Mg(OAc)_2$, 60 mM NH_4Cl, 1 mM DTT, 100 μg/mL CHX, 200 U/mL SUPERase·In™ RNase Inhibitor, 1 M sucrose (Sigma Aldrich, 8510-500GM)) and centrifuge at 100,000 rpm at 4°C using a Beckman TLA120.2 rotor for 1 hour. Ribosome cushion pellets were gently washed and resuspended in 300 μL binding buffer (20 mM HEPES-KOH, pH 7.6, 15 mM $Mg(OAc)_2$, 60 mM NH_4Cl, 1 mM DTT, 100 μg/mL CHX, 200 U/mL SUPERase In RNase inhibitor, 20 U/mL TURBO DNase,) at 4 °C in a Thermomixer with 1,000 rpm for 1 hour. Ribosomal RNA concentration was quantified by Qubit™ RNA HS kit (Invitrogen, Q32852) following manufacturer's instructions using Qubit™ 4 Fluorometer (Invitrogen, Q33238).

Isolation of poly(A) RNA

Total RNA was first extracted from mESCs. A frozen cell pellet from a confluent 10-cm plate of mESCs was thawed on ice, resuspended in 1 mL cold TRIzol, and incubated at room temperature for 5 minutes. Then, 200 μL chloroform (Sigma Aldrich, 3150) was added, and the tube was manually shaken for 15 seconds. The tube was then incubated at room temperature for 2 minutes. The sample was centrifuged at 12,000 ×g for 15 minutes at 4°C. Then, 510 μL top aqueous layer was pipetted out into a fresh, chilled tube. This was then mixed with 510 μL 70% ethanol (Gold Shield, 412804). The RNA was purified using a Purelink RNA Mini kit (Thermo Fisher, 12183025) following the manufacturer's instructions with the following exceptions. The sample was transferred to a PureLink spin cartridge and centrifuged at 12,000 ×g for 15 seconds at room temperature. The flowthrough was discarded, and the cartridge was reinserted into the same collection tube. This centrifugation step was repeated so the entire sample was bound to the cartridge. Washes were performed according to the manufacturer's protocol. To elute, the cartridge was inserted into a DNA lo-bind tube, and 50 μL RNase-free water was added to the center of the cartridge. The sample was incubated at room temperature for 1 minute. Finally, the sample was centrifuged at 12,000 ×g for 1 minute at room temperature. The resulting eluate was stored at -80°C.

Poly(A) RNA was enriched using NEBNext® Poly(A) mRNA Magnetic Isolation Module (New England Biolabs (NEB), E7490L) according to the manufacturer's instructions with some modifications. Each sample that was destined to be incubated with cysteine-charged resin derived from 8 poly(A) reactions with 5 μg RNA each. All steps except for the elution were performed as described in the manufacturer's protocol up until the final elution. For the final elution, the beads from 8 reactions were combined and resuspended in 60 μL RNase-free water by pipetting six times. The sample was incubated at 80°C for 2 minutes and then cooled to 25°C to elute the poly(A) RNA. The tube was then placed on a magnetic rack for about 2 minutes, or until the solution was clear. Then, 57 μL of supernatant was collected and stored at -80°C.

Chromatography with cysteine-charged resin

To perform the cysteine-charged sulfolink characterization, sucrose cushion pellet and poly(A) samples were thawed on ice, and the RNA concentrations were measured using a Qubit RNA high sensitivity (HS) assay kit. Samples were diluted to RNA concentrations in the range of 4.53 - 7.07 ng/μL using RNase-free water and then kept on ice while the resin was prepared.

First, 500 μL Sulfolink coupling resin (Thermo Fisher, 20402) was added to a falcon tube and centrifuged at 850 ×g for 1 minute at room temperature, and the supernatant was decanted. The resin was then resuspended in 1 resin volume (e.g., 500 μL) coupling buffer (50 mM Tris-HCl, pH 8.5 (Fisher Scientific, BP153-500), 5 mM ethylenediaminetetraacetic acid (EDTA; Invitrogen, AM9262)), and then centrifuged at 850 ×g for 1 minute at room temperature. The supernatant was decanted, and the resin was washed twice more with 1 volume (i.e., 500 μL) coupling buffer as previously described. After the last wash was decanted, the resin was resuspended in 1 volume (i.e., 500 μL) 50 mM L-cysteine (Sigma Aldrich, 168149-25G) in coupling buffer and left on a rocker at room temperature for at least one hour. Then, the resin was centrifuged at 850 ×g for 1 minute at room temperature. The supernatant was decanted, and then the resin was resuspended in 1 volume (i.e., 500 μL) coupling buffer and centrifuged at 850 ×g for 1 minute at room temperature. The supernatant was decanted, and this washing step was repeated twice more. The resin was then washed three times with 2 volumes (i.e., 1 mL) priming buffer (20 mM HEPES-KOH, pH 7.6, 15 mM $Mg(OAc)_2$, 60 mM NH_4Cl, 1 mM DTT, and 100 μg/mL CHX) by resuspending the resin in the priming buffer, centrifuging at 850 ×g for 1 minute, and decanting the supernatant. The wash with priming buffer was repeated twice more, and then the resin was resuspended in 1 volume (i.e., 500 μL) priming buffer. For each sample, 12.5 μL resin slurry was added to a micro-spin column (Thermo Fisher Scientific, 89879), which was placed in a DNA lo-bind tube. The caps were removed. The micro-spin columns were centrifuged at 1,000 ×g for 1 minute at room temperature to remove the priming buffer from the resin, and then the bottom caps were put on again.

For each sucrose cushion pellet or poly(A) RNA sample, 42 - 48 μL was added to the resin for a total of 190 - 339 ng of RNA. The top caps were screwed on, and the columns were briefly vortexed to mix. The capped columns were put in DNA lo-bind tubes and put on ice for 15 minutes under foil. Then, the caps were removed, the columns were moved to fresh DNA lo-bind tubes, and the samples were centrifuged at 1,000 ×g for 1 minute at room temperature. The bottom caps were replaced, the flowthroughs were re-applied to the resin, and the top caps were screwed on. The columns were again briefly vortexed to mix, and then they were returned to the DNA lo-bind tubes and left on ice for 15 minutes under foil. Then, the caps were removed, and the samples were centrifuged at 1,000 ×g for 1 minute at room temperature. The flowthroughs were kept on ice, and the bottom caps were put on to the columns, which were moved to fresh DNA lo-bind tubes. The resin was then washed by adding 1 volume, (i.e., 12.5 μL) priming buffer to each column, capping the columns, vortexing the columns briefly to mix, uncapping the columns and returning them to their DNA lo-bind tubes, and centrifuging the samples at 1,000 ×g for 1 minute at room temperature. This washing step was repeated three more times

for a total of four washes. The bottom caps of the columns were put on, and the columns were moved to fresh DNA-lo bind tubes. To elute, 12.5 μL elution buffer (20 mM HEPES-KOH, pH 7.6, 15 mM $Mg(OAc)_2$, 500 mM KCl (Invitrogen, AM9010), 1 mM DTT, and 100 μg/mL CHX) was added to each column. The top caps were screwed on, and the columns were vortexed briefly to mix and then returned to their DNA lo-bind tubes. The samples were then rested on ice for 2 minutes under foil. Finally, the caps were removed, and the eluates were collected by centrifuging at 1,000 ×g for 1 minute at room temperature. The eluates were kept on ice.

After collecting eluate, 50 μL TRIzol (Invitrogen, 15596026) was added to the resin and incubated at room temperature for 5 min. TRIzol was collected by centrifuging at 1,000 ×g for 1 min at room temperature. RNA was extracted from each resin using RNA Clean and Concentrator-5 kit (Zymo Research, R1016). The RNA was eluted in 10 μL RNase-free water, and RNA concentrations were measured by Qubit RNA HS Kit.

Characterization of cysteine-charged sulfolink resin binding using 80S ribosomes from samples treated with puromycin, RNase A, or high salt

Related to Figures 1C and S1C–S1E. E14 mESCs were grown in 15-cm plates coated with 0.1% (w/v) gelatin (Sigma Aldrich, G9391) to ~80% confluency. The media was changed to fresh mESC media 1 hour prior to harvesting. The cells were then incubated with 100 μg/mL CHX in mESC media for 3 minutes at 37°C, 5% CO_2. The media was removed, and the cells were rinsed once with 10 mL 100 μg/mL CHX DPBS, lifted with 100 μg/mL CHX in 0.05% trypsin-EDTA (Thermo Fisher, 15400-054, diluted with DPBS), and pelleted by centrifuging at 200 ×g for 3 minutes at 4°C. The cell pellets were flash frozen and stored at -80°C.

Cells were then thawed on ice and lysed using 600 μL cold lysis buffer A and clarified as in "Characterization of cysteine-charged sulfolink resin, mESC ribosome cushion pellet preparation." For samples that were going to be treated with RNase A, the lysis buffer omitted SUPERase·In™ RNase Inhibitor.

RNase A treatment was performed by adding 3 μg RNase A per 600 μg RNA and incubating at room temperature on a head-to-tail rotor for 30 minutes. Digestion was stopped by adding SUPERase·In™ RNase Inhibitor to a final concentration of 200 U/mL.

To isolate untreated 80S and RNase A-treated 80S ribosomes, clarified lysates were loaded onto sucrose gradients (10-50% (w/v) sucrose, 20 mM Tris pH 7.5, 100 mM NaCl,15 mM $MgCl_2$,100 μg/mL cycloheximide, made on a Biocomp Model 108 Gradient Master) and centrifuged in a Beckman SW41 rotor at 40,000 rpm for 2.5 hours at 4°C in a Beckman L8-80M ultracentrifuge. Sucrose gradients were then fractionated on a density gradient fraction system (Brandel, BR-188) using PeakChart software with continuous A260 measurement. The 80S peak fractions of each treatment were collected and buffer exchanged to priming buffer using 3 kDa Amicon® Ultra Centrifugal Filters (Sigma Aldrich, UFC8003). Buffer exchange was performed by filling the column to the top with priming buffer and centrifuging at 4,000 rpm at 4°C until the sample did not further condense. This procedure was repeated two more times.

To purify puromycin-treated 80S ribosomes, buffer-exchanged (to priming buffer) 80S ribosomes from the untreated sample were combined with 1 mM puromycin (Invivogen, ant-pr-1) and 100 mM GTP (Thermo Fisher Scientific, R1461) and incubated at 37°C with rotation for 30 minutes. The reaction mixture was then loaded onto a 1 M sucrose cushion (cushion buffer) and centrifuged at 100,000 rpm at 4°C for 1 hour using a TLA120.2 rotor. The resulting cushion pellet contained the nascent polypeptide-depleted ribosomes.

Untreated, puromycin-treated, and RNase A-treated 80S ribosomes were further analyzed by western blotting to probe for RPs and control RAPs to confirm the treatments had worked as expected. To do this, equal amounts of RNA for each sample were combined with 2x Laemmli buffer and denatured by boiling at 95°C for 5 minutes with shaking at 1,000 rpm. Sample sets were loaded in duplicates onto a 4-20% TGX Criterion gel, and the proteins were separated with constant voltage. Transfer of the proteins to a PVDF membrane was performed as in "Western blotting for mESCs, human cells, and mouse embryonic tissues." The membrane was blocked in 5% milk 1x PBST by rocking at room temperature for 1 hour and subsequently washed three times with 1x PBST. Then the membrane was cut so that individual pieces could be probed by western blotting for RP or RAP markers. One sister blot was probed for Naa15, Pabp1, and Rps5. The other sister blot was probed for Metap1. This was done by rocking the membrane pieces overnight at 4°C in 5% BSA 0.02% NaN_3 1x PBST containing the primary antibody dilutions: 1:1,000 anti-Naa15, 1:1,000 anti-Pabp1, 1:1,000 anti-MetAP1, or 1:5,000 anti-Rps5. Then, the membranes were washed. For Naa15, Pabp1, and MetAP1, the membranes were washed 3 times for 10 minutes each time at room temperature in 1x PBST. The Rps5 membrane was washed 4 times for 5 minutes each time at room temperature. The Naa15 and Pabp1 membranes were rocked in 1:5,000 anti-rabbit HRP in 5% milk 1x PBST for one hour at room temperature. The MetAP1 and Rps5 membranes were rocked in 1:5,000 anti-mouse HRP in 5% milk 1x PBST. Washes for each membrane were performed as after the primary antibody incubation. The Naa15, Pabp1, and MetAP1 blots were developed with Femto reagent and then imaged. The Rps5 membrane was developed with Clarity reagent and then imaged. The MetAP1 membrane was then washed twice with 1x PBST for 5 minutes each time and stripped by rocking in the Restore™ PLUS Western Blot Stripping Buffer (Thermo Fisher Scientific, 46430) for 15 minutes at room temperature. The membrane was then washed 4 times for 5 minutes each time with 1x PBST and then blocked by rocking in 5% milk 1x PBST for 1 hour at room temperature. The membrane was washed 3 times with 1x PBST for 5 minutes each time, and then it was rocked in 1:3,000 anti-Rpl4 in 5% BSA 0.02% NaN_3 1x PBST overnight at 4°C. The next day, the membrane was washed 4 times for 5 minutes each time with 1x PBST, rocked in 1:5,000 anti-rabbit HRP in 5% milk 1x PBST, washed 4 times for 5 minutes each time with 1x PBST, developed with Clarity reagent, and imaged.

To purify high salt-washed 80S ribosomes, mESC lysate and cushion pellet were prepared as previously described. The cushion pellet, which contained the ribosomes, was resuspended in high salt binding buffer (20 mM HEPES, adjusted to pH 7.6 using KOH,

15 mM $Mg(OAc)_2$, 0.5 M NH_4Cl, 1 mM DTT, 200 U/mL SUPERase·In™ RNase Inhibitor). The resuspended cushion pellet material was loaded onto a high salt sucrose gradient (10-45% (w/v) sucrose, 20 mM Tris pH 7, 0.7 M NH_4Cl, 15 mM $MgCl_2$) in a Beckman SW41 rotor at 40,000 rpm for 2.5 hours at 4°C in a Beckman L8-80M ultracentrifuge to specifically enrich for 80S ribosomes.The 80S fraction was collected, buffer-exchanged to priming buffer using a 3 kDa Amicon® Ultra Centrifugal Filter as above.

Untreated and high salt-treated 80S ribosomes were also analyzed by western blotting. Samples were processed for western blotting as for the untreated, puromycin-treated, and RNase A-treated sample comparison. As before, samples were run in duplicate so there were sister blots. The membrane was blocked and washed as for the untreated, puromycin-treated, and RNase A-treated sample comparison. The membrane was then cut to probe for individual proteins. One set of samples for one of the sister blots was probed for Naa15 and MetAP1 as above. The other sister blot was probed for Pabp1 by blocking with 5% milk 1x PBST for 1 hour at room temperature, washing the membrane 3 times with 1x PBST for 5 minutes each time, and then proceeding with the rest of the western procedure as in "Western blotting for mESCs, human cells, and mouse embryonic tissues." The primary antibody solution was 1:1,000 anti-Pabp1 in 5% BSA 0.02% NaN_3 1x PBST, and the secondary antibody solution was 1:5,000 anti-rabbit HRP in 5% milk 1x PBST. The blot was developed with Clarity reagent. Then, the MetAP1 membrane piece and the corresponding lower membrane piece for the sample set probed with Pabp1 antibody were both washed twice with 1x PBST for 5 minutes each time and then rocked in 0.1% NaN_3 in 1x PBST for 45 minutes at room temperature to inactivate HRP. The membranes were washed 4 times with 1x PBST for 5 minutes each time, and then blocking and probing with antibodies was performed as in "Western blotting for mESCs, human cells, and mouse embryonic tissues." The MetAP1 membrane was reprobed using an antibody against Rpl4, and the other membrane piece was used to probe for Rps5. The procedure to probe for these RPs was the same as the procedure used to probe for Rpl4 for the untreated, puromycin-treated, and RNase A-treated 80S ribosomes.

Validated 80S ribosome samples were divided into 3 technical replicates for each treatment and then subjected to chromatography with the sulfolink resin as in "Characterization of cysteine-charged sulfolink resin." The RNA in the flowthrough, eluate, and TRIzol-extracted (representing the RNA that remained bound to the resin after the elution step) samples was measured by a Qubit RNA HS Kit. To generate the bar graphs in Figures 1C and S1E, the RNA in the eluate and TRIzol-extracted resin samples was summed and divided by the amount of input RNA to represent the fraction of RNA that had bound to the resin. Then, this fraction was divided by the average of the fraction of input RNA that was bound to the resin for the untreated sample to represent the fraction of 80S ribosomes bound to the resin relative to the untreated control. Error bars represent +/- standard error of the mean (SEM), where the propagated standard error was calculated using average errors.

RAPIDASH for E14 mouse embryonic stem cells

Harvest and cytoplasmic lysis

Related to Figure 1. Approximately 15 x 10^6 cells each of FLAG-tagged S17 and FLAG-tagged L36 mESCs as characterized previously[5] were seeded onto 15-cm plates (1:4 ratio from ~80% confluent plate). After one day, the media was replaced with 18 mL fresh mESC media. One hour post-media change, 2 mL 1 mg/mL CHX in mESC media was added to each 15-cm plate for a final concentration of 100 μg/mL CHX, and the plates were returned to the cell culture incubator for 3 minutes. The cells in each 15-cm plate were rinsed twice with pre-warmed 10 mL 100 μg/mL CHX in DPBS and were dissociated with 4 mL 100 μg/mL CHX, 0.05% trypsin-EDTA solution in DPBS. The plates were returned to the incubator briefly, after which the trypsin solution was quenched by adding 4 mL 100 μg/mL CHX in cold mESC media. The cells were pelleted in a tabletop centrifuge at 200 ×g at 4°C for 3 minutes, and the supernatant was aspirated out. Each pellet was washed once with 2 mL cold 100 μg/mL CHX in DPBS, transferred to a 2 mL tube, and then pelleted again in a tabletop centrifuge at 200 ×g at 4°C for 3 minutes. The supernatant was aspirated out, and each pellet was flash frozen in liquid nitrogen and stored at -80°C. Each pellet was lysed in 400 μL cold lysis buffer A. Cells were then lysed by vortexing at high speed for 30 seconds and putting them back on ice for 30 seconds. This was repeated another two times for a total of 3 minutes. The samples were then incubated on ice for 30 minutes and vortexed briefly for 10 seconds every 10 minutes. The cytoplasmic fraction was enriched by centrifuging the lysates twice at 800 ×g for 5 minutes at 4°C, then once at 8,000 ×g for 5 minutes at 4°C, and finally once at 20,817 ×g for 5 minutes at 4°C, with the supernatants being moved to fresh chilled tubes after each centrifugation.

Sucrose cushion ultracentrifugation

High density complexes were enriched by sucrose cushion ultracentrifugation. To do this, 300 μL of cytoplasmic lysate from each sample was layered onto 700 μL of sucrose cushion buffer in a polycarbonate centrifuge tube (Beckman Coulter, 343778) and centrifuged using a TLA120.2 rotor at 100,000 rpm for 1 hour at 4°C.

Preparation of L-cysteine charged sulfhydryl resin

The amount of L-cysteine charged sulfhydryl resin required for each experiment was prepared while the samples were undergoing sucrose cushion ultracentrifugation. Per sample, 1 mL of SulfoLink™ coupling resin slurry was pipetted into a polypropylene tube (Corning, 352059), which was used in order to minimize resin loss during decanting. The slurry was initially centrifuged at 800 ×g for 1 minute at 4°C to pellet the resin, and the storage solution was decanted. The resin was then washed three times by adding a volume of cold coupling buffer equal to twice the bed volume, resuspending the resin by inverting gently, centrifuging at 800 ×g for 1 minute at 4°C, and decanting the supernatant after each centrifugation. Afterwards, a volume of 50 mM L-cysteine in coupling buffer equal to twice the bed volume was added to the resin. The tube was wrapped in aluminum foil and then rocked for 1 hour on a platform rocker at room temperature. The resin was then centrifuged at 800 ×g for 1 minute at 4°C, and the supernatant was decanted to collect the L-cysteine charged sulfhydryl resin. The charged resin was washed three times with cold priming buffer. For each

wash, cold priming buffer with four times the bed volume was added to the resin, which was resuspended by gently inverting the tube and then collected by centrifuging at 800 ×g for 1 minute at 4°C and decanting the supernatant. After the final wash, the charged resin was resuspended in a volume of the cold priming buffer equal to twice the bed volume, 1.5 mL charged resin slurry was aliquoted into one 5 mL spin column (Thermo Scientific, 89897) for each sample. Charged resin can be stored overnight at 4°C.

Affinity enrichment with L-cysteine charged sulfolink resin

After the sucrose cushion ultracentrifugation step, the supernatant was removed by pipetting with a P1000 micropipette without disturbing the pellet, which contains high density protein complexes. Each pellet was dislodged with a pipette tip and resuspended in 1 mL of cold binding buffer by pipetting for 30 seconds. The tube was then sealed with parafilm wrap and shaken on a thermomixer at 1,000 rpm for 30 minutes at 4°C to further resuspend the protein. Immediately prior to incubation, the twist-off bottoms of the spin columns containing the charged resin were snapped off, and the columns were placed in 15 mL falcon tubes. The columns were then centrifuged at 1,000 ×g for 1 minute at 4°C to remove the priming buffer and subsequently capped with the provided bottom closures. The priming buffer was discarded. Then, for each sample, half of the resuspended protein pellet was transferred into a charged resin-containing spin column. The other half of each sample was retained to analyze the sucrose cushion ultracentrifugation step. The spin columns were flicked several times to mix and then incubated on ice for 15 minutes under foil. The bottom closures were then removed, and the flowthroughs were collected by centrifuging at 1,000 ×g for 1 minute at 4°C. The spin columns were capped with the bottom closures and replaced into the 15 mL falcon tubes, and the flowthroughs were added back to their respective resins. The resin was resuspended by flicking the spin columns and then incubated for another 15 minutes on ice under foil. The bottom closures were removed, the centrifugation step was repeated, and the flowthroughs were set aside for other analyses. The resin in each spin column was then washed with a volume of cold priming buffer equal to twice the bed volume by capping the spin column with a bottom closure and inverting by hand several times. The bottom closures were then removed, and the columns were centrifuged again at 1,000 ×g for 1 minute at 4°C to discard the wash buffer. This washing step was repeated three more times. After the final wash, the bottom closures were reattached to the columns. Each sample was then eluted by adding a volume of cold elution buffer equal to half the bed volume, resuspending the resin by flicking the tubes gently, incubating on ice for 2 minutes under foil, and centrifuging the samples at 1,000 ×g for 1 minute at 4°C. The elution step was repeated three more times with volumes of fresh elution buffer equal to half the bed volume each time. All four elutions for each sample were pooled together.

Sucrose gradient fractionation for RAPIDASH characterization

Related to Figures S1A and S1B. For the gradient in Figure S1A, two 15-cm plates of E14 mESCs were grown and harvested as described in "RAPIDASH for E14 mouse embryonic stem cells - Harvest and cytoplasmic lysis." Both cell pellets were flash frozen in liquid nitrogen. The cytoplasmic lysate for Figure S1A was derived from these cell pellets, which were lysed and clarified as in "RAPIDASH for E14 mouse embryonic stem cells."

RNA concentrations were measured using a NanoDrop™ 2000c Spectrophotometer (Invitrogen, ND-2000C) to normalize the amount of RNA loaded for each sample. Linear sucrose gradients (10-45% sucrose (w/v), 20 mM Tris-HCl pH 7.5 (Invitrogen, AM9010), 15 mM $MgCl_2$ (Invitrogen, AM9010), 150 mM NaCl (Invitrogen, AM9010), 1 mM DTT, 100 μg/mL CHX, in nuclease-free water) were made in 14x89 mm open-top thinwall polypropylene centrifuge tubes (Beckman Coulter, 331372) using a gradient maker (Biocomp, 108). Before layering the samples onto the gradient, 200 μL sucrose gradient solution was removed from each centrifuge tube; then, 180 μg of RNA was loaded. The samples were centrifuged using a SW 41 Ti swinging bucket rotor (Beckman Coulter, 331362) at 40,000 rpm for 2.5 hours at 4°C.

Fractions were collected for 30 seconds each using the Density Gradient Fraction System with a flow rate of 1.5 mL/minute. Proteins were precipitated from fractionated samples as described above, except 600 μL -20°C Precipitation Agent was added to each fraction as described in "Mass spectrometry of unlabeled tryptic digests - Protein precipitation." After the protein pellets were dried, they were immediately prepared for western blotting.

For the gradients in Figure S1B, E14 mESCs were grown at the 10-cm plate scale until approximately 50-60% confluent. Cells were harvested from three 10-cm plates as in "Characterization of cysteine-charged sulfolink resin binding using 80S ribosomes from samples treated with puromycin, RNase A, or high salt," and the three cell pellets were flash frozen in liquid nitrogen. The cell pellets were subsequently thawed on ice, lysed in 500 μL lysis buffer A, and clarified as in "Characterization of cysteine-charged sulfolink resin binding using 80S ribosomes from samples treated with puromycin, RNase A, or high salt." Each of the three lysate samples below were approximately 600 μg of RNA at a 1.2 μg/μL concentration.

The lysate from one pellet underwent the entire RAPIDASH protocol as in "RAPIDASH for E14 mouse embryonic stem cells." First, the lysate was split equally across two 700 μL 1 M sucrose cushions, and ultracentrifugation was performed as in "RAPIDASH for E14 mouse embryonic stem cells." Each resulting ribosomal pellet was resuspended in 250 μL binding buffer and then combined into one sample. This material then underwent chromatography with 1 mL of cysteine-charged sulfolink resin prepared as in "RAPIDASH for E14 mouse embryonic stem cells" up until the elution step. The flowthrough of the cysteine-charged sulfolink resin chromatography was collected. Elution was performed by adding 250 μL elution buffer to the resin, incubating on ice for 2 minutes, and centrifuging the sample in conicals at 1,000 ×g for 1 minute. This elution step was repeated, and the eluate was combined with the first eluate.

The lysate from a separate pellet was subjected to chromatography with 1 mL cysteine-charged sulfolink resin prepared as in "RAPIDASH for E14 mouse embryonic stem cells." The flowthrough was collected.The elution was performed as above, with two rounds of elution with 250 μL elution buffer each. The eluates were combined.

These two eluate samples and the two flowthrough samples from each chromatography procedure described above, as well as lysate generated by lysing the final pellet in 500 μL lysis buffer A and clarifying the lysate as in "RAPIDASH for E14 mouse embryonic stem cells," were analyzed by sucrose gradient fractionation as above, except the gradients were 10-50% (w/v) sucrose gradients.

RNA-seq analysis of cysteine-charged resin input and eluate samples

Related to Figure S2. E14 mESCs were grown in 10-cm plates to approximately 50-60% confluency. The cells from 3 plates were harvested as described in "Characterization of cysteine-charged sulfolink resin binding using 80S ribosomes from samples treated with puromycin, RNase A, or high salt" and flash frozen. Frozen cell pellets were thawed on ice. Each cell pellet was lysed in 300 μL lysis buffer A, and the lysates were subjected to sucrose cushion ultracentrifugation as in "Characterization of cysteine-charged sulfolink resin." Each input sample for sucrose cushion ultracentrifugation contained approximately 75 μg of RNA. The pelleted material from each cushion, which contains ribosomes, was resuspended in 1 mL binding buffer. Half of each sample was subjected to total RNA extraction using TRIzol LS (Invitrogen, 10296010). To do this, 500 μL of sample was mixed with 1.5 mL TRIzol LS and then aliquoted into two 2 mL DNA lo bind tubes. Then, chloroform was added at one fifth of the volume of TRIzol LS, and the tubes were vigorously shaken by hand and then left at room temperature for 3 minutes. The tubes were then centrifuged at 12,000 ×g. The upper aqueous layers for the tubes deriving from one cell pellet were combined with an equal volume of ethanol and put onto one column from a Zymo RNA Clean and Concentrator-5 kit, and the RNA was purified following the manufacturer's instructions. The final elution step in the recommended protocol was eluted for a combined total of 30 μL eluate for each sample.

The other half of each sample underwent chromatography with sulfhydryl-charged sulfolink resin. Each input sample consisted of 500 μL sucrose cushion pellet in binding buffer. Ribosomes were enriched using 1 mL cysteine-charged sulfolink resin, prepared as in "Characterization of cysteine-charged sulfolink resin." Chromatography was performed as in "Characterization of cysteine-charged sulfolink resin" up until the elution step. To elute, 500 μL of elution buffer was added to the resin for each sample, and the resin was incubated on ice for 2 minutes. The eluate was collected by centrifuging into a clean tube for 1 minute at 1,000 ×g. This elution step was repeated. The RNA from the eluate was then extracted using the TRIzol LS and chloroform protocol above and subsequently purified using a Zymo RNA Clean and Concentrator-5 kit. Samples were then submitted to Novogene for poly(A) enrichment of transcripts and library preparation. Libraries were then sequenced by Novogene on a NovaSeq X Plus Series instrument with paired-end 150 base pair reads.

RNA-seq analysis

Related to Figure S2. Cutadapt version 4.7 was used to trim adapter sequences from the paired end reads with parameters: "-j 0 –minimum-length=20 -a AGATCGGAAGAGCACACGTCTGAACTCCAGTCA -A AGATCGGAAGAGCGTCGTGTAGGGAAAGAGTGT -o <Read1.trimmed.fq.gz> -p <Read2.trimmed.fq.gz> <Read1.fq.gz> <Read2.fq.gz>". Genome index for GRCm39 primary assembly was built using basic annotation from GENCODE release M34 and STAR version 2.7.11b with parameters: "–runThreadN 16 –runMode genomeGenerate –genomeDir <GRCm39_dir/> –genomeFastaFiles <GRCm39.primary_assembly.genome.fa> –sjdbGTFfile <gencode.vM34.primary_assembly.basic.annotation.gtf> –sjdbOverhang 149". Subsequently, trimmed reads were then aligned using STAR version 2.7.11b with parameters: "–runThreadN 16 –readFilesCommand zcat –genomeDir <GRCm39_dir/> –readFilesIn <Eluate_1_Read1.trimmed.fq.gz>,<Eluate_2_Read1.trimmed.fq.gz>,<Eluate_3_Read1.trimmed.fq.gz>,<Input_1_Read1.trimmed.fq.gz>,<Input_2_Read1.trimmed.fq.gz>,<Input_3_Read1.trimmed.fq.gz> <Eluate_1_Read2.trimmed.fq.gz>,<Eluate_2_Read2.trimmed.fq.gz>,<Eluate_3_Read2.trimmed.fq.gz>,<Input_1_Read2.trimmed.fq.gz>,<Input_2_Read2.trimmed.fq.gz>,<Input_3_Read2.trimmed.fq.gz> –outSAMattrRGline ID:Eluate1, ID:Eluate2, ID:Eluate3, ID:NC1, ID:NC2, ID:NC3 –outSAMtype BAM Unsorted –quantMode TranscriptomeSAM". Transcriptome database was generated using gffread version 0.12.7, to parse out transcriptome data from GRCm39 primary assembly using GENCODE release M34 basic annotation. This transcriptome was first indexed using salmon version 1.10.3[113] with parameters: "-p 16 –gencode -t". Afterwards, transcript abundance was quantified with parameters: "–gencode -t <transcriptome_from_genome.fa> -p 16 –gcBias -l ISR -a <Sample.toTranscriptome.bam> -o <sample_out/>". Output files from salmon (quant.sf) were subjected to differential gene expression analysis using DESeq2 version 1.44.0. Cutoff for differentially enriched genes is: $|FC| > 2$, Benjamini-Hochberg adjusted p-value < 0.05. Analysis scripts will be available on GitHub.

SYPRO Ruby for mESCs

Related to Figure S3D. Protein samples were prepared and ran on 4-20% Mini-PROTEAN® TGX™ Precast Protein Gels as in "Western blotting for mESCs, human cells, and mouse embryonic tissues." After electrophoresis, the gel was opened into a clean 15-cm plate and rinsed in distilled water briefly. The gel was then fixed by adding 100 mL of fixative solution (50% methanol (Fisher Scientific, A452SK-1), 7% glacial acetic acid (Fisher Scientific, A38-212), in high performance liquid chromatography (HPLC) water (Fisher Scientific, W5-4) prepared in glass container) and rocking on orbital shaker for 30 minutes. Fixative solution was then discarded by pipetting it out into a designated waste container, and the fixing step was repeated one more time. Afterwards, the gel was moved to a separate container wrapped in foil. SYPRO Ruby (Invitrogen, S12000) was added until the gel was submerged. The gel was then incubated overnight on an orbital shaker. On the next day, the gel was transferred into another clean container covered with foil and then washed with 100 mL of wash solution (10% methanol, 7% glacial acetic acid, in HPLC water) by rocking for 30 minutes. After the washing step, the solution was decanted, and the gel was rinsed three times with HPLC water by rocking for 5 minutes each time before imaging it with a ChemiDoc XRS+ System using SYPRO Ruby filter.

Mass spectrometry of unlabeled tryptic digests

Protein precipitation

Related to Figures 1G, 1H, and 2A. Proteins were precipitated from mESC samples by adding one volume equivalent of -20°C Precipitation Agent from the ProteoExtract® Protein Precipitation Kit (Millipore, 539180) to each sample. For RAPIDASH samples from E12.5 mouse tissues, four volume equivalents of Precipitation Agent were mixed with each sample instead. All samples were then placed at -20°C for at least 16 hours. Precipitated protein samples were then pelleted by centrifugation at 10,000 ×g for 10 minutes at room temperature. The supernatant was then removed from each sample by pipetting and discarded. Each protein pellet was then washed with 1 mL of prepared Wash Solution from ProteoExtract® Protein Precipitation Kit that was chilled at -20°C. The samples were vortexed briefly and centrifuged at 10,000 ×g for 2 minutes at room temperature. The supernatant was removed from each sample, and the wash and centrifugation step was repeated one more time. The pellets were then dried. by leaving the tubes open to allow the remaining wash buffer to evaporate.

Trypsin/Lys-C digestion

Each protein sample was solubilized by pipetting with a low retention pipette tip (Fisher Scientific, 02-717-135) in 50 μL denaturing buffer (50 mM NH_4HCO_3 (Sigma Aldrich, 09830-500G), 6 M urea (Sigma Aldrich, U1250-1KG), in HPLC water). The protein concentration for each sample was then quantified using a Bradford assay (Bio-Rad, 5000006) with technical duplicates following the manufacturer's protocol. For each mESC RAPIDASH sample (Figures 1G and 1H), 80 μg protein was denatured and reduced by adding 0.5 μL 500 mM DTT to each sample for a final concentration of 5 mM and incubating in a thermomixer at 37°C for 1 hour at 500 rpm. The samples were alkylated by adding 1 μL 500 mM iodoacetamide (Pierce, A39271) to each 50 μL sample for a final concentration of 15 mM and incubating them in the dark at room temperature for 30 minutes. A 0.2 μg/μL Trypsin/Lys-C stock solution in Resuspension Buffer (Promega, V5073) was subsequently added to each sample at a 1:50 trypsin/Lys-C:sample ratio by mass to digest the protein into tryptic peptides. The samples were mixed and then shaken at 500 rpm for 4 hours in a thermocycler at 37°C for the initial digestion by Lys-C. Afterwards, each sample was diluted sixfold by adding 250 μL 50 mM NH_4HCO_3 to reduce the urea concentration to 1 M to allow trypsin to refold. The samples were then incubated for another 12 hours in a 37°C water bath to complete the digestion. Trypsinization was then quenched by adding 3 μL 50% (v/v) heptafluorobutyric acid (HFBA; Sigma Aldrich, 52411-5ML-F) in HPLC water to each sample. The samples were then either stored at -80°C or immediately desalted.

Peptide desalting

Each sample was desalted using an OMIX C18 pipette tip (Agilent technologies, A57003100) attached to a P200 pipette set to 150 μL. Each OMIX C18 pipette tip was conditioned by pipetting 50% (v/v) acetonitrile (Fisher Scientific, A955-1) up and down three times. No air was allowed to pass through the sorbent after it was conditioned. The OMIX C18 pipette tip was then equilibrated with 1% (v/v) HFBA by pipetting up and down three times. Acidified peptides were bound to the OMIX C18 sorbent by pipetting up and down for seven times carefully. After the peptides were bound, each tip was rinsed with 0.1% (v/v) HFBA by pipetting up and down three times. To elute the peptides, 7 μL 0.1% (v/v) formic acid (Fisher Scientific, A117-50) in 50% (v/v) acetonitrile by carefully pipetting up and down five times. A second elution was performed by pipetting up and down with 7 μL 0.1% (v/v) formic acid in 75% (v/v) acetonitrile five times. The two elutions were then pooled together and dried completely using a speed-vac (~45 minutes). The dried peptide samples were stored at -80°C. The peptides were resuspended in 15 μL 0.1% formic acid for analysis by mass spectrometry.

Liquid chromatography tandem mass spectrometry

Mass spectrometry was performed on an Acquity UPLC (ultra performance liquid chromatography) M-class system (Waters) coupled online to an Orbitrap Elite mass spectrometer (Thermo Fisher Scientific). Peptides were separated by reversed-phase chromatography using a Self-Pack PicoFrit column (New Objective, PF360-75-15-N-5) with a 360 μm outer diameter, 75 μm inner diameter, and a tip size of 15 μm packed to approximately 22 cm with HALO Peptide ES-C18 Bulk Packing 2.7 μm beads (MAC-MOD Analytical, 942120202). The UPLC solvents A and B were 0.1% (v/v) formic acid and 0.1% formic acid (v/v) in/100% acetonitrile, respectively. For each sample, 2 μL was loaded at 1% B at 0.3 μL/minute for 20 minutes. Peptides were then separated at 0.3 μL/minute over a linear gradient from 1% B to 40% B for 90 minutes, followed by a linear gradient from 40% B to 100% B for 20 minutes, followed by a constant flow at 100% B for 10 minutes. Then, there was a linear ramp back down to 1% B over 5 minutes and then constant flow at 1% B for 5 minutes.

The Orbitrap Elite was operated in a data-dependent mode using Xcalibur v3.0 (Thermo Fisher Scientific). Collision-induced dissociation (CID) MS/MS scans were recorded after each MS1 scan (R = 120,000) for the top 15 most abundant precursor ions in the Orbitrap. The isolation width was 1.8 m/z, the normalized collision energy was 35%, and the activation time was 10 milliseconds. The dynamic exclusion parameters were: a repeat count 1 with a 45 second repeat duration, an exclusion list size of 500, an exclusion duration of 80 seconds, and a +/- 10 ppm exclusion mass width. Only charge states of 2 or 3 were not rejected; others, including unassigned charges, were rejected.

RAPIDASH and proteomic analysis of ribosomal complexes for PC3 cells

Related to Figure S3F. PC3 cells were grown on 15-cm tissue-culture treated plates, where per replicate 10 plates of PC3 cells were left untreated and 10 plates of PC3 cells were treated with 3 nM Rapalink-1 for 24 hours. PC3 cells were processed for RAPIDASH and TMT-MS as described in "RAPIDASH for E14 mouse embryonic stem cells." Rapalink-1 was a kind gift from Kevan Shokat's lab at UCSF.

Proteomic analysis of ribosomal complexes

In solution digestion. Aliquots of ribosomal samples were digested with trypsin for proteomic analysis. Samples (30 μg protein) were prepared at a concentration of 0.6 mg/ml in a solution containing 8 M Urea and 50 mM ammonium bicarbonate and frozen until processing. After thawing, samples were added 10 mM tris(2-carboxyethyl)phosphine and incubated for 1 hour at 56°C. This was followed by addition of 20 mM iodoacetamide and a 30 minute incubation at room temperature in the dark. The samples were then diluted with 20 mM ammonium bicarbonate to reach a concentration of 1 M Urea. For digestion, the samples were then added 3% (w/w) Lysyl Endopeptidase®, Mass Spectrometry Grade (Lys-C) (FUJIFILM Wako Chemicals U.S.A. Corporation) and incubated at 37°C on a shaker overnight. After that, samples were added to 3% (w/w) trypsin MS grade (Pierce- Thermo Fisher) and digested for 6 additional hours. After this, samples were acidified with formic acid to a final concentration of 5% formic acid, and the digests were then desalted using 100 μL OMIX C18 pipette tips (Agilent) following the manufacturer's protocol. Eluates were dry-evaporated in preparation for direct label free MS analysis or for labeling with tandem mass tag (TMT) reagents for quantitative comparison.

Tandem mass tag (TMT) labeling

Dried samples were labeled according to TMT-6plex kit instructions (ThermoFisher Scientific), with some modifications. Briefly, samples were resuspended in 16 μL 0.1 M triethylammonium bicarbonate, pH 8.0. TMT reagents were dissolved in acetonitrile at 25 μg/μL, and 5 μL of these stocks added to the samples. After incubation for 1 hour at room temperature, samples were quenched with 1 μL 5% hydroxylamine, then all 6 samples combined and partially evaporated in speedvac until volume was around 5 μL. Each sample then had 100 μL 1% formic acid added, and then the peptides were desalted using OMIX tips. The OMIX tip eluate was dried and resuspended in 20 μL 0.1% formic acid for mass spectrometry analysis.

Mass spectrometry analysis

Peptide digests resuspended in 0.1% formic acid were injected (approximately 2 μg) onto a 2 μm 75 μm x 50 cm PepMap RSLC C18 EASY-Spray™ column (Thermo Scientific, ES903). For peptide elution, 3-hour water/acetonitrile gradients (2–25% in 0.1% formic acid) were used, at a flow rate of 200 nL/minute. Analysis was performed in an Orbitrap Eclipse (Thermo Scientific) in positive ion mode. MS spectra were acquired between 375 and 1500 m/z with a resolution of 120000. For each MS spectrum, multiply charged ions over the selected threshold (2E4) were selected for MS/MS in cycles of 3 seconds with an isolation window of 0.7 m/z. Precursor ions were fragmented by higher energy collision dissociation (HCD) using stepped relative collision energies of 30, 35 and 40 to ensure efficient generation of sequence ions as well as TMT reporter ions. MS/MS spectra were acquired in centroid mode with resolution 60000 from m/z=120. A dynamic exclusion window was applied which prevented the same m/z from being selected for 30 seconds after its acquisition.

Peptide and protein identification and quantitation

Peak lists were generated using PAVA in-house software.[120] All generated peak lists were searched against the human subset of the SwissProt database (SwissProt.2019.07.31, 20432 entries searched), using Protein Prospector[107] with the following parameters: enzyme specificity was set as Trypsin, and up to 2 missed cleavages per peptide were allowed. Carbamidomethylation of cysteine residues, and TMTsixplex labeling of lysine residues and N-terminus of the protein, were allowed as fixed modifications. N-acetylation of the N-terminus of the protein, loss of protein N-terminal methionine, pyroglutamate formation from peptide N-terminal glutamines, oxidation of methionine were allowed as variable modifications. Mass tolerance was 10 ppm in MS and 30 ppm in MS/MS. The false positive rate was estimated by searching the data using a concatenated database which contains the original SwissProt database, as well as a version of each original entry where the sequence has been randomized. A 1% FDR was permitted at the protein and peptide level. For quantitation only unique peptides were considered; peptides common to several proteins were not used for quantitative analysis. For TMT based quantitation, relative quantization of peptide abundance was performed via calculation of the intensity of reporter ions corresponding to the different TMT labels, present in MS/MS spectra. Intensities were determined by Protein Prospector. Median intensities of the reporter ions (each TMT channel) for all peptide spectral matches (PSMs) were used to normalize individual (sample specific) intensity values. For each PSM, relative abundances were calculated as ratios vs the average intensity levels in the 3 channels corresponding to control (non-stimulated) samples. For total protein relative levels, peptide ratios were aggregated to the protein levels using median values of the $\log_2$ ratios. Significance was calculated using Student's t-test.

RAPIDASH for E12.5 tissues

Related to Figure 4. Limbs, forebrain, and liver tissues were microdissected from E12.5 FVB/NJ mouse embryos. Uterus was washed in DPBS twice to remove the blood. Each embryo was transferred into a plate containing filming media one by one, where microdissection was performed to take out the tissues. Filming media (10% FBS (Sigma Aldrich, TMS-013-B) in DMEM/F-12 with HEPES without phenol red (Gibco, 11039021)) was used during microdissection, and the tissues were collected with P1000 pipette. Excess media was removed by pipette without centrifugation, and the sample was then flash frozen in liquid nitrogen. Each biological replicate consisted of tissues pooled from the same litter (9-12 embryos).

For lysis, 100 μL of cold lysis buffer A was initially added into each sample. The tissues were rapidly ground by hand for 30 seconds using a disposable microcentrifuge pestle. Then, an additional 300 μL of cold lysis buffer A was added to each sample. RAPIDASH was then performed as described in "RAPIDASH for E14 mouse embryonic stem cells" starting from the vortexing step during lysis, with the following modifications: after the sucrose cushion ultracentrifugation step, each protein pellet was resuspended in 500 μL cold binding buffer instead of 1 mL, and the entire volume was subjected to affinity enrichment with L-cysteine charged sulfhydryl resin.

TMT mass spectrometry

Related to Figures 1D, 4B, S3B, and S3C. For the comparison of the original sulfhydryl-charged resin chromatographic purification of eukaryotic ribosomes and the RAPIDASH protocol, mammalian ribosomes were purified from one 70% confluent 10-cm plate of mESCs following the previously published protocol[10] or using the "RAPIDASH for E14 mouse embryonic stem cells" protocol.

Proteins were precipitated from mESC sucrose cushion pellet, mESC RAPIDASH, or E12.5 mouse tissues RAPIDASH samples as described in "Mass spectrometry of unlabeled tryptic digests."

The protein samples were then digested into peptides as described in "Mass spectrometry of unlabeled tryptic digests - Trypsin/Lys-C digestion." To prepare samples for TMT, equal amounts of protein by mass were aliquoted into separate tubes according to Table 1.

TMT labeling

TMTsixplex™ Isobaric Label Reagents (Thermo Scientific, 90066) were freshly prepared for each experiment by resuspending the entire 0.8 mg of labeling reagent in the tube with 100 μL 100% ethanol. For every 1 μg of peptide, 0.5 μL 8 μg/μL of freshly resuspended TMT label reagent was used. To do this, the peptides were first resuspended in 20 mM HEPES, pH 8.0 (Fisher Scientific, AAJ63578AK). The volume of HEPES buffer used was three times the volume of the TMT label that would be added. TMT label reagents were then added into the resuspended peptides, and the samples were incubated for 1 hour at room temperature in the dark. The labeling reaction was subsequently quenched by adding a volume of 5% (v/v) hydroxylamine (Sigma Aldrich, 467804-10ML) equal to 1/20 of the sample volume at room temperature for 15 minutes. The samples for a single injection for relative quantification with different TMT labels were then mixed together according to Table 1. The combined sample was then acidified by adding 50% HFBA to a final concentration of ~0.5% (v/v) and 100% formic acid to a final concentration of 5% (v/v). Then, the combined samples were desalted using OMIX C18 pipette tips and dried with a speed-vac as described earlier. Peptides were resuspended in 8 μL 0.1% (v/v) trifluoroacetic acid (Fluka, 40967) in 5% (v/v) acetonitrile and subjected to ultra performance liquid chromatography (UPLC) tandem mass spectrometry (MS/MS) analysis using an Acquity UPLC M-class system (Waters) coupled online to an Orbitrap Elite mass spectrometer (Thermo Fisher Scientific).

Liquid chromatography tandem mass spectrometry for TMT

Peptides were separated by reversed-phase chromatography using the same column as in "Mass spectrometry of unlabeled tryptic digests - Liquid chromatography tandem mass spectrometry." UPLC solvent A was 0.1% (v/v) formic acid, and UPLC solvent B was 0.1% (v/v) formic acid/100% acetonitrile, respectively. For each sample, 3 μL was injected and loaded for 30 minutes at 1% B at a flow rate of 0.3 μL/minute. Peptides were separated at the same flow rate over a linear gradient of 5% B to 40% B for 180 minutes, followed by a linear ramp to 100% B for 10 minutes, followed by constant flow at 100% B for 10 minutes. Finally, there was a ramp down to 1% B over 1 minute, where it was held for 9 minutes at constant flow.

The Orbitrap Elite (Thermo Fisher Scientific) was operated in a data-dependent mode using Xcalibur v3.0 (Thermo Fisher Scientific). HCD MS/MS scans (R = 15,000) were recorded after each MS1 scan (R = 60,000) for the top 15 most abundant precursor ions in the Orbitrap. The following HCD parameters were used: an isolation width of 1.6 m/z, a normalized collision energy of 40%, and an activation time of 0.1 milliseconds. Dynamic exclusion parameters were set as follows: a repeat count 1 with a 30 second repeat duration, an exclusion list size of 500, an exclusion duration of 60 seconds, and a +/- 10 ppm exclusion mass width. Charge state rejection was enabled for charge states that were less than 2 or unassigned.

Mass spectrometry data analysis

Related to Figures 1D, 1G, 1H, 2A, 4B, S3B, and S3C. The raw spectra were analyzed using MaxQuant (v2.4.2.0) against *Mus musculus* SwissProt reviewed proteome database downloaded on June 7, 2024 with the following parameters: a maximum of 2 missed trypsin enzyme cleavage sites, first search mass tolerance of 20 ppm, main search mass tolerance of 4.5 ppm, and MS/MS match tolerance of 20 ppm. Deamidation (NQ), oxidation (M), and N-terminal acetylation were searched as variable modifications, and carbamidomethyl (C) was searched as a fixed modification. For identification, a minimum of one razor + unique peptide was required, and the result was filtered with 1% false discovery rate (FDR) at the peptide and protein levels. For TMT quantification, a minimum of two razor + unique peptides present was required instead.

For data related to Figures 1H (Table S3) and 2A (Table S5), proteins that were identified only by site, contaminants, and reverse hits were filtered out. Proteins that were identified in three out of six mESC samples (Figure 1H) or two out of three forebrain samples (Figure 2A) were used for subsequent analysis. Gene ontology molecular function (GOMF) terms were obtained by first converting SwissProt IDs into Entrez Gene IDs. The Entrez Gene IDs were then analyzed by Manteia[16] to obtain gene ontology terms that are significant. These were filtered so that level 4 terms were the most broad term level that was utilized (e.g. for terms that had more than one level associated, those that were level 1, 2, or 3 in any branch were filtered out).

For the TMT mass spectrometry data, contaminants, reverse hits, and peptides only identified by site were filtered out, and reporter intensity for each protein was $\log_2$ transformed and median-normalized. For the data related to Figures 1D and S3B (Table S2), only proteins that were detected in all three replicates were selected. Subsequently, the proteins were categorized to separate core RPs from other proteins. The significance of enriched protein groups in each replicate was evaluated with Welch's t-test. For the data related to Figure 4B (Table S8), proteins that were detected in three out of four replicates were selected, the missing values were imputed by random numbers from a normal distribution, and the reporter intensity values between each pair of tissues were analyzed

with a paired Welch's t-test using Perseus (v2.0.11) Proteins with a fold change $\geq$ 2 and a permutation-based FDR < 10% were deemed to be significantly enriched in one E12.5 mouse embryo tissue over another.

Sucrose gradient fractionation of mESC lysates and subsequent western blotting

Related to Figures 2B–2D. For the gradients in Figures 2B and 2C, the media on these E14 mESCs was changed to fresh mESC media approximately 45 minutes before harvesting. Treatment with CHX and pelleting the cells proceeded as in "Characterization of cysteine-charged sulfolink resin binding using 80S ribosomes from samples treated with puromycin, RNase A, or high salt." Cell pellets were lysed by adding 250 μL chilled polysome lysis buffer (20 mM Tris, pH 7.5, 15 mM $MgCl_2$, 150 mM NaCl, 1% Triton X-100, 0.5% sodium deoxycholate, 8% glycerol, 1 mM DTT, 100 μg/mL CHX, 20 U/mL TURBO DNase, 200 U/mL SUPERase·In™ RNase Inhibitor, 1x Halt protease and phosphatase inhibitor in UltraPure water). The lysates were kept on ice and then alternatively vortexed in the cold room and put back on ice three times for 30 seconds each time. The lysates were then incubated on ice for 20 minutes and vortexed briefly every 10 minutes. The lysates were clarified by centrifuging at 1,300 ×g for 5 minutes at 4°C, moving the supernatants to fresh chilled tubes, centrifuging at 10,000 ×g for 5 minutes at 4°C, and moving the supernatants to fresh chilled tubes again. The RNA amounts and concentrations were normalized, and 200 μL lysate was layered onto linear 10-45% (w/v) sucrose gradients (20 mM Tris pH 7.5, 150 mM NaCl, 15 mM $MgCl_2$, 1 mM DTT, 100 μg/mL CHX, made on a Biocomp Model 108 Gradient Master). For the gradient in 2C, the sucrose gradient also contained 50 mM EDTA. Centrifugation of the samples through the gradients, fractionation, and the collection of samples were performed as in "Sucrose gradient fractionation for RAPIDASH characterization." Fractions were precipitated using a ProteoExtract Protein precipitation kit following the manufacturer's instructions.

For the gradients in Figure 2D, E14 mESCs were cultured at the 10-cm plate scale until they reached approximately 50-60% confluency. Cells from one 10-cm plate were harvested as in "Characterization of cysteine-charged sulfolink resin binding using 80S ribosomes from samples treated with puromycin, RNase A, or high salt" and flash frozen. One cell pellet was thawed on ice and lysed using 300 μL chilled lysis buffer (20 mM Tris, pH 7.0, 15 mM $MgCl_2$, 150 mM NaCl, 0.5% Triton X-100, 8% glycerol, 1 mM DTT, 100 μg/mL CHX, 20 U/mL TURBO DNase, 1x Halt protease and phosphatase inhibitor in UltraPure water). The lysate was divided evenly across two tubes. One tube was designated the non-treated control sample, and SUPERase·In™ RNase Inhibitor was added to a final concentration of 200 U/μL. The lysate in the other tube was treated with RNase A such that 3 μg of RNase A was added per 600 μg RNA. This sample was then incubated at room temperature with rotation for 30 minutes. RNase A activity was stopped by adding SUPERase·In™ RNase Inhibitor to a final concentration of 200 U/mL. The non-treated and RNase A-treated lysate samples were each loaded on 10-45% (w/v) sucrose gradients (20 mM Tris, pH 7.0, 150 mM NaCl, 15 mM $MgCl_2$, 100 μg/mL CHX, made on a Biocomp Model 108 Gradient Master) and centrifuged in a Beckman SW41 rotor at 40,000 rpm for 2.5 hours at 4°C in a Beckman L8-80M ultracentrifuge. Sucrose gradients were then fractionated on a density gradient fraction system using PeakChart software with continuous A260 measurement. Fractions were collected and precipitated using a ProteoExtract Protein precipitation kit. Briefly, each fraction was mixed with 700 μL Precipitation Agent and then left at -20°C to precipitate overnight, after which the manufacturer's instructions were followed to complete the protein precipitation.

Protein precipitates were resuspended in 30 μL 2x Laemmli buffer and boiled at 95°C at 1,000 rpm for 5 minutes on a Thermoshaker. Samples were loaded by equal volume and separated on a 4-20% Criterion™ TGX™ Precast Midi protein gel and transferred to a PVDF membrane using a Trans-Blot® Turbo™ Transfer System as in "Western blotting for mESCs, human cells, and mouse embryonic tissues." In Figures 2B and 2C, the membranes were cut horizontally to facilitate probing with primary antibodies against Dh30, Rps26, and Rpl29 at a 1:1000 dilution. For Figure 2D, the membranes were blocked in 5% milk 1x PBST for 1 hour at room temperature and then washed 3 times with 1x PBST. The membranes were cut across horizontally to separately probe for the presence of Dhx30, Pabp1, and Rpl4. The membranes were rocked in primary antibody solution at a 1:1,000 dilution in 5% BSA 0.02% NaN_3 in 1x PBST overnight in the cold room. The next day, the membranes were washed three times for 10 minutes each time at room temperature using 1x PBST. The membranes were then rocked in 1:5,000 anti-rabbit HRP in 5% milk 1x PBST for 1 hour at room temperature. The membranes were washed three times for 10 minutes each time at room temperature using 1x PBST and then developed using Clarity reagent for Pabp1 and Rpl4 or Femto reagent for Dhx30.

siRNA-mediated knockdown and OP-puromycin labeling

Related to Figure 2E. Before transfection, 6-well plates were coated overnight with 0.1% gelatin prior to use. Cultured mESCs were trypsinized, washed, and resuspended in Opti-MEM (Gibco, 11058021) at a density of 5.0 x 10^5 cells/mL. Cells were then transfected with 25 nM of non-targeting control siRNA #2 (siFluc; Dharmacon, D-001210-02-05) or siRNA target against mouse *Dhx30* (Dharmacon, M-053738-00-0005) using Dharmafect Reagent I (Dharmacon, T-2001) as per manufacturer's protocol. Cells (1 mL) were then plated into each well of a 6-well plate and incubated for 24 hours at 37°C in antibiotic-free media. Following incubation, global protein synthesis was measured using O-propargyl-puromycin (OPP). Briefly, cells were labeled with 20 μM of OPP (Vector Laboratories, CCT-1407) in mESC media for 30 minutes at 37°C.

Following metabolic labeling, cells were harvested and washed twice with 1x PBS. Subsequent cell pellets were resuspended in Zombie Violet Live-Dead Stain (1:500 in PBS; BioLegend, 423113) and incubated for 15 min in the dark. Cells were then washed with Cell Staining Buffer (0.1% NaN_3, 2% FBS in Hanks' Balanced Salt Solution (HBSS; Thermo Fisher Scientific, 14175095)) before being fixed in 1% paraformaldehyde (Fisher Scientific, 43368-9M) for 15 minutes on ice. Cells were then permeabilized in Perm Buffer

(0.1% Saponin (Sigma Aldrich, 47036), 0.1% NaN_3, 3% FBS in PBS) for 1 hour on ice. Cells were next washed twice with Cell Staining Buffer (without 0.1% NaN_3), labeled with an Alexa Fluor 555 Picolyl Azide dye (Thermo Fisher, C10642) and incubated for 30 min at room temperature in the dark. Labeled cells were washed and resuspended in Cell Staining Buffer before being analyzed on a LSRII flow cytometer (BD Biosciences) using software packages CellQuest and FlowJo v10. The data are plotted as the average median fluorescence intensity normalized to the siFluc control, and the error bars are +/- standard error of the mean (SEM). The propagated standard error was calculated using average errors.

Transfection of Dhx30 mutant constructs, sucrose cushion ultracentrifugation, and western blotting

Related to Figures 2G and 2H. V5-tagged constructs of Dhx30 (wild type Dhx30, ΔOB-fold, R805/8A, ΔdsRBD-1, and ΔdsRBD-1/2) were cloned into pCAG plasmids. Prior to use, 6-well plates were coated overnight with 0.1% gelatin. For transfections, 250 μL of Opti-MEM was mixed with 4 μg of plasmid in one tube and separately 250 μL of Opti-MEM was mixed with 10 μL of Lipofectamine 2000 (Invitrogen, 11668019). Both tubes were incubated for 5 minutes at room temperature. Following incubation, both tubes were mixed together and incubated for 15 minutes at room temperature. Cultured mESCs were trypsinized, washed, and resuspended in Opti-MEM at a density of 1.0 x 10^6 cells/mL. After incubation of the Lipofectamine:DNA mixture, 1 mL of cells was added to each tube, mixed gently with a pipet, and immediately transferred to a 6-well plate. After incubation for 3 hours, the media was replaced with complete mESC media. Plates were then incubated at 37°C for an additional 24 hours before downstream experiments.

The next day, approximately 45 minutes prior to harvesting, the media on these cells was changed to fresh mESC media. Treatment with cycloheximide and harvesting the cells proceeded as in "Sucrose gradient fractionation of mESC lysates and subsequent western blotting." Cell pellets were lysed by adding 300 μL chilled polysome lysis buffer without sodium deoxycholate. The lysates were alternatively rested on ice and vortexed three times for 30 seconds each time. The lysates were then incubated on ice for 20 minutes and vortexed briefly every 10 minutes. Lysates were clarified by two centrifugation steps: first, the lysate was centrifuged at 2,600 rpm for 5 minutes at 4°C, and the supernatant was moved to a fresh chilled tube; second, the lysate was centrifuged at 10,000 rpm for 5 minutes at 4°C, and the supernatant was moved to a fresh chilled tube. Samples were normalized so that each lysate had the same amount of RNA in equal volumes of polysome lysis buffer without sodium deoxycholate.

For each sample, 300 μL clarified lysate was layered onto a 700 μL sucrose cushion (1 M sucrose, 20 mM Tris, pH 7.5, 15 mM $MgCl_2$, 150 mM NaCl, 1 mM DTT, 100 μg/mL CHX in UltraPure water). Samples were then centrifuged at 100,000 rpm at 4°C using a Beckman TLA120.2 rotor for 1 hour. The cushion pellets were each resuspended in 150 μL polysome lysis buffer and stored at -80°C. The supernatants were each mixed with 1 mL of chilled Precipitation Agent from the ProteoExtract Protein Precipitation kit and stored at -80°C. Protein precipitation was completed according to the manufacturer's instructions. The lysate, supernatant, and pellet fractions were analyzed by western blotting using antibodies against the V5 tag (1:5000 dilution), Rps6 (1:1000 dilution), and Gapdh (1:1000 dilution). The data in 2H are plotted as the average percentage of total amount of Dhx30 found in the pellet and supernatant. The error bars are +/- standard deviation. Significance was calculated using a two-tailed Welch's t test.

Sucrose gradient fractionation of P493-6 cells

Related to Figures 3B and S4A. P493-6 cells were treated with 0.1 μg/mL tetracycline (Sigma Aldrich, T7660) 24 hours prior to harvest. The cells were then treated with 100 μg/mL CHX for 5 minutes at 37°C in P493-6 culture media. Cells were harvested and then lysed in P493-6 cell lysis buffer (10 mM HEPES, pH 7.4, 100 mM NaCl, 5mM $MgCl_2$, 1% Triton X-100, 100 μg/mL CHX, 2 mM DTT). Lysates were clarified by centrifuging for 10 minutes at 12,500 rpm. To assess whether LLPH association with the ribosome depends on RNA, cytoplasmic lysate containing 240 μg RNA in 200 μL lysis buffer was digested with or without 0.4 μg RNase A diluted from a 10 mg/mL RNase A stock (Qiagen, 12125) for 5 minutes at 25°C on a thermomixer. Digestion was stopped by adding 2 μL SUPERase·In™ RNase Inhibitor. The samples were loaded onto 10-50% (w/v) linear sucrose gradients (10 mM HEPES, pH 7.4, 100 mM NaCl, and 5 mM $MgCl_2$) and centrifuged at 38,000 rpm for 2.5 hours at 4°C. For the samples treated with or without EDTA, the cells were not treated with tetracycline prior to harvesting, and the lysis buffer contained SUPERase·In™ RNase Inhibitor at a 1:100 dilution. Cytoplasmic lysates containing 240 μg RNA in 200 μL lysis buffer were layered onto 10-50% (w/v) linear sucrose gradients (10 mM HEPES, pH 7.4, and 100 mM NaCl) with or without 50 mM EDTA. Samples were fractionated using a Piston Gradient Fractionator (Biocomp Instruments, 152). The proteins in the fractions were precipitated using a ProteoExtract kit. Equal volumes of precipitated protein from each fraction were analyzed by western blotting using antibody solutions against LLPH, RPS20, and RPL8 (primary antibodies at a 1:1000 dilution).

H1-hESC cell culture and CRISPR

Related to Figure 3. To generate homozygous Llph knockout H1-hESCs, guide RNAs (gRNAs) (AAGCCTGCTGGCCTCCTTTG, GAGAATACTTTTAAGCCTGC, CTCTTGGCAATGTTTGGGTT) targeting Llph exon 2 were designed using Benchling, and single gRNA (sgRNA) synthesized using the Gene Art Precision gRNA Synthesis Kit (Thermo Fisher, A29377) according to kit instructions. In all, 3.43 μg of sgRNA mix was complexed with 40 pmol of Cas9-NLS protein (UC Berkeley Macrolab) for 10 minutes at room temperature. The Cas9-sgRNA RNP along with 0.3 μg of pCE-mp53DD (Addgene #41856, to promote cell survival) were then nucleofected into 4 x 105 hESCs using the P3 Primary Cell 4D-Nucleofector™ X Kit S (Lonza, V4XP-3032) with program CB-150 following manufacturer's instructions. Cells were then plated in 1 well of a 6-well plate post nucleofection and cultured until confluent to split.

Clonal selection was then performed by sparse seeding of 3000 cells in a 10-cm dish, followed by manual picking of clones into individual wells of a 96-well plate.

Lentivirus production

Related to Figures 3C–3G, S4E, and S4F. Replication incompetent lentiviruses were produced in COS1 cells by cotransfection of packaging plasmids pMD2.G (Addgene #12259) and psPAX2 (Addgene #12260) with lentiviral vectors: 1) FUW-TetO-Ngn2-T2A-Bsd, where TetO promoter drives expression of full length mouse Neurogenin2 (Ngn2) and Blasticidin S deaminase (Bsd) via cleavage of T2A peptide sequence; 2) FUW-rtTA, to allow for dox-inducible expression of Ngn2-T2A-Bsd construct that is under TetO promoter.[57]

In brief, for each 15-cm plate, 1.05 X 10^7 of COS1 cells were seeded one day before transfection. 1.9 μg of pMD2.G and 5.63 μg of psPAX2 were mixed with 2.24 μg of each lentiviral vector in 1.5 mL Opti-MEM and 75 μL of 1x polyethylenimine (Sigma Aldrich, 764965-1G) for 20 minutes at room temperature. Afterwards, plasmid mix was added dropwise onto the plate. Media was replaced the next day with 17 mL of fresh prewarmed DMEM + 10% FBS without Penicillin/Streptomycin. The first collection was done 24 hours after media replacement, and the virus-containing media was stored at 4°C. The second collection was done 48 hours after media replacement, and both collections of virus-containing media were combined. Lenti X concentrator (Takara, 631232) was then used to concentrate the virus 100x following the manufacturer's instructions.

Generation of human induced neurons from H1-hESC with Ngn2 overexpression

Related to Figures 3C–3G, S4E, and S4F. Prior to plating cells for induced neurons (iN) differentiation, a 6-well plate was coated with 1:200 Matrigel (Corning, 356234) for at least 2 hours. On day 0, approximately 500k of H1-hESCs are plated per well of 6-well plate in 1mL of mTeSR1 + 2 μM thiazovivin + 2 μg/mL polybrene (Tocris, 7711). Then, 2 μL each of Ngn2-Bsd and rtTA lentivirus were added per well. On day 1, after approximately 18 hours of infection, media was replaced to 2 mL of N3 media (DMEM/F12 1:1 (Gibco, 11320-033) + 1x N2 supplement (Gibco, 17502-048) + 1x non-essential amino-acids, 5 mg of insulin (dissolved in 10 mM NaOH) (Sigma Aldrich, I6634-100MG), 0.5x Penicillin/Streptomycin) + 2 μg/mL doxycycline (Dox) (Fisher Scientific, BP26535). On days 2 and 3, media was replaced to 2 mL of N3 media + 2 μg/mL Dox + 2 μg/mL puromycin (Sigma Aldrich, P8833-25MG). On day 4, media was replaced to 2 mL of N3 media + 2 μg/mL Dox + 2 μg/mL puromycin + 4 μM Cytosine β-D-arabinofuranoside (AraC) (Sigma Aldrich, C1768)S4.

To prepare iN for imaging, on day 4, glass coverslips were first placed in a 24-well plate, sterilized by washing 3x with 70% ethanol for 5 minutes each, and then UV-irradiated for 30 minutes as the ethanol evaporated. Afterwards, the coverslips were coated with 1:200 matrigel overnight. On day 5 morning, approximately 50k mouse glial cells from newborn wild-type CD1 mice were plated on each coverslip with NBP media (Neurobasal (Gibco, 21103-049), 1x Glutamax, 1x Gem21 NeuroPlex™ Serum-Free Supplement (Gemini, 400-160), 0.5x Penicillin/Streptomycin, 5% iN grade serum - Cytiva HyClone™ (Cytiva, SH30396.03)). On day 5 evening, premature iN cells were detached gently with Accutase, and approximately 150k cells per well were re-plated with 800 μL NBP media + 2 μg/mL doxycycline. On day 7, the cells were washed gently with pre-warmed NB zero media (NBP without 5% serum) to remove any dead cells, and the media was replaced with 800 μL NB-2% (NBP with 2% serum instead) + 2 μg/mL Dox + 4 μM AraC. On day 10, the spent media was partially replaced with 300 μL NB-2% + 2 μg/mL Dox + 4 μM AraC. On day 14, Dox and AraC were no longer added, and the spent media was partially replaced with 300 μL NB-2%. On day 21, the spent media was partially replaced again with fresh 300 μL NB-2%.

Sucrose gradient fractionation of human induced neurons treated with or without RNase A and subsequent western blotting

Related to Figure S4E. H1-hESCs were cultured at the 15-cm plate scale and subjected to human iN differentiation as described in "Generation of human induced neurons from H1-hESC with Ngn2 overexpression" until days *in vitro* (DIV) 5. The cells were processed as in "Sucrose gradient fractionation of mESC lysates and subsequent western blotting," except that Accutase with 100 μg/mL CHX was used instead of trypsin to gently detach the cells. Anti-Pabp1 and anti-Rps5 antibodies were used for western blotting as in "Characterization of cysteine-charged sulfolink resin binding using 80S ribosomes from samples treated with puromycin, RNase A, or high salt." The primary antibody solution for LLPH was 1:1000 dilution of anti-Llph in 5% BSA in PBST.

Human induced neurons morphology analysis

Related to Figures 3C and 3D. Glia co-cultured LLPH$^{+/+}$ and LLPH$^{Nterm/Nterm}$ hiNs were grown until DIV 30 as mentioned above in "Generation of human induced neurons from H1-hESC with Ngn2 overexpression." Cells on the glass coverslips were washed carefully with cold PBS once and then fixed in 4% paraformaldehyde, 4% sucrose, in PBS for 20 minutes at 4°C. Afterwards, the coverslips were washed three times with room temperature PBS and blocked in 2.5% goat serum (MP Biomedicals, 092939249), 2.5% BSA, and 0.2% Triton X-100 in PBS for 1 hour at room temperature. Primary antibody MAP2 (chicken, 1:1000, Encor, CPCA-MAP2) was added in the same blocking buffer and left to incubate overnight at 4°C. Coverslips were then washed in PBS three times and incubated with fluorescence-labeled secondary antibodies (goat anti chicken Alexa 647, 1:1500, Invitrogen, A-21449) in PBS for 1 hour at room temperature. Coverslips were again washed in PBS three times and then incubated with (4',6-diamidino-2-phenylindole) (DAPI; Thermo Fisher, 62248) diluted 1:10,000 in PBS. Afterwards, slides were mounted on microscope slides with

Fluoromount-G (SouthernBiotech, 0100-01). Images were taken by Zeiss LSM 780 and analyzed by SNT plugin in Fiji.[108] The images were then exported for neurite length analysis in ImageJ. Neurite length was measured using SNT.[109] Significance was calculated using a Wilcoxon signed-rank test.

LLPH-Flag immunoprecipitation

Related to Figure S4B. To generate lentiviruses, 293T cells were transfected with either a doxycycline-inducible pHR-TRE3G-LLPH-FLAG-P2A-BFP plasmid or a control pHR-TRE3G-GFP-FLAG-P2A-BFP plasmid together with pMD2.G and psPAX2 plasmids in the presence of PolyFect Transfection reagent (Qiagen, 301105). A549 cells were transduced with lentivirus encoding either a doxycycline-inducible pHR-TRE3G-LLPH-FLAG-P2A-BFP or a control pHR-TRE3G-GFP-FLAG-P2A-BFP construct. For mass spectrometry experiments, LLPH-FLAG was induced by treatment of A549 cells with 1 μg/mL doxycycline for 48 hours prior to cell harvest. Cells stably expressing blue fluorescent protein (BFP) were sorted by fluorescence activated cell sorting on a BD Biosciences FACSAria III to generate A549 cell lines with inducible LLPH-Flag or GFP-Flag. Cells were treated with 1 μg/mL Dox for 48 hours to induce LLPH-Flag or GFP-Flag expression. Cells were then harvested with CHX treatment as described previously (RAPIDASH for E14 mouse embryonic stem cells - Harvest and cytoplasmic lysis). Mock pull downs prepared in lysates expressing GFP-flag were performed in parallel as controls for non-specific binding. To prepare cytoplasmic lysate, cells were lysed with cold lysis buffer C (20 mM HEPES-KOH pH 7.5, 150 mM potassium acetate (KOAc), 5 mM $MgCl_2$, 2 mM DTT, 8% glycerol, 1% Triton X-100, 0.5% sodium deoxycholate, 100 μg/mL CHX, 100 U/mL SUPERase·In™ RNase Inhibitor, 25 U/mL TURBO DNase, and 1× Halt™ Protease and Phosphatase Inhibitor) by vortexing at high speed for 30 seconds and putting them back on ice for 30 seconds. This was repeated another two times for a total of 3 minutes. Afterwards, samples were incubated for 30 minutes on ice with vortexing every 10 minutes. Lysates were cleared by sequential centrifugation at 800 ×g for 5 minutes, 800 ×g for 5 minutes, 8000 ×g for 5 minutes and 21,300 ×g for 10 minutes at 4°C. Cytoplasmic lysates were then treated with 1 μL RNase T1 and 1 μL MNase (Thermo Fisher, EN0181) for 30 minutes at room temperature. The reaction was quenched by addition of 5 μL of SUPERase·In™ RNase Inhibitor and leaving the samples on ice. To perform the immunoprecipitation, 300 μL of cytoplasmic lysate was incubated with 50 μL of ANTI-FLAG® M2 Affinity Gel (Sigma Aldrich, A2220) for 2 hours on a turning wheel at 4°C. Beads were then transferred into 15 mL falcon tubes and batch washed two times with 10 mL wash buffer A (20 mM HEPES-KOH pH 7.5, 150 mM KOAc, 5 mM $MgCl_2$, 1 mM DTT, 2% glycerol, 0.01% NP40 (Thermo Fisher, 85124)) each time and then batch washed once with 10 mL of buffer B (20 mM HEPES-KOH pH 7.5, 150 mM KOAc, 5 mM MgCl2, 1 mM DTT, 2% glycerol, 0.05% octaethylene glycol monododecyl ether (Nikkol; Sigma Aldrich, P8925)). Afterwards, 5 mL buffer B was added to each sample, and the slurry was transferred to a Mobicol column (Boca Scientific, M1050) with a 10 μm pore size Mobicol filter inserted (Boca Scientific, M2110) to perform the last column wash. Proteins were then eluted in 100 μL of 250 μg/mL Flag peptide (Sigma Aldrich, F3290) in buffer B by incubating the column on a turning wheel at 4°C for 45 minutes. Proteins were partially separated on SDS-PAGE gels, allowing the bromophenol blue marker to reach 1 cm inside the gel. Gel was stained using ProtoBlue Safe Colloidal Coomassie Blue G-250 stain (National Diagnostics, EC-722). The upper portion of the lanes containing the proteins was excised and digested in-gel with trypsin as described previously.[121] The extracted digests were vacuum-evaporated and dried samples were resuspended in 5 ul 0.1% formic acid and subjected to mass spectrometry analysis. Figure S4

Mass Spectrometry Analysis

Peptide digests were subjected to chromatographic separation using a 2 μm, 50 μm x 150 mm, EASY-Spray C18 Reversed Phase HPLC column (Thermo Scientific, ES801). Water-acetonitrile gradients (2–25% in 0.1% formic acid over 60 minutes) were used to separate peptides at a flow rate of 200 nL/minute for analysis in an Orbitrap Lumos Fusion (Thermo Scientific) in positive ion mode. MS spectra were acquired between 375 and 1500 m/z with a resolution of 120000. For each MS spectrum, multiply charged ions over the selected threshold (2E4) were selected for MSMS in cycles of 3 seconds with an isolation window of 1.6 m/z. Precursor ions were fragmented by HCD using a relative collision energy of 30. MSMS spectra were acquired in centroid mode with resolution 30000 from m/z=110. A dynamic exclusion window was applied which prevented the same m/z from being selected for 30s after its acquisition.

Peptide and protein identification and quantitation

Peak lists were generated using PAVA in-house software.[120] All generated peak lists were searched against the human subset of the SwissProt database (SwissProt.2019.07.31) using Protein Prospector.[107] The database search was performed with the following parameters: a mass tolerance of 10 ppm for precursor masses; 30 ppm for MS/MS, cysteine carbamidomethylation as a fixed modification and acetylation of the N terminus of the protein, pyroglutamate formation from N terminal glutamine, and oxidation of methionine as variable modifications. All spectra identified as matches to peptides of a given protein were reported, and the number of spectra (PSM) used for label free quantitation of protein abundance in the samples.

Cell viability assay

Related to Figure S4D. H1-hESCs were passaged as described in "H1-hESC cell culture and CRISPR," and cells were counted to ensure even plating across genotypes. Cells were plated in Geltrex-coated black-sided clear-bottomed 96-well tissue culture dishes (Sigma Aldrich, CLS3603). Wells on the edge of the dish were excluded. Cell viability was measured using the CellTiter-Glo® 2.0 Cell Viability Assay (Promega, G9242) following kit instructions. Significance was measured using Student's t tests.

CellPress

Ribosome profiling on human induced neurons

Related to Figures 3E–3G. LLPH$^{+/+}$ and LLPH$^{Nterm/Nterm}$ hiNs were grown until DIV 14 as mentioned above in "Generation of human induced neurons from H1-hESC with Ngn2 overexpression" with modifications as stated below. Glia was not added on day 5 and premature iN cells were not detached and instead left growing on matrigel coated 6-well plate for the full 14 days. On day 5, media was fully replaced to NB zero + 2 μg/mL Dox + 4 μM AraC. On day 10, 50% of spent media was replaced with NB zero + 2 μg/mL Dox + 4 μM AraC. hiNs were harvested using Accutase in the presence of 100 μg/mL CHX and lysed with lysis buffer B (20 mM Tris-HCl pH 7.5, 15 mM $MgCl_2$, 150 mM NaCl, 1 mM DTT, 100 μg/mL CHX, 1% Triton X-100, 0.5% sodium deoxycholate, 8% glycerol, 20 U/mL TURBO DNase, 200 U/mL SUPERase In™ RNase inhibitor, 1x Halt™ protease and phosphatase inhibitor in nuclease-free water). Lysis was performed and the cytoplasmic fraction was enriched by serial centrifugation as described in "RAPIDASH for E14 mouse embryonic stem cells."

Ribosome profiling libraries were prepared by generally following the published protocol of McGlincy and Ingolia[122] with modifications below. To isolate RNA input samples for RNA-seq, 10 μL of cytoplasmic lysate is transferred into 500 μL of cold TRIzol, mixed by pipetting, and stored at -80°C for subsequent RNA extraction using NEBNext® Ultra II Directional RNA Library Prep Kit for Illumina (NEB, E7760L). The remaining lysate (~375 μg total RNA) was treated with 0.33 μg RNase A (Thermo Scientific, AM2271) and 200 U RNase T1 (Thermo Scientific, EN0541) for 30 min on rotator at room temperature. Digestion was stopped by adding 10 μL SUPERase·In™ RNase Inhibitor and transferring the samples on ice. Meanwhile, to isolate intact 80S ribosomes and ribosome footprints (RFPs), 10-50% linear sucrose gradients were made in 14x89 mm open-top polyallomer centrifuge tubes using a gradient maker (Biocomp, 108). Before layering the lysates onto the gradient, 200 μL sucrose gradient solution was removed from each centrifuge tube. Then, 200 μL cytoplasmic lysate containing 20 μg RNA was used for each RFP sample. The tubes were centrifuged using a SW 41 Ti swinging bucket rotor at 40,000 rpm for 2.5 hours at 4°C.

Fractions were collected for 30 seconds each using the Density Gradient Fraction System with a flow rate of 1.5 mL/minute). 80S were found in fraction 7 for hiN D14 LLPH$^{+/+}$ rep 2 and LLPH$^{Nterm/Nterm}$ rep 1, and fraction 6 and 7 for the other samples. A 3x volume of TRIzol LS (Thermo Fisher, 10296028) was added to these fractions. RFP samples were then extracted from TRIzol using the Direct-Zol Microprep Kit (Zymo, R2060) according to the manufacturer protocol. Subsequently, these samples were treated with TURBO DNase at 37°C for 30 minutes according to the manufacturer protocol and cleaned up with Zymo RNA Clean & Concentrator Kit with some modifications to enrich for small RNAs (>17 nt, <200 nt). Adjusted binding buffer was prepared by mixing equal volumes of 100% ethanol and RNA binding buffer. Samples were first adjusted to 100 μL with nuclease free water. Then, 200 μL of adjusted binding buffer was added and mixed, followed by adding 450 μL of 100% ethanol and mixed. Samples were then processed with spin columns as per manufacturer protocol and eluted twice with 6 μL of nuclease free water each.

RFPs were denatured at 80°C for 90 seconds in denaturing sample loading buffer (10 mM EDTA and bromophenol blue (Fisher Scientific, MBX14107), in formamide (Promega, H5052)), then incubated on ice for 5 minutes before running on a 15% Tris-borate-EDTA-urea (TBE-urea) polyacrylamide gel. Fragments were size-selected using NI-800 and NI-801[122] as 26–34 nt markers. Gel slices were freeze-thawed for at least 30 minutes at -80°C and 3 minutes at room temperature. They were then crushed by forcing the gel through a hole in a 0.5 mL tube pierced by a 20 gauge needle (Santa Cruz Biotechnology, sc-359535) by centrifuging at 15,000 ×g for 2 minutes. RNA were then extracted from the minced gel at room temperature overnight in 400 μL RNA extraction buffer,[122] then re-extracted with an additional 200 μL RNA extraction buffer for additional 3 hours, removing the minced gel by using 0.22 μm cellulose acetate centrifuge tube filters (Corning, 8160) and spinning at max speed for 2 minutes at room temperature. The combined 600 μL extraction was precipitated with 2 μL GlycoBlue (Thermo Fisher, AM9516) and 750 μL 100% isopropanol (Sigma Aldrich, PX1835-6) overnight at -80°C. Precipitated RFPs were pelleted at 21,000 ×g for 30 minutes at 4°C, washed with ice-cold 80% ethanol in water, air dried at room temperature for 10 minutes, then dissolved in 4 μL of 10 mM Tris pH 8, dephosphorylated, and ligated to barcoded linkers as per the published protocol. RNA linkers were pre-adenylated beforehand using Mth RNA ligase (NEB, E2610S). Unreacted linker was deadenylated and digested as per the published protocol. The barcoded RFPS were then purified using Zymo Oligo Clean & Concentrator column (Zymo, D4060) according to the manufacturer's protocol, and subsequently reverse-transcribed as per the published protocol. Template RNA was degraded by alkaline hydrolysis, and cDNA was purified using Zymo Oligo Clean & Concentrator column, denatured in sample loading buffer, and size selected on a 10% TBE-urea gel, as marked by NI-800 and NI-801 that had been processed in parallel with the samples. Gel slices were processed as described previously, and cDNA was extracted at room temperature overnight in 400 μL DNA extraction buffer,[122] then re-extracted with an additional 200 μL DNA extraction buffer for 3 hours. The cDNA was pelleted, washed, and dried as described above, then resuspended in 15 μL 10 mM Tris pH 8. cDNA was circularized by adding 2 μL 10X CircLigase I buffer, 1 μL of 1 mM ATP, 1 μL of 50 mM $MnCl_2$, and 1 μL of CircLigase I (Biosearch Technologies CL4111K) to the 15 μL of cDNA and incubating at 60°C for 12 hours, then 80°C for 10 minutes. Using 1 μL of circularized DNA template per 50 μL reaction, library construction to add indexing primers was performed as per the published protocol using a different reverse primer for each replicate. PCR products were purified using a Zymo DNA Clean & Concentrator column (Zymo, D4003). Size selection was performed on a 8% TBE-urea gel, with the lower bound marked by NI-803[122] that had undergone library construction in parallel with the samples, and the upper bound at 170 nt as marked by O'Range 20 bp DNA ladder (Thermo, SM1323). Gel slices were extracted as described above. DNA was precipitated as described above, except using 1.25 μL of 20 μg/mL glycogen (Invitrogen, 10814-010) instead of GlycoBlue. The pellet was resuspended in 15 μL of 10 mM Tris pH 8. Library quality was analyzed on an Agilent 2100 Bioanalyzer (High-Sensitivity DNA) at the Stanford Protein and

Nucleic Acid Facility. Library concentration was measured using Qubit dsDNA high sensitivity kit (Thermo Fisher, Q33231), and the RFP samples were then pooled in equal amounts.

Poly(A)-enriched RNA samples were mixed together with RFP samples in 4:6 ratio. Libraries were sequenced by Novogene (Sacramento, CA) on a full lane Illumina NovaSeq X Plus with paired-end 150 bp reads.

Ribosome profiling analysis

Related to Figures 3E–3G. For Ribo-seq data from RFP samples, only analysis of Read 1 was necessary due to the short insert length. cutadapt version 2.4[110] was used to trim adapter sequences in both poly(A)-enriched RNA and RFP samples. For RFP samples, only sequences from Read 1 were trimmed from 3' adapter sequences with parameters "-j 0 -u 3 -a AGATCGGAAGAGCACAGTCT GAACTCCAGTCAC –discard-untrimmed -m 15", whereas in poly(A)-enriched RNA samples, both 3' and 5' adapters were trimmed from Read 1 and Read 2, respectively, with parameters "-a AGATCGGAAGAGCACACGTCTGAACTCCAGTCA -A AGATCGG AAGAGCGTCGTGTAGGGAAAGAGTGT". For RFP samples, in-line barcodes were demultiplexed using fastx_barcode_splitter.pl (http://hannonlab.cshl.edu/fastx_toolkit/) with parameters "–eol". Unique molecular identifiers and in-line barcodes were extracted using UMI-tools version 1.0.1[115] with parameters "extract –extract-method=string –bc-pattern=NNNNNCCCCC –-3prime". Reads were filtered by quality using fastq_quality_filter (http://hannonlab.cshl.edu/fastx_toolkit/) with parameters "-Q33 -q 20 -p 70 -z". GENCODE release 43[103] was used as a reference. To remove reads originating from rRNA, transfer RNA (tRNA), and small nuclear RNA (snRNA), reads aligning to these sequences using bowtie2 version 2.3.4.3[116] with parameters "-L 18" were discarded. PCR duplicates were then removed using UMI-tools. Ribosome A site positions were determined by offsetting the distance of the 5' end of each RFP read to canonical start sites in each length group and adding 4 nucleotides. Reads aligning to the CDS were used for RFP libraries, while reads aligning to the entire transcript were used for RNA-seq libraries. Transcript abundance for RNA-seq samples were quantified using salmon version 1.4.0.[113] Reads mapping to mitochondrial DNA genes were excluded from further analysis. Transcripts with counts per million (CPM) >2 were retained for downstream analysis RFP and RNA-seq libraries were normalized separately by the trimmed mean of M-values method in edgeR.[117] Differential RFP and RNA-seq abundance and enrichment were analyzed using voom[119] and limma.[118] Multiple testing correction was performed using the Benjamini-Hochberg method.

Sucrose Gradient Fractionation for mouse E12.5 tissues

Related to Figure 4C. For Figure 4C, each sample consisted of tissues pooled from the same litter prepared as described above in "RAPIDASH for E12.5 tissues." However, cold lysis buffer B was added to each sample instead of cold lysis buffer A. Lysis was performed as described in "RAPIDASH for E12.5 tissues," and the cytoplasmic fraction was enriched by serial centrifugation as described in "RAPIDASH for E14 mouse embryonic stem cells.".

Linear sucrose gradients were made in 11x60 mm open-top polyallomer centrifuge tubes (Seton Scientific, 5010) as in "Sucrose gradient fractionation for RAPIDASH characterization." For EDTA treated samples, 50 mM EDTA was included in the sucrose gradient solution. Before layering the cytoplasmic lysates onto the gradient, 130 μL sucrose gradient solution was removed from each centrifuge tube. Typically, 125 μL cytoplasmic lysate containing 80-120 μg RNA was used for each sucrose gradient fractionation experiment. The tubes were centrifuged using a SW 60 Ti swinging bucket rotor (Beckman Coulter, 335649) at 35,000 rpm for 2.5 hours at 4°C.

Fractions were collected for 28 seconds each using the Density Gradient Fraction System with a flow rate of 0.75 mL/minute. Proteins were precipitated and prepared as described in "Mass spectrometry of unlabeled tryptic digests - Protein precipitation." After the protein pellets were dried, they were immediately prepared for western blotting.

RAPIDASH on macrophages

Related to Figures 5A, 5B, and S5. RAPIDASH isolation of ribosome complexes from macrophages was performed as described above with the following exceptions. For each sample, ~100 million macrophages were used as starting material. For CHX treatment of macrophages, 100 μg/mL CHX was added to the BMDM culture media for seven minutes before cells were washed twice in ice cold PBS containing 100 μg/mL CHX and harvested with a cell scraper.

Proteomic analysis of ribosomal complexes in macrophages

Related to Figures 5A, 5B, and S5. Samples were processed for mass spectrometry as in "RAPIDASH and proteomic analysis of ribosomal complexes for PC3 cells" with the following exceptions.

In solution digestion and TMT labeling

For "In solution digestion," samples were prepared at a concentration of 1 mg/mL in a solution containing 8 M Guanidinium Hydrochloride (GndHCl; Sigma Aldrich, G3272) and 50 mM ammonium bicarbonate and frozen until processing. The next steps, including reduction, treatment with iodoacetamide, dilution with ammonium bicarbonate, digestion with trypsin, and acidification of the digests was performed as in "RAPIDASH and proteomic analysis of ribosomal complexes for PC3 cells." Digests were desalted using either C18 ZipTip (Millipore, ZTC18S960) or 100 μL OMIX C18 pipette tips (Agilent) following the manufacturer's protocol. Eluates were dry-evaporated in preparation for direct label free MS analysis or for labeling with TMT reagents for quantitative comparison.

TMT labeling was performed as in "RAPIDASH and proteomic analysis of ribosomal complexes for PC3 cells," except a TMTpro™ 18-plex kit (Thermo Scientific, A52045) was used. After the TMT labeling was quenched with hydroxylamine, all 15 samples were

combined and partially evaporated in speedvac until volume was around 5 μl. Samples were acidified with 100 μL 1% formic acid, and the peptides were desalted using a C18 SepPak (Waters, WAT051910). The SepPak eluate was dried in preparation for fractionation by high pH reverse phase chromatography.

High pH reverse phase chromatography

SepPak cleaned, TMT labeled samples were resuspended in 240 μL 20 mM ammonium formate (Sigma Aldrich, 09735) pH 10.4 for fractionation of the peptide mixture by high pH reverse phase chromatography using a Gemini 5 μm C18 110Å 150 x 4.60 mm column (Phenomenex, 00F-4435-E0), operating at a flow rate of 0.550 mL/min. Buffer A consisted of 20 mM ammonium formate (pH 10), and buffer B consisted of 20 mM ammonium formate in 90% acetonitrile (pH 10). Gradient details were as follows: 1 % to 30% B in 49 min, 30% B to 70% B in 4 min, 70% B down to 1% B in 4 min. Peptide-containing fractions were collected, evaporated, and resuspended in 0.1% formic acid for mass spectrometry analysis.

Mass spectrometry analysis

Resuspended peptide digests were injected onto the same column and separated using the same gradient and flow rate as in "RAPIDASH and proteomic analysis of ribosomal complexes for PC3 cells." Analysis of the label free samples was performed in an Orbitrap Lumos Fusion (Thermo Scientific) in positive ion mode. MS acquisition parameters were the same as in "RAPIDASH and proteomic analysis of ribosomal complexes for PC3 cells," except an isolation window of 1.6 m/z and the precursor ions fragmentation by HCD using a relative collision energy of 30 were used. MSMS spectra were acquired in centroid mode with resolution 30000 from m/z=110. A dynamic exclusion window was applied which prevented the same m/z from being selected for 30 seconds after its acquisition.

For analysis of the TMT experiments, aliquots of 10 non-consecutive chromatographic fractions were analyzed in an Orbitrap Exploris 480 (Thermo Scientific) in positive ion mode with the same parameters as in "RAPIDASH and proteomic analysis of ribosomal complexes for PC3 cells."

Peak lists were generated using PAVA in-house software[120] and searched against the mouse subset of the SwissProt database (SwissProt.2019.07.31, 17026 entries searched), using Protein Prospector[107] with the same allowances for fixed and variable modifications as in "RAPIDASH and proteomic analysis of ribosomal complexes for PC3 cells," except TMT16plex labeling of lysine residues and N-terminus of the protein was allowed as a fixed modification instead of the TMTsixplex label. Mass tolerance parameters and the estimation of false positive rate was the same as in "RAPIDASH and proteomic analysis of ribosomal complexes for PC3 cells." In addition, as before, 1% FDR was permitted at the protein and peptide level. Only unique peptides were used for quantitation. TMT-based quantitation was performed as in "RAPIDASH and proteomic analysis of ribosomal complexes for PC3 cells." Significance was calculated using Student's t-test.

The analysis performed to obtain the GO terms in S5A was performed using Manteia as in "Mass spectrometry data analysis." To obtain the top 15% enriched proteins in the RAPIDASH eluate from unstimulated BMDMs, the fraction of peptide counts belonging to a protein in each replicate was normalized by the protein's molecular weight. Then, the average of the three replicates (Table S9, column N) was ranked from highest to lowest, and the top 186 proteins were selected.

Sucrose gradient fractionation experiments for macrophages

Related to Figures 5C–5F. For Puromycin treatment of BMDMs, 2 mM Puromycin was added to the BMDM culture media for 10 minutes before cells were washed twice in ice cold PBS and harvested with a cell scraper. Cell pellets were lysed immediately or frozen and stored at -80°C.

For sucrose gradient fractionation experiments, 30-40 million macrophages were lysed in one of two polysome buffers: buffer A (20 μM HEPES-KOH, pH 7.6, 15 mM magnesium acetate, 60 mM ammonium chloride, 1 mM DTT, 1% Triton X-100, 0.5% sodium deoxycholate, 8% glycerol, 20 U/mL TURBO DNase, 1x Halt Protease Inhibitor Cocktail) or buffer B (20 mM Tris pH 7.4, 150 mM NaCl, 15 mM $MgCl_2$, 1 mM DTT, 0.5% Triton X-100, 8% glycerol, 20 U/mL TURBO DNase, 1x Halt Protease Inhibitor Cocktail). Lysates were vortexed three times for 30 seconds, then incubated on ice for 30 minutes. Macrophages lysed in buffer A were centrifuged at 800 ×g for 5 minutes, then 8000 ×g for 5 minutes, then at max speed for 5 minutes in a tabletop microcentrifuge at 4 °C. Macrophages lysed in buffer B were centrifuged at 1,800 ×g for 5 minutes, then at 10,000 ×g for ten minutes in a tabletop microcentrifuge at 4 °C.

Puromycin-treated macrophages were lysed in buffer A supplemented with 2 mM puromycin and 200 U/mL SUPERase·In™ RNase Inhibitor. Non-puromycin-treated (control) macrophages were lysed in buffer A supplemented with 100 μg/mL CHX and 200 U/mL SUPERase·In™ RNase Inhibitor. Puromycin and non-puromycin-treated macrophage lysates (300 μL) were loaded onto a 10-50% (w/v) sucrose gradient (20 mM Tris pH 7.4, 100 mM KCl, 4 mM $MgCl_2$) generated using a Gradient Master 108 (Biocomp).

For RNase treatment of macrophage samples, macrophages were treated *in vitro* with CHX and lysed in polysome buffer B supplemented with 100 μg/mL CHX. Control samples were lysed in buffer B supplemented with 100 μg/mL CHX and 200 U/mL SUPERase·In™ RNase Inhibitor. Following centrifugation, the RNA concentration in each sample was measured using a Nanodrop 2000c Spectrophotometer. For every 75 μg of RNA, 0.5 μL RNase A and 0.3 μL RNase T1 were added, and samples were incubated with rotation at room temperature for 30 minutes (control samples were meanwhile kept on ice.) After 30 minutes, SUPERase·In™ RNase Inhibitor was added to the RNase-treated samples, such that the volume of SUPERase·In™ RNase Inhibitor added was equal

to twice the volume of the combined RNases that were added. RNase-treated and control macrophage lysates were loaded onto a 10-50% (w/v) sucrose gradient (20 mM Tris, pH 7.4, 150 mM NaCl, 15 mM $MgCl_2$).

All samples were centrifuged at 38,000 rpm for 2.5 hours at 4°C in a Beckman L8-70M ultracentrifuge. Samples were separated into 14 fractions on a Piston Gradient Fractionator (Biocomp Instruments, 152).

Western blotting for macrophage gradient fractions

Related to Figures 5C–5F. Protein was precipitated from polysome fractions using the ProteoExtract Protein Precipitation kit according to the manufacturer's instructions with the following modifications: 700 μL of Precipitation Agent was added to 700 μL of each polysome fraction, and samples were incubated for at least 24 hours at -20°C. All centrifugation steps were performed at max speed at room temperature in a tabletop microcentrifuge (Eppendorf).

Precipitated protein was resuspended in 35 μL of 1x Laemmli Sample Buffer supplemented with 10% 2-mercaptoethanol. 10 μL of each sample was loaded into 4-15% Mini-PROTEAN TGX Precast protein gels and transferred onto nitrocellulose membranes. Membranes were blocked in tris-buffered saline with TWEEN 20 (TBST) with 5% milk and incubated overnight in TBST with 5% milk at 4°C with the following primary antibodies: anti-RPL23 (A305-008A, Bethyl), anti-RPS6 (2317S, Cell Signaling), anti-RPS12 (16490-1-AP, Proteintech), anti-USP15 (14354-1-AP, Proteintech), anti-Viperin (MaP.VIP, Abcam), anti-CMPK2 (H00129607-A01, Abnova), anti-HO-1 (ADI-SPA-895-F, Enzo), anti-RACK1 (4716S, Cell Signaling), and anti-OAS3 (21915-1-AP, Proteintech). Membranes were washed and incubated for one hour at room temperature with either Promega Anti-Mouse (W402B) or Anti-Rabbit (W401B) IgG HRP Conjugates. Membranes were incubated for two minutes with SuperSignal West Dura Extended Duration Substrate (Protein Biology) and visualized using the BioRad ChemiDoc Touch Imaging System.

QUANTIFICATION AND STATISTICAL ANALYSIS

Information regarding statistical analyses and the parameters used can be found in the Figure legends and in the method details section. No strategies for randomization, stratification, or the inclusion or exclusion of data were used. Sample size was chosen to conform to the standards in the literature.